ANTIMALARIAL ACTIVITY OF QUINOLINE THIOSEMICARBAZONES: SYNTHESIS AND ANTIPLASMODIAL EVALUATION

A THESIS SUBMITTED IN FULFILMENT OF THE REQUIREMENT FOR THE DEGREE

OF

MASTER OF SCIENCE (CHEMISTRY)

AT

RHODES UNIVERSITY

BY

LUKHANYISO NQENO

2021

Abstract

Africa is one of the regions that is most affected by malaria, as 90% of all malaria deaths occur in sub-saharan Africa. Malaria is a life threatening disease responsible for an estimated 800000 deaths each year, the majority of these deaths occurred in children under the age of five. The disease is a mosquito-borne, and it is transmitted to humans by the female *Anopheles* mosquito. The parasite responsible for this disease belong to the *Plasmodium* genus with *Plasmodium falciparum* causing the most severe cases of the disease in humans.

The most widely available anti-malarials were designed to specifically target the pathogenic blood stage in humans, however, in order to completely eradicate malaria there is a need for the development of medicines that not only target the pathogenic blood stage of the parasite but also block parasite transmission and eliminate asymptomatic and cryptic hepatic forms of the parasite. Iron chelators have recently gained importance as potent antimalarials, to cause infection nearly all protozoa obtain growth essential iron from their hosts. Iron is required for the development of the parasite. Deprivation of utilizable iron by chelation is a proficient approach to arrest parasite growth and associated infection. Thiosemicarbazones are known iron chelating agents by bonding through the sulfur and azomethine nitrogen atoms.

This study is aimed at the identification of thiosemicarbazone based derivatives as possible antimalarial agents. Due to their iron chelation abilities there has been increasing interest in the investigation of thiosemicarbazones as possible antimalarials. During the course of this project, several thiosemicarbazone derivatives were synthesized and their structure confirmed using routine analytical techniques (NMR, FTIR, and HRMS). The synthesized compounds were evaluated *in vitro* against the chloroquine sensitive strain (3D7) of *P. falciparum* for antimarial activity. The compounds were also evaluated agsinst Hela cells for overt cytotoxicity. The compounds generally showed poor antimalarial activity. One compound (**LKN11**) was identified to possess intrinsic and moderate antimalarial activity of 6.6 μM. The compounds were generally not cytotoxic against Hela cell at concentrations of up to 20 μM, with only compound **LKN10** showing modest cytotoxic activity of 9.5 μM. This research went on to identify two thiosemicarbazone based derivatives which had a significant effect on HeLa and pLDH cells.

Table of Contents

Table of Figures

Dedication

Dedicated to my late grandfather, Benjamin Monwabisi Nqeno

Acknowledgements

I would not be where I am today if it was not for a handful of people God placed in my life. However, my first acknowledgement has to be the Almighty, if it had not been for God's grace and mercy in my life I do not know where I would be. I have dwelled in the secret place of the most high and true to His word I have abided under the shadow of the Almighty. All the praise and all the glory goes to Him.

My mother is my rock and my anchor and I do not know where I would be without her. She has been patient and understanding even when I did not have patience for myself. Mama wam ndikuthanda ngentliziyo yam yonke andazi ndingayintoni ngaphandle kwakho. UThixo akusikelele akugcine mama wam. I love you so much.

I would also like to thank my supervisor, Dr. Khanye, for always being there when I needed his help and for answering my never-ending questions. I know very well I can be a handful but Sir I cannot thank you enough for your patience, understanding and your abundance of knowledge and wisdom. I pray God blesses you with more success and joy in your life.

Lastly, I would like to acknowledge Rhodes University and the Chemistry department of this prestigious university for affording me the opportunity to continue my studies further and thus allow me to undergo this research. I would also like to thank my financial backers, NRF without whom I would not have had this opportunity.

CHAPTER 1

INTRODUCTION AND LITERATURE REVIEW

1.1 History of Malaria and its discovery

In the twentieth century alone, malaria has claimed between 180- 300 million lives, accounting for 2-5% of all deaths worldwide. Ancient writings and artifacts testify to malaria's long reign, with the malaria antigen having been recently detected in ancient Egyptian remains dating back from 3200 and 1304 BC. In recent years, by virtue of climate, ecology, and poverty, sub-Saharan Africa has been home to 80-90% of the world's malaria cases and deaths, although predictions state that resurgent malaria in southern Asia is already altering that proportion[4].

Malaria has been linked with swamps since the condition known as Roman fever inspired the name malaria meaning "bad air". A French doctor, during the Franco-Prussian war, by the name of Charles Louis Alphonse Lavernan knew that many diseases previously ascribed to as evil vapors were in fact caused by microbes. In 1880 he identified a brownish black pigment in crescent shaped bodies from the body of a febrile soldier, he later discovered that these pigments were found in the blood of malaria victims by several investigators. He ultimately recognized four distinct forms in human blood that would prove to be the malaria parasite in different stages of its life cycle. Although at first his findings were viewed with skepticism, he was later affirmed and received the Nobel Prize for discovering the single-celled protozoan that caused malaria. Several years later the mode of transmission of the disease was demonstrated by surgeon-major Ronal Ross[4].

1.2 Malaria

Malaria is a life-threatening mosquito-borne disease transmitted to humans by the female Anopheles mosquito. The parasites responsible for the spread of malaria belong to the *Plasmodium* genus, with over 100 types of *Plasmodium* species capable of infecting a variety of species⁵⁵⁵, however, only five types of *Plasmodium* parasites can infect humans[5]. These five *Plasmodium* parasites are *Plasmodium ovale*, *P. vivax*, *P. malariae*, *P. knowlesi* and *P. falciparum*[6]. The most severe cases of malaria in humans are caused by *P. falciparum*.[7]

Malaria occurs primarily in tropical regions, as well as some sub-tropical regions, of Africa, Central, and South America, Asia, and Oceania[8]. According to the World Health Organisation (WHO) Malaria report 2011, a total of 216 million estimated malaria cases occurred in 2010, 81% of which were reported in the African region, followed by Southeast Asia with 13% and Eastern Mediterranean Region with 5%, with an estimation of 655000 malaria-related deaths. About 91% of these deaths occurred in the African region, 6% in the Southeast Asian region and 3% in the East Mediterranean region[9]. The latest malaria report by the WHO reported that in the last year malaria-affected 228 million people, which is almost 5% more infected than in 2010, however, the number of malaria deaths decreased to 405 000, most reported cases were found in Sub- Saharan Africa[10–12]. Africa is one of the countries most affected by malaria in the world, with about 90% of all malaria deaths in the world occurring in Africa south of the Saharan. There is a high abundance of *P. falciparum* in Sub-Saharan Africa depicted in **Figure 1.1** below, due to failure to eradicate the most effective malaria vector, the female Anopheles mosquito which is abundant in the Sub-Saharan Africa region[13].

An estimated 1 million people die in Africa from malaria each year with 90% of these deaths occurring in pregnant women and young children under the age of five[14]. Pregnancy reduces a woman's immunity to malaria making her more susceptible to infection and at greater risk of illness, severe amnesia and death[10–12]. Most of these aforementioned children experience their first malaria infections during the first two years of life when they have not yet acquired adequate clinical immunity.[14]

There are three principal ways in which malaria can contribute to death in young children:

1) An acute infection, which often presents itself as seizures or coma, may kill a child directly and quickly.
2) Repeated malaria infections contribute to the development of severe anemia, which significantly increases the risk of death.
3) Low birth weight due to malaria infection in pregnant women is the major risk factor for death in the first month of life.

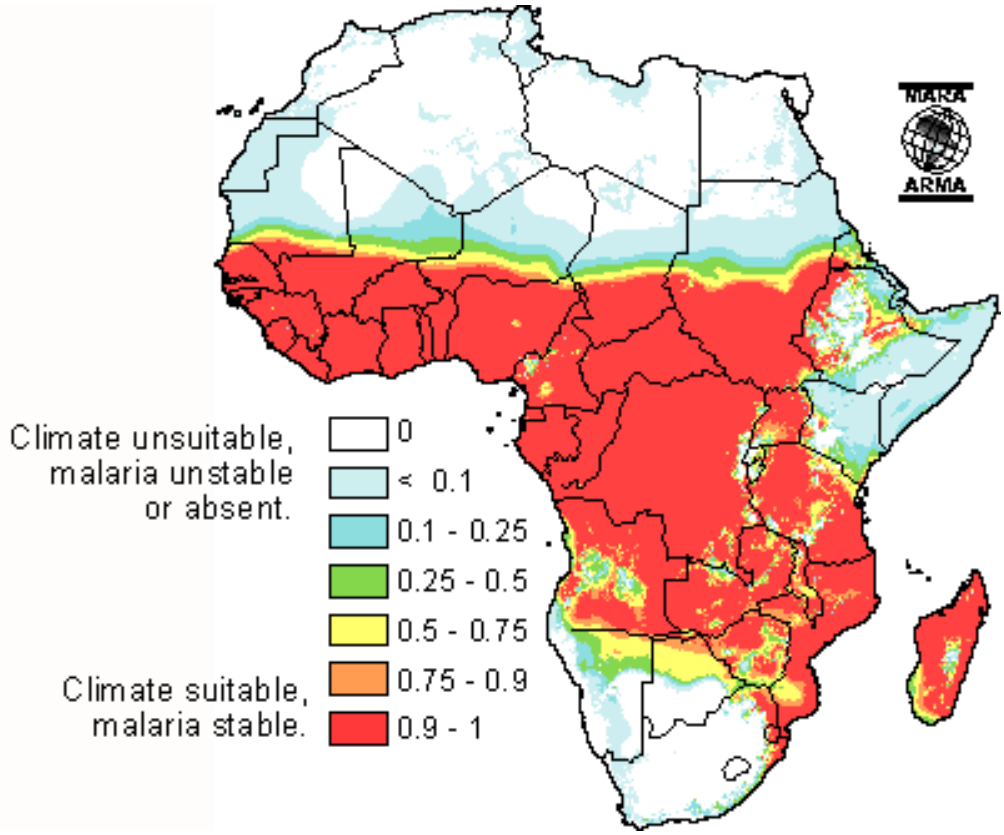

Figure 1.1**: Distribution of Malaria in Sub-Saharan Africa**[15]

1.2.1 Malaria Life cycle

Malaria is typically transmitted by the bite of an infected female Anopheles mosquito. During a blood meal by a female Anopheles mosquito certain forms of blood-stage parasites, known as gametocytes, are ingested by the mosquito. The gametocytes mate in the gut of the mosquito and begin a cycle of growth and multiplication, known as the sexual stage, in the mosquito. A form of the parasite called a sporozoite migrates to the mosquitos salivary glands after 10-18 days. When the Anopheles mosquito takes a blood meal on another human, anticoagulant saliva is injected together with the sporozoites, which migrate to the liver thereby starting a new cycle. The infected mosquito acts as a vector, carrying the disease from one human to another, however, the mosquito itself is not affected by the presence of the parasite, unlike the human host[16].

The **Figure 1.2** below shows a simple representation of the transmission of the *P. falciparum* parasite from the vector, the female Anopheles mosquito, to the human host.

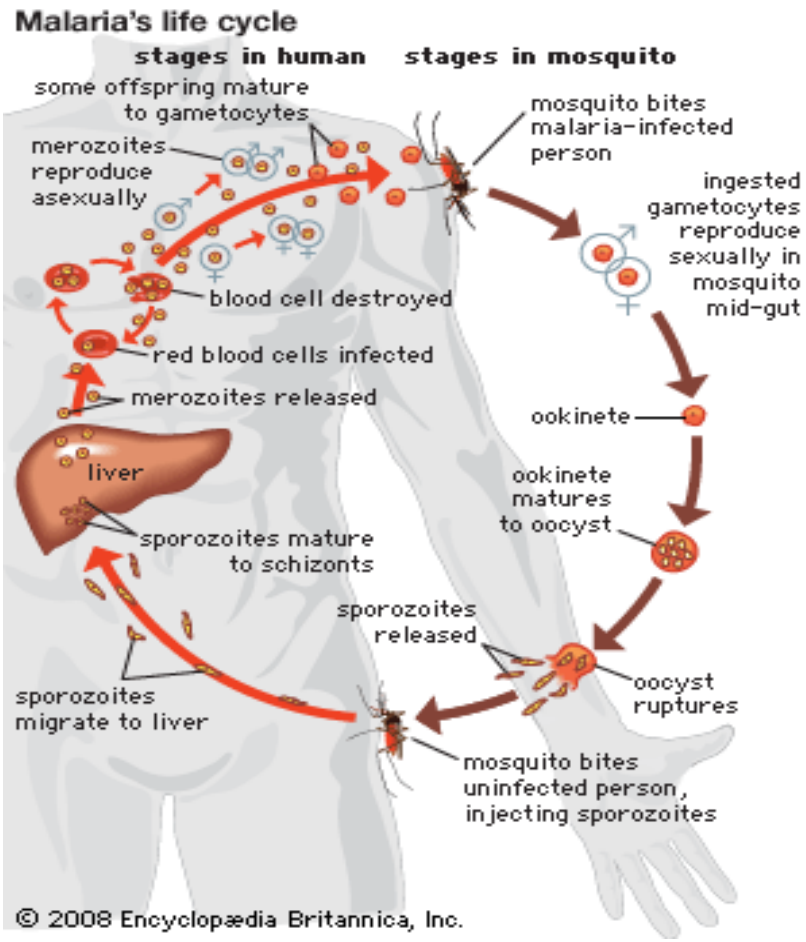

Figure 1.2: The Life cycle of Malaria[17]

The lifecycle of the malaria parasite involves a host and a vector, the vector being the female Anopheles mosquito, which does not suffer from the presence of the parasite and simply carries it to the human host who is affected and thus suffers from the presence of the parasite.

The sporozoites migrate, infect liver cells and mature into schizonts, which rupture and release merozoites. After initial replication in the liver, the parasites undergo asexual multiplication in the erythrocytes. The merozoites infect red blood cells, the ring stage trophozoites mature into schizonts, which rupture releasing merozoites. Some parasites differentiate into sexual erythrocytic stages known as gametocytes. The gametocytes- male gametocytes are known as microgametocytes and female gametocytes are known as macrogametocytes[7].

The parasite multiplication in the mosquito is known as the sporogonic cycle. While in the mosquito's stomach the microgametes penetrate the macrogametes creating zygotes. The zygotes, in turn, become motile and elongated, at this stage, they are referred to as ookinetes and invade the

midgut wall of the mosquito where they develop into oocysts. The oocysts grow, rupture and release sporozoites that make their way to the mosquitos' salivary glands. The inoculation of the sporozoites into a new human host continues the malaria life cycle.[7]

1.2.2 Treatment of malaria

In recent years great progress has been made to reduce the high level of suffering caused by malaria worldwide. The development of resistance to anti-malarial drugs has highlighted the need for continued research to completely eradicate this disease[18]. There are currently fourteen medicines for curative treatment of malaria and four medicines for prophylactic treatment, listed on the WHO model list of essential medicines. The most effective of these are the artemisinin-based combinations that use a combination of artemisinin derivatives with one or more complementary compounds, which unlike the artemisinin derivatives are long-acting and possess a different mechanism of action[18]. Artemisinin is effective against several multi-drug resistant forms of *P. falciparum*. The first report of resistance to artemisinin was in western Cambodia in 2008, ten years later in 2018, a report was published identifying more than 30 independent cases of artemisinin resistance in Southeast Asia[18]. Several compounds have been discovered and developed as potential anti-malarial candidates with the hopes of progressing into clinical trials. One of these compounds was a chiral 8-aminoquinoine derivative which was developed at the University of Mississippi and was still in preclinical trials in 2014. Another was MK4815, an amino-tert-butylphenol derivative, which was developed in 2012 at Merck but is still in preclinical studies due to safety issues.

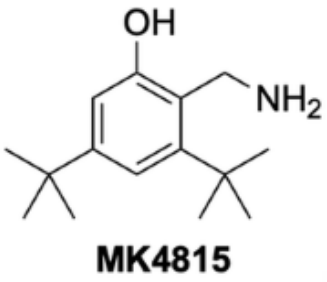

MK4815

Figure 1.3: Structure of MK4815, an amino-tert-butylphenol derivative[18].

In 1967 modern malaria vaccine development began with seminal studies in mice using irradiated sporozoites[19]. Almost 50 years later and there still is no licensed product. However, steady progress is being made especially in regards to the breakthroughs in the understanding of the

cellular and molecular mechanisms mediating protection in animal models and humans[20]. The revised Malaria Vaccine Technology Roadmap to 2030 calls for a next-generation vaccine to achieve 75% efficacy over 2 years against *P. falciparum*, while also retaining its original goal of the first-generation vaccine with protective efficacy of more than 50% lasting over a year and more. To achieve this next-generation goal a need to build on the success of current pre-erythrocytic subunits and whole sporozoite-based vaccines, as well as new strategies to add blood-stage or transmission-blocking immunity are required[20].

The most extensively tested vaccine candidate for the prevention of *P. falciparum* malaria infection is RTS,S/A801. This vaccine directs immune responses against the major circumsporozoite protein (PfCSP) covering the surface of the infecting sporozoite[20]. RTS,S, formulated with the potent liposomal adjuvant system AS01 from GlaxoSmithKline, is the only vaccine that has demonstrated protective efficacy against clinical malaria in a Phase III clinical trials. However, protection from *P. falciparum* malaria is partial, wanes over time and may be dependent on age as protection was lower in infants of 6-12 weeks old than in young children of 5-17 months of age[20]. According to WHO two safety signals, namely meningitis, and cerebral malaria, emerged from the phase III trial and a confirmed risk of febrile convulsions within 7 days of vaccination in the 5-17 month age category was noted. In July 2015 WHO recommended large scale pilot implementations to further evaluate the vaccine's potential for reducing childhood deaths and to provide additional data on safety in the context of routine use[20].

1.2.3 History of Antimalarials

During the seventeenth century, infusions of Cinchona bark were the only effective antimalarial treatment until quinine, which is the active component in the bark, was isolated in 1820[21]. Since this initian the isolation of quinine, other natural and synthetic compounds have been developed. However, strains of the parasite began to show signs of resistance towards these drugs, rendering them less effective. Accordingly, their use has ceased or is restricted to particular situations[21].

Quinine had been used as one of the most effective treatments for malaria until resistance to this drug was first reported in the 1980s and since 2006, is no longer in use as a front-line treatment for malaria[21].

Mepacrine was predominantly used throughout the Second World War as a prophylatic. This compound is a derivative of methylene blue, another anti-malarial that was discovered in 1891[21]. The use of Mepacrine has declined over the years, however. methylene blue and its derivatives are still used with a combination with primaquine currently in clinical trials. Mepacrine itself is no longer used today due to the high chance of undesirable side efects such as toxic psychosis.

Chloroquine was used to treat all forms of malaria, especially during the 1940s, with few side effects[21]. The first resistance to chloroquine was reported in the 1950s and over the years many strains of malaria have developed resistance to this drug. Despite this, chloroquine is on the World Health Organisations Model List of Essential Medicines (MLEM) for the treatment of *P. vivax* in regions where resistance has not yet developed[21].

Mefoquine was developed in the 1970s and was originally introduced for the treatment of chloroquine-resistant malaria. It is thought that the structurally related quinoline drugs (such as quinine, mepacrine, chloroquine and mefoquine) act through the disruption of haemoglobin digestion in the blood stage of the parasite[21]. These drugs are commonly used in combination with a complementary drug (e.g. mefoquine and artesunate) to reduce the chance of resistance development to the quinoline family of compounds. Mefoquine is commonly sold in its racemic form, however, due to the perception of central nervous system toxicity that has been suggested to affect a large number of its users it is no longer widely used as an antimalarial drug[21].

Halofantrine was developed between the 1960s and 1970s and was initially used for treatment against all forms of the Plasmodium parasite. Due to a number of undesirable side efects, such as the potential for high levels of cardiotoxicity, the use of this drug has diminished. Halofantrine is used only in cases where patients are known to be free of heart disease and where infection is due to severe and resistant forms of malaria[21].

1.2.4 Currently Used Antimalarials

There are currently 14 medicines listed on the WHO Model List of Essential Medicines for curative treatment of malaria and 4 medicines for prophylactic treatment , with the treatments formulated either as single compounds or as combinations. The most efective of these drugs are the artemisinin-based combinations which use an artemisinin derivative in combination with one or more complementary compounds[22]. Medicines for Malaria Venture (MMV) have been involved in the progression of nine new anti-malarial treatments based on different combinations of

approved drugs[22]. Artemisinin and its derivatives were first isolated in 1971 by Tu Youyou from the plant *Artemisia annua*. Artemisinin has been shown to be effective against all multi-drug resistant forms of *P. falciparum*. The most common derivatives of artemisinin are artemether, artesunate and arteether[22]. These semi-synthetic derivatives are prodrugs which are transformed to the active metabolite, dihydroartemisinin. The first report of resistance to artemisinin was in western Cambodia in 2008 and then ten years later a report was published identifying more than 30 independent cases of artemisinin resistance in southeast Asia, specifcally with resistance to the dihydroartemisinin–piperaquine combination therapy[22]. The mechanism of action through which artemisinin acts is thought to be that the molecule is activated by haem to generate free radicals, which in turn damage proteins required for parasite survival. In 2015, artemisinin was shown to be associated with the up-regulation of the unfolded protein response pathways which may be linked to decreased parasite development[22].

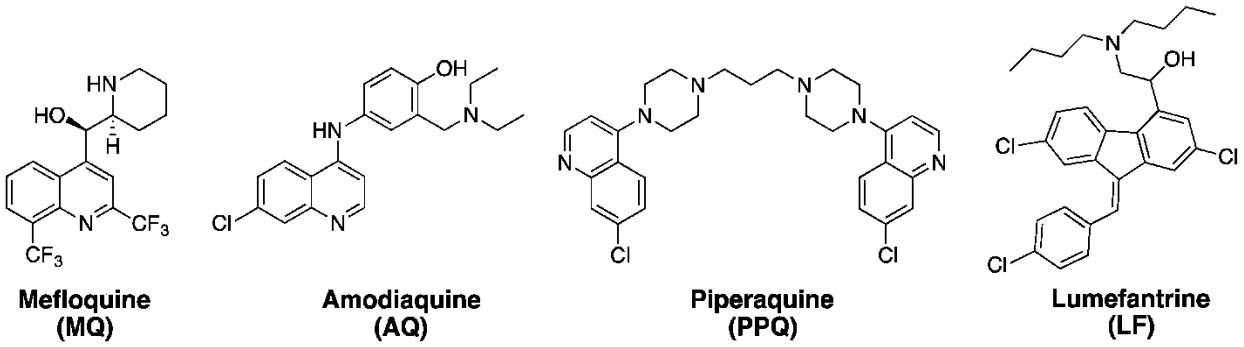

Figure 1.4: Structure for a few artemisinin based drugs[23]

Amodiaquine was first synthesized in 1948 and is mainly used for the treatment of uncomplicated malaria casued by *P. falciparum* when used in combination with artesunate. Similar to chloroquine, amodiaquine's mode of action is thought to involve complexation with haem and inhibition of haemozoin formation[22].

Piperaquine was developed in the 1960s and was initially used throughout China as a replacement for chloroquine, before resistance led to its diminished use as a monotherapy[22]. The mode of action of piperaquine is not completely understood, studies have suggested that it acts by accumulating in the digestive vacuole and inhibiting haem detoxifcation through the binding of haem-containing species[22].

Lumefantrine was first synthesized in 1976, the exact MoA of lumefantrine is unknown, however studies suggest that it inhibits nucleic acid and protein synthesis through the inhibition of β - haematin formation by complexation with haemin. Lumefantrine is currently used only in combination with artemether[22].

Proguanil was first reported as one of the first antifolate anti-malarial drugs in 1945 while atovaquone was first reported in 1991 for the treatment of protozoan infections . The combination of these two compounds is commonly sold as Malarone™ and has proven to be a very effective anti-malarial due to the synergistic effect of the two components[22]. This is, in large part, due to the diferent MoAs for each compound. Atovaquone acts as a cytochrome bc1 complex inhibitor which blocks mitochondrial electron transport. Proguanil acts as a dihydrofolate reductase (DHFR) inhibitor through its metabolite, cycloguanil which disrupts deoxythymidylate synthesis. When used in combination with atovaquone however, proguanil does not act as a DHFR inhibitor but has instead been shown to reduce the concentration of atovaquone required for treatment. Generic atovaquone/proguanil is still available today for the treatment of chloroquine-resistant malaria[22].

Pyrimethamine was developed in the early 1950s. Sulfadoxine was developed in the early 1960s and due to high levels of resistance is no longer used as a preventative drug[22]. The combination of pyrimethamine and sulfadoxine was approved for use for the treatment of malaria in 1981. Both drugs are known to target the parasite folate biosynthesis pathway. Pyrimethamine inhibits dihydrofolate reductase, while sulfadoxine inhibits dihydropteroate synthetase[22].

Pyronaridine was first synthesized in the 1970s and has been found to be effective against chloroquine resistant strains of malaria and has been in use for over 40 years. Like lumefantrine, pyronaridine has been found to act through the inhibition of β-haematin formation[22] .

Tafenoquine was first discovered in 1978 and was recently approved by the United States Food and Drug Administration for use as the first new single-dose for the radical treatment of *P. vivax* malaria in over 60 years . Tafenoquine is thought to be a prodrug which is metabolized to the active quinone tafenoquine, however the mode of action is not well known[22].

1.2.5 Potential Pathogen Vulnerabilities in the Malaria Life Cycle

Complete eradication of malaria requires the development of medicines that not only target the pathogenic blood stage of the parasite but also block parasite transmission and eliminate asymptomatic and sometimes cryptic hepatic forms of the parasite[24]. However, the most widely available anti-malarial drugs were designed to specifically target the pathogenic blood stage in humans[24]. It would be decidedly desirable for candidate drugs to have activity against hepatic and asexual forms of the malaria parasite as some potential pathogen vulnerabilities could be explored, however, few clinical trials have examined these vulnerabilities. Additionally, few studies have investigated the impact of drugs on the transmission of parasites from human blood to the mosquito vector, nor have many been designed to evaluate anti-hepatic stage activity.[24]

One of the first potential pathogen vulnerabilities that could be targeted by small molecules is a bottleneck population at the liver stage[24]. Within minutes of being released by the bite of an infected female *Anopheles* mosquito, *Plasmodium falciparum* sporozoites reach the mammalian liver, where they invade hepatocytes and either lie dormant or develop over several days, eventually forming the schizonts that are the prelude to a blood-stage infection[24–27]. Developing molecules that efficiently target the parasitic stages in the liver would offer protection from infection and could theoretically eliminate the cryptic hypnozoite (dormant parasite) infection reservoirs formed by *P. vivax* and *P. ovale*[26,27]. Considering that only one hundred or so sporozoites may be introduced during a blood meal by a mosquito, there are likely to be fewer parasites at this stage than in the active blood-stage infection this reduces the possibility of resistance arising[24].

A second bottleneck occurs during sexual development[28]. At each round of schizogony, about 1% of merozoites differentiate into gametocytes, and it is these developmentally arrested cells that are transmitted to the mosquito. Mature gametocytes are sexually dimorphic thus forming micro- and macrogametocytes that escape the red blood cells and produce male and female gametes in the blood meal of the mosquito by processes known as exflagellation and activation, respectively[24,28]. Following fertilization, the zygote differentiates into motile and invasive ookinete within which the briefly diploid genome undergoes meiosis. These processes occur within an environment almost entirely derived from host blood, which can provide a novel and ideal conduit for the delivery of drugs to inhibit parasite transmission to the mosquito[24,28]. Having crossed the midgut wall the very few surviving ookinetes differentiate into oocysts that undergo endomitosis,

eventually producing thousands of daughter sporozoites. The sporozoites migrate from the midgut of the mosquito to its salivary glands where the lifecycle begins again[24,28].

Given that it would be highly desirable for candidate drugs to have activity against hepatic and sexual forms of the malaria parasite, it is surprising that few clinical trials have examined whether gametocyte carriage can be reduced following drug treatment[29]. Additionally, few studies have investigated the impact of drugs on the transmission of parasites from human blood to the mosquito vector, nor have many been designed to evaluate anti-hepatic stage activity[24]. In the context of malaria eradication, these gaps in our understanding of the full potential of the drug armory are problematic.[24]

1.3 Rationale for the search of new drugs

Malaria is a disease that still affects several people all over the world, leading to many deaths. The parasite causing the disease has gained resistance against several antimalarial drugs, and thus there is a great need for the development of drugs that are not only effective against the malaria parasite but can also completely eradicate it. Measures need to be put in place for the development of antimalarial compounds that could in theory target various phases of the parasite's development. The basis of this project is the synthesis of compounds that could theoretically inhibit several stages in the development of malaria parasite and thus completely eradicate the growth of the parasite.

Thiosemicarbazides are known iron chelators of extracellular protozoan by binding through the sulfur and azomethine nitrogen groups, it has been thought that one of the ways thiosemicarbazides inhibit cell growth is by the inhibition of cellular iron uptake. While α-phenols have demonstrated inhibitory factors of malaria parasite by possible inhibition of hemozoin formation, phenol- thiosemicarbazone derivatives are a group of the compounds investigated for possible inhibition of cell growth for this very reason. Quinoline scaffold is found in several pharmaceutically active compounds, these compounds are thought to interfere with hemoglobin digestion in the blood stages of malaria, interfering with this process in such a way that the parasite is effectively killed with its waste. Quinoline- thiosemicarbazone scaffolds are the second group of compounds under investigation for the effects these compounds may have as possible antimalarial agents.

1.4 Thiosemicarbazones: General overview and chemistry

This chapter focuses on the synthesis and characterization of various thiosemicarbazone derivatives. These compounds were synthesized using conventional synthetic methods, shown in various schemes below, and were fully characterized using common analytical techniques such as nuclear magnetic resonance (NMR), mass spectrometry (MS), infrared spectroscopy (IR), elemental analysis and melting point determination.

Recently hydrazine- hydrazide derivatives have gained great importance due to their diverse biological properties including antibacterial, anti-fungal, anti-inflammatory, anti-malarial and anti-tuberculosis activities. Hydrazone- hydrazide derivatives are molecules that contain highly reactive azomethine groups and are thus useful in new drug development. They are derived from aldehydes and ketones by reaction with different hydrazine derivatives to give the following grouping: R_1R_2C=N-NHR. Hydrazones can react with electrophilic and nucleophilic reagents and are thus widely used in organic synthesis especially for the preparation of heterocyclic compounds.[30]

These compounds have a C=N bond, which is conjugated with a lone pair of electrons of the functional nitrogen atom. The nitrogen atoms of the hydrazones are nucleophilic and the carbon atom has both electrophilic and nucleophilic nature. The α-hydrogen of hydrazones is more potent than that of acidic ketones. The combination of hydrazones with other functional groups lead to compounds with unique physical and chemical character. Owing to their biological and pharmacological properties, they are considered important for the synthesis of heterocyclic compounds.[31]

1.5 Medicinal applications of thiosemicarbazones

1.5.1 Anti-tubercular Activity

Tuberculosis is a disease caused by the pathogenic bacterium *Mycobacterium tuberculosis* (*Mtb*)[32]. This bacterium infects about one third of the world population, however, a healthy immune system can suppress the growth and multiplication of *Mtb* maintaining the bacteria in an inactive state. When the immune system is compromised or weakened, as is the case during treatment of rheumatoid arthritis, HIV infection, diabetes, old age and malnutrition, *Mtb* reactivates and latent tuberculosis is converted to active pulmonary tuberculosis[33]. This disease has been managed using a first line regiment consisting of rifampicin, isoniazid, pyrazinamide and ethambutol, which must

be taken daily over a period of six months[33]. This treatment process is complicated and the emergence of multi-drug resistant and extensively drug resistant forms of *Mtb* strains has only worsened the situation. Therefore, there is a great need for research of new chemical agents with the potential to inhibit *Mtb* infection. Thioacetozone, a thiosemicarbazone-containing compound has been found to be a potent anti-tubercular drug. With research from Trotsko *et al.* having shown thioacetozone to have displayed minimum inhibitory concentrations against clinical isolates of *Mtb*, including multidrug resistant ones. The prodrug thioacetozone requires activation of its thiocarbonyl moiety by the Flavin-dependent monooxygenase EthA for bactericidal activity[32]. Following this activation, thioacetozone inhibits the dehydration of β-hydroxyacyl-acyl carrier protein (β-hydroxyacyl-ACP) step of the type II fatty acid synthase (FAS-II) elongation cycle and abolition of mycolic and biosynthesis, thus resulting in bacterial death of *M. tuberculosis*[32]. This inhibition of mycolic acid synthesis is also the target of the first-line anti-tubercular drugs such as isoniazid. However, the toxicity issues of thioacetozone especially in situations of HIV infection, have halted further clinical development of this drug. Flouroquinolones are a subclass of quinolones which have been recommended as second line therapy for TB and have also been reported for their antimalarial activity potential[33]. Research performed by Beteck *et al.* found that compounds incorporating both thiosemicarbazones and quinolone frameworks might be worth exploiting as potential compounds to target both malaria and TB infections as the series of compounds synthesized exhibited good activities against *P. falciparum* and *M. tuberculosis*[33].

1.5.2 Antifungal Activity

As shown through the development of research in the field of mycology there has been an increase in the frequency of opportunistic fungal infections, particularly those caused by *Candida sp.* and *Crptococcus sp*. The increased incidence of these yeast caused fungal infections has presented a challenge for clinicians of different specialties because of difficulty in the diagnosis and treatment of these infections[34]. In addition, the infection of the bloodstream caused by *Candida* species is associated with substantial morbidity and mortality, with the average mortality rate for candidaemia being 43% which is substantially higher than for any other blood flow infection[34]. Cryptococcosis is the most prevalent fatal fungal disease in the world with one million cases and about 6000000 deaths per year and is largely related with HIV infection. Additionally, there is also an increase in invasive infection caused by species of antifungal resistant *Candida*, with *Candida albicans* showing a 0-5% fluconazole resistance rate with higher values in South Africa[34].

Despite the availability of several classes of antifungal agents currently available in therapy, such as azoles and particularly triazoles, polyeres and echinocandins, the discovery of new active drugs against *Candida* species has been of great importance since those available have a related toxicity such as hepatotoxicity of azoles, cardiopathy of echinocandins and nephrotoxicity of amphotericin B[34]. At the same time cases of resistance to these three classes of drugs have been demonstrated by several studies in the USA. In view of the need for new antifungal drugs thiosemicarbazones have received prominence in the medicinal chemistry field for their chemical versatility and promising biological applications. In addition, the chemotherapeutic activity of nitro-heterocycles has been associated with compounds having the nitro group attached to C-5 of the five membered heterocycles. Compounds with the 5-nitrothiophene moiety in various heterocyclic systems have demonstrated improved biological activity as potent antifungal agents[34]. This knowledge taken into account was the reasoning behind the research performed by the research group of de Araujo Neto *et al.* where twelve N-substituted 2-(5-nitro-thiophene)-thiosemicarbazone derivatives were synthesized and characterized. These compounds were found to exhibit promising antifungal activity especially against *Candida neoformins*[34]. Thiosemicarbazones and semicarbazones are known to be a class of compounds with widespread biological activities including activity as antiviral, antitumor, antiparasitic and antifungal agents. These compounds are capable of complexing with metal ions and their biological activity is modulated by the nature of the metal[35]. The research team of de Oliveira Paiva *et al.* found that thiosemicarbazones had the greatest activity against *Aspergillus spp* and showed a chelating effect and decreased the ergesterol in lipidic content[35]. Research performed by Dinh Thanh *et al.* indicated that thiosemicarbazone derivatives with a sydnone ring and D-glucose moiety showed activity against bacterial and fungal strains with the group of compounds containing a halogen group showing the highest activity against all the tested strains of bacterial and fungal organisms[36].

1.5.3 Antiviral Activity

The antiviral activities of thiosemicarbazones have been explored since the 1960s, with 1-N-methyl-β-thiosemicarbazone, which was used to treat smallpox[37]. However, since then they have been neglected for a great deal of time with the principal concern for researchers being the enhancement of these compounds as antitumor and antiprotozoal agents. Only in recent years has there been a rediscovery of the antiviral activity of thiosemicarbazones[37]. In the year 2000 the research group of Hoston and Verela reported antiviral activities of three 3-deoxy-D-erythro-

hexos-2-ulose bis(thiosemicarbazone) complexes of copper(II), platinum(II), and palladium(II) ions against poliovirus type 1[37]. Genova *et al.* discovered the antiviral properties of benzyle bis(thiosemicarbazone) and 3,5-diacyl-1,2,4-triazole bis(4-methylthiosemicarbazone) palladium(II) complexes against herpes simplex virus strain 1 and 2, on acyclovir resistant cells[37]. For the first time menthone thiosemicarbazones were evaluated by Mishra *et al.* against the human immunodeficiency (HIV) types 1 and 2, the reported results from the compound revealed a promising antiviral activity. The research group of Bal *et al.* in 2005 reported a marked anti-HIV-1 activity for a series of isatin β-thiosemicarbazone derivatives designed on the basis of a 3D-pharmacophoric mapping of the existing non-nucleoside reverse transcriptase inhibitors (NNRTIs) with the thiosemicarbazone moeity[37].

Over the years considerable progress has been made in the identification of HIV-1 treatments with limited side effects and low capacity of inducing the emergence of drug resistant variants. However, there has not been a considerable amount of effort made towards the study of the effects of HIV therapeutic strategy in the presence of related infections. The use of drugs that interfere with related infectious agents during an HIV infection can dramatically alter the progression of the disease, including the development of the diseases provoked by these agents[37]. It is for this reason why the investigation of new anti-HIV drugs should also include the study of their activity against co-infecting microbes. The research group of Pelosi *et al.* reported the evaluation of anti-HIV activity of thiosemicarbazone derivatives which had also been tested against human T-cell leukemia viruses (HTLV)[37]. This study was one of the first the discovery of new potential anti-HIV drugs took into account the screening of the compounds against other retroviruses which frequently co-infect HIV-1 positive patients and interfere with AIDs progression. The results obtained from this study warranted further research and development aimed towards the investigation of the mechanism and the candidate factors by which these anti-retrovirals act[37].

In a publication reported by Pham *et al.* the synthesis and biological activities of thiosemicarbazones containing an adamantine skeleton were investigated[38]. Amantadine was one of the first adamantine derivatives and was found to have antiviral activities resulting in the synthesis and biological activities of adamantine derivatives being pursued by a number of researchers. In the investigation by the research team of Pham *et al.* the researchers combined two moieties, namely a thiosemicarbazone constituent and an adamantine skeleton, which could

potentially help to confer new molecules with promising biological activities[38]. Results from this investigation yielded thiosemicarbazones with good inhibition against *Candida albicans* fungus. Among synthesized thiosemicarbazones, those containing hydroxyl groups on the phenyl ring showed good inhibitory activity against tested cancer cell lines which were Hep3B, A549 and MCF-7[38].

1.5.4 Antitumor Activity

One of the most clinically investigated thiosemicarbazones is *N*-methylsatin thiosemicarbazone, which was commercialized in the 1960s[39]. These compounds were originally developed as an agent used against smallpox but were rendered obsolete with the introduction of smallpox vaccines. Clinical anticancer research focused mainly on α-*N*-heterocyclic thiosemicarbazones, as these compounds are potent chelators of metal ions, especially iron, and were originally developed with the aim of targeting the enhanced demand cancer cells have for iron[39]. Since as early as 1956 the first derivative of this class of thiosemicarbazones were reported to show activity against leukemia in mice. After extensive structure activity studies 5-hydroxyl-2-formylpyridine thiosemicarbazones, which was one of the most promising compounds of that particular study, was tested in clinical phase 1 trials and was shown to possess anticancer activity in leukemia patients. However, the results of these tests yielded negative and severe side effects, mainly gastrointestinal toxicity, and fast inactivation by glucordination, leading to the withdrawal of the compound[39]. Further optimization of these compounds led to the development of 3-aminopyridine-2-carboxaldehyde thiosemicarbazone, most commonly known as Triapine, a compound that has meanwhile been tested in more than 30 clinical phase I and II trials[39]. Triapine showed promising activity against hematological diseases, whereas solid cancers proved unresponsive. The probable reasoning behind the inefficiency of Triapine monotherapy against solid tumors include inappropriate drug delivery due to very short plasma half-life, fast metabolism or excretion and/or rapid development of drug resistance[39]. Despite these drawbacks thiosemicarbazones have remained the focus of interest, this interest resulting in several recent phase 1 studies being performed for testing the safety of Triapine in combination therapy. In addition two new α-*N*-heterocyclic thiosemicarbazones are undergoing clinical evaluation[39].

In 2015 a thiosemicarbazone derivative known as COTI-2 entered a clinical phase 1 trial for the treatment of advanced or recurrent gynecologic malignancies. According to the information provided by the compony Critical Outcome Technologies, Inc., COTI-2 displayed strong

anticancer activity in the nanomolar range especially in p53-mutant cell lines, as this thiosemicarbazone restores the wildtype function of the p53 protein[39]. The second most commonly tested thiosemicarbazone is di-2-pyridylketone 4-cyclohexy-4methyl-3-thiosemicarbazone which has been under clinical phase 1 evaluation since January of 2016 to assess its pharmaceutical characteristics and the maximum tolerated dose in patients with a range of advanced and resistant tumors. In contrast to a number of other drugs such as desferrioxamine (DFO) which is used for the treatment of iron overload and selectively chelate iron(III)[39]. Whereas, α-*N*-heterocyclic thiosemicarbazones usually form stable complexes with iron(II) and iron(III) and are therefore able to redox cycle between these two oxidation states under physiological conditions[39].

1.5.5 Antiparasitic Activity

Tropical diseases, such as Human African Trypanosomiasis (HAT), Chagas disease and visceral and cutaneous leishmaniasis, are caused by infectious agents called *Trypanosomatids* of the genera *Trypanosoma* and *Leishmanias*[40]. The treatment of these parasitic infections relies on pentamidine (PEN), suramine and melarsoprol as first choice drugs for the treatment of HAT, whereas benznidazole (BZD) and nifartimox are routinely used for the treatment of Chagas disease. The current therapy of leishmaniasis is based on antimalarial organic complexes and amphoterian B (AmB) with miltefosine having been approved in 2002 as the first oral antileishmanial agent[40]. All these drugs, however, suffer from high toxicity and development of resistance against them. Thus, the discovery and development of new chemotherapeutic agents against these parasitic diseases is vital. The thiosemicarbazone scaffold was already known in the field of antiparasitic agents[40]. Thiosemicarbazones were originally designed as parasitic cysteine protease inhibitors, inhibiting cruzain in *Trypanosoma cruzi* and rodhesain in *Trypanosoma brucei*, which are two enzymes that play a vital role at every stage of the parasites lifecycle. The formation of strong metal chelating thiosemicarbazones or their metal complexes suggest that the mechanism of action is mainly due to a dual pathway involving production of toxin free radicals by thiosemicarbazone bioreduction or metal complex-DNA interaction[40].

Malaria is currently the third leading cause of deaths from a single infective agent and has reportedly led to deaths of 445000 people in 2016 alone[41]. Sub-saharan Africa has been the most affected by this parasitic disease wherein 88% of the reported malarial cases 90% of the reported cases resulted in the deaths of the patients. The death toll caused by malaria has declined in the

past several years, however, despite this decline malaria is still a great global health challenge with at least 40% of the world's population living in places endemic to this disease[41]. Thiosemicarbazone containing compounds have been reported to exhibit antimalarial activity as well as Flouroquinolones. After taking various literature reports into consideration the research team of Beteck *et al.* reasoned that design and development of novel compounds incorporating both thiosemicarbazones and quinolone frameworks may be worth exploring as potential compounds to target both malaria and TB infections. The compounds reported in their study exhibited good activities against *Plasmodium falciparum* and *M. tuberculosis*, suggesting that quinolone thiosemicarbazones are a compound class worth further exploitation in search of cheaper molecules with dual activities against disease causing microorganisms[41].

1.6 **Thiosemicarbazones: Possible mode of action**

1.6.1 Iron Chelation

To cause infection, nearly all protozoa obtain growth essential iron from their hosts. Iron is required for the development of the parasite since many enzymes of the plasmodial metabolic pathways depend on the presence of this element[42]. Deprivation of utilizable iron by chelation is a proficient approach to arrest parasite growth and associated infection. A strong iron chelator, deferoxamine (DFO), seen in **Figure 1.5** below, reportedly diminishes the activity of Fe(III)-containing enzymes in parasitic protozoa[42]. Therefore, iron chelators have recently gained importance as potent antimalarial compounds. It is proposed that iron chelator antimalarials mainly arrest iron-dependent ribonucleotide reductase-mediated production of nucleotides, although the precise mechanistic details of antiparasitic action are still unclear[42]. The intraerythrocytic stages during malaria are mainly responsible for clinical symptoms related to malaria. During that stage, the malaria parasite digest enormous amounts of hemoglobin inside the food vacuole and thereby releasing high quantities of toxin-free heme. Free heme can change membrane permeability by intercalating into the cell membrane and also may induce oxidative stress, which may lead to parasite death[42]. However, by converting heme into less-toxic hemozoin, parasites cleverly evade the toxicity of free heme. Heme contains an iron atom at the center of its tetrapyrrole ring; therefore, an iron-chelating molecule may be able to interact with free heme through its iron. Furthermore, it is worth noting that this sort of heme-intercalating molecule may inhibit hemozoin formation to induce parasite death[42]. Therefore, a small molecule, which can both chelate free iron

and prevent hemozoin formation through heme-binding would be a novel, dual-target antimalarial agent. Sarkar et al., reported the designing synthesis and antimalarial activities of conjugated hydrazones[42]. These molecules chelated free iron, interacted with free heme, inhibited hemozoin formation, and prevented *P. falciparum* growth in vitro. The lead compound of this research also showed antimalarial activity in vivo against the MDR strain of *P. yoelii* in Swiss albino mice.[42]

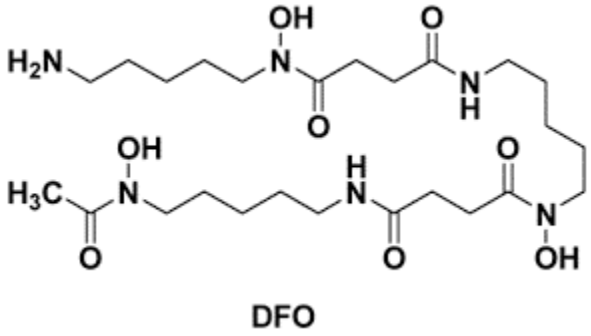

Figure 1.5 : Structure of Deferoxamine[1]

Deferoxamine is the standard iron-chelating agent in clinical use, with the developmental stage of action for this drug identified as trophozoite or schizont and the major putative target was assumed to be iron-dependent enzyme ribonucleotide reductase[43]. DFOs inhibitory effect on enzyme activity is probably due to scavenging iron from the iron pool with which the enzyme is in dynamic equilibrium[43]. The possibility of DFO acting on parasites by destabilizing the iron-containing hemozoin, thus leading to release of toxic heme-derived material was also raised[43]. This drug, however, is considered of little use in most areas affected by malaria because it is expensive, has to be given intravenously and penetrates infected red blood cells slowly[44]. The major drawback of DFO is its relatively slow speed of action in biological systems, due to limited membrane permeation across biological membranes[43].

The antimalarial activity of DFO prompted several authors and investigators to study antimalarial activity of three aroylhydrazone iron chelators, namely, pyridoxal isonicotinoyl hydrazone, 2-hydroxy-1-naphthaldehyde *m*-flourobenzoyl hydrazone and salicylaldehyde isonicotinoyl hydrazone[2]. These studies showed promising results, and chelators of this class are orally effective and very economical to synthesize thus overcoming some of the disadvantages of DFO. The studies have been further expanded to include some newly synthesized aroylhydrazones and thiosemicarbazones[2]. The compounds in the investigations were members of a new class of iron

chelators that are Schiff bases formed between acid hydrazides of thiosemicarbazides and an aldehyde or ketone. Results from a particular investigation performed performed by *Walcourt et al.* demonstrated that several aroylhydrazone chelators, in particular 2-hydroxy-1-naphthylaldehyde isonicotinoyl hydrazone and 2-hydroxy-1-naphthylaldehyde-4-phenyl-3-thiosemicarbazone, which can be seen in **Figure 1.6** and **Figure 1.7** respectively, were shown to have greater activity than DFO as anti-malarial agents against chloroquine-resistant and sensitive parasites[2]. Given the increased resistance of malaria to standard chemotherapeutic regimens in many regions of the world, these studies suggest that this class of agents deserves further in-depth investigation as potential antimalarials[2].

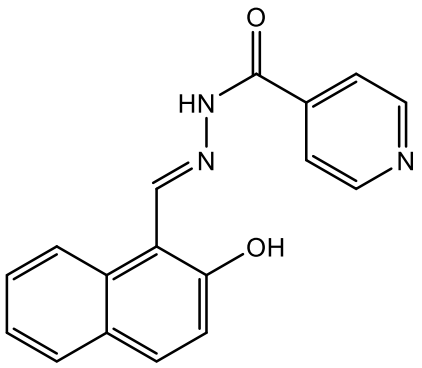

Figure 1.6: Structure of 2-hydroxy-1-naphthylaldehyde isonicotinoyl hydrazine[2]

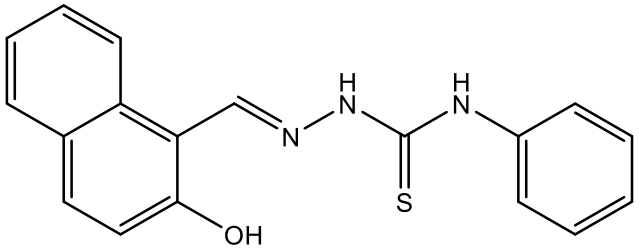

Figure 1.7: Structure of 2-hydroxy-1-naphthylaldehyde-4-phenyl-3-thiosemicarbazone[2]

Thiosemicarbazones are analogs of semicarbazones with a sulfur atom in place of the oxygen atom. They are readily prepared by the condensation reaction between a ketone or an aldehyde and a thiosemicarbazide. These compounds are versatile chelators towards an extensive range of metal ions, such as divalent metal ions (Zn^{2+}, Cu^{2+}) and trivalent metal ions (CO^{3+}, Fe^{3+}, Re^{3+}, Ga^{3+}, In^{3+}) with sulfur and azomethine nitrogen atoms. Biologically, these atoms have a broad spectrum of therapeutic properties with antibacterial, antimalarial, antiviral, and antitumor activities, by potentially binding to cellular copper, iron, or zinc ions.[45]

There have been numerous recent studies using iron-chelating agents as a possible treatment for malaria. Thiosemicarbazones are known iron-chelating agents by bonding through the Sulphur and azomethine nitrogen atoms. Their activity against extracellular protozoan such as *P. falciparum*, *Trichomonas vaginalis*, *Trypanosoma cruzi*, and other parasites have been demonstrated by several researchers.[46]

Iron is an essential element that is necessary for several cellular processes, such as cellular proliferation. Although iron chelators, such as desferrioxamine, have been clinically utilized for the treatment of iron overload disease, novel thiosemicarbazones chelators have been widely investigated as potential anti-cancer agents. Although the molecular mechanisms involved in the activity of thiosemicarbazones have not been completely elucidated, several modes of action have been reported. These include 1) the inhibition of cellular iron uptake from the iron transport protein transferrin; 2) the mobilization of iron from cells; 3) the inhibition of the ribonucleotide reductase activity; 4) the upregulation of the metastasis suppressor protein; 5) the formation of redox-active metal complexes that produce reactive oxygen species.[47]

1.6.2 Inhibition of cysteine proteases

The increasing resistance of malaria parasites to various drugs has greatly limited the treatment and control of this disease[48]. Therefore new antimalarial agents, ideally those directed towards new targets, are an urgent priority. One of the potential targets for drugs directed against *P.falciparum* are proteases that hydrolyze hemoglobin to provide amino acids for parasite protein synthesis. Multiple proteases appear to participate in this process, among them being the cysteine proteases falcipain-2 and falcipain-3[48]. Cysteine protease inhibitors block parasite hemoglobin hydrolysis and development, indicating that cysteine protease plays a key role in hemoglobin degradation, a necessary function of erythrocytic trophozoites[49]. Cysteine protease inhibitors also block the rupture of erythrocytes by mature parasites, suggesting an additional role for cysteine proteases in the hydrolysis of erythrocyte cytoskeletal proteins[49]. *Plasmodium falciparum* is known to express three papain-family cysteine proteases, known as falcipains. These three proteases are expressed by trophozoites and hydrolyze hemoglobin at acidic pH, signifying roles in this process[49].

Hemoglobin degradation in the *P. falciparum* parasites food vacuole is an essential function for parasite survival, and the *P. falciparum* depends on hemoglobin degradation by the partially

redundant proteolytic activities of the falcipains and plasmepsins. Three members of the falcipain family of cysteine proteases are known to be involved in hemoglobin catabolism. Significant effort has been directed towards developing inhibitors of these proteases to discover new antimalarials. These studies have resulted in potent falcipain inhibitors with promising antimalarial activity both in vitro and vivo. The thiosemicarbazones have been reported to have antimalarial activity, though they may act through alternative methods[50]. A study on a series of thiosemicarbazones which had recently been shown to inhibit a *Trypanosoma cruzi*-derived cysteine protease, cruzain, generated basic structure activity relationships (SAR) against cruzain around three positions. The authors of this study found that halides such as bromine and chlorine were tolerated at the 3′- and/or 5′-position on the aryl ring of the aryl-thiosemicarbazone[3]. In addition they found that the sulfur and methine bonds were critical to the inhibition of cruzain[3]. The data supporting structure-activity relationships of thiosemicarbazones with cruzain found by the research group of *Greenbaum et al.* can be seen in the **figure 1.8** below.

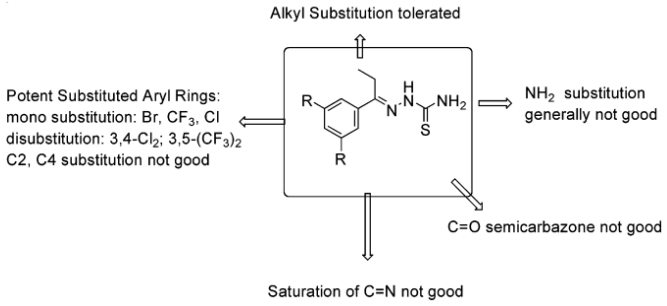

Figure 1.8: Summary of known thiosemicarbazone structure-activity relationships with cruzain[3]

1.7 Rationale: Synthesis of thiosemicarbazones

Thiosemicarbazides are known iron chelators of extracellular protozoan by binding through the sulfur and azomethine nitrogen groups, it has been thought that one of the ways thiosemicarbazides inhibit cell growth is by the inhibition of cellular iron uptake[51]. While α- phenols have demonstrated inhibitory factors of malaria parasite by possible inhibition of hemozoin formation, phenol- thiosemicarbazone derivatives are a group of the compounds investigated for possible inhibition of cell growth for this very reason. Quinoline scaffold is one found in a number of pharmaceutically active compounds, these compounds are thought to interfere with hemoglobin

digestion in the blood stages of malaria, interfering with this process in such a way that the parasite is effectively killed with its own waste. Quinoline- thiosemicarbazone scaffolds are the second group of compounds under investigation for the effectiveness these compounds may have in inhibiting malaria and as possible antimalarial agents.

1.8 Aims and Objectives

1.8.1 Aims

This study primarily aims to identify and characterize novel thiosemicarbazone based derivatives as potential anti-malarial agents.

1.8.2 Specific aims

- To synthesize and fully characterize thiosemicarbazone based derivatives as potential anti-malarial agents.

- To pharmacologically evaluate achieved compounds *in vitro* for their potential antiparasitic activity against a selection of *Plasmodium falciparum* strains.

CHAPTER 2

RESULTS AND DISCUSSION

2.1 Results and discussion

2.1.1 Retrosynthetic Analysis of quinolone-thiosemicarbazone

The retrosynthetic analysis of quinolone-thiosemicarbazone target compounds can be found in the **scheme 2.1** below. The synthesis of this group of target compounds was hypothesized to be achievable from various carbaldehyde derivatives which would in turn have been synthesized from acetanilides synthesized from commercially available anilines.

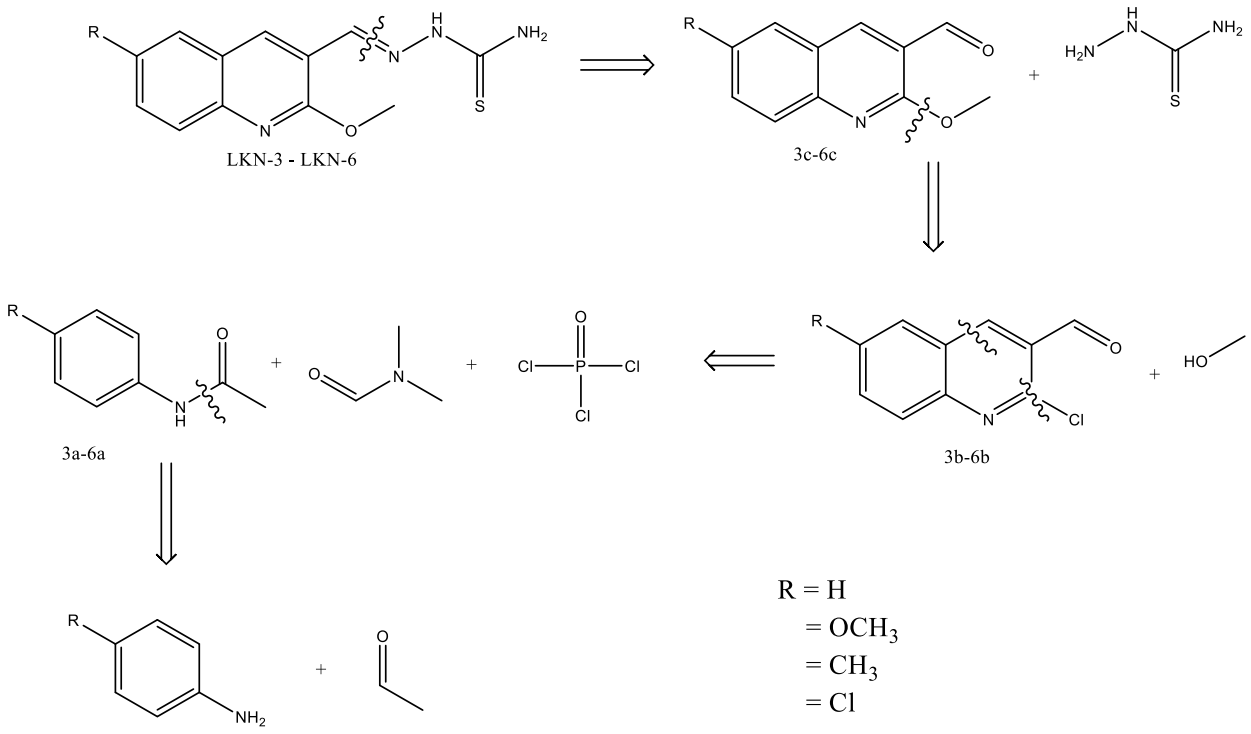

Scheme 2.1: Retrosynthetic analysis of quinoline-thiosemicarbazones

2.1.2 Synthesis of targeted quinolone-thiosemicarbazone derivatives

The overall synthetic route for the synthesis of quinolone – thiosemicarbazone derivatives can be found in the **scheme 2.2** below. This reaction scheme was used to synthesize final compounds **LKN-3**, **LKN-4**, **LKN-5**, and **LKN-6**.

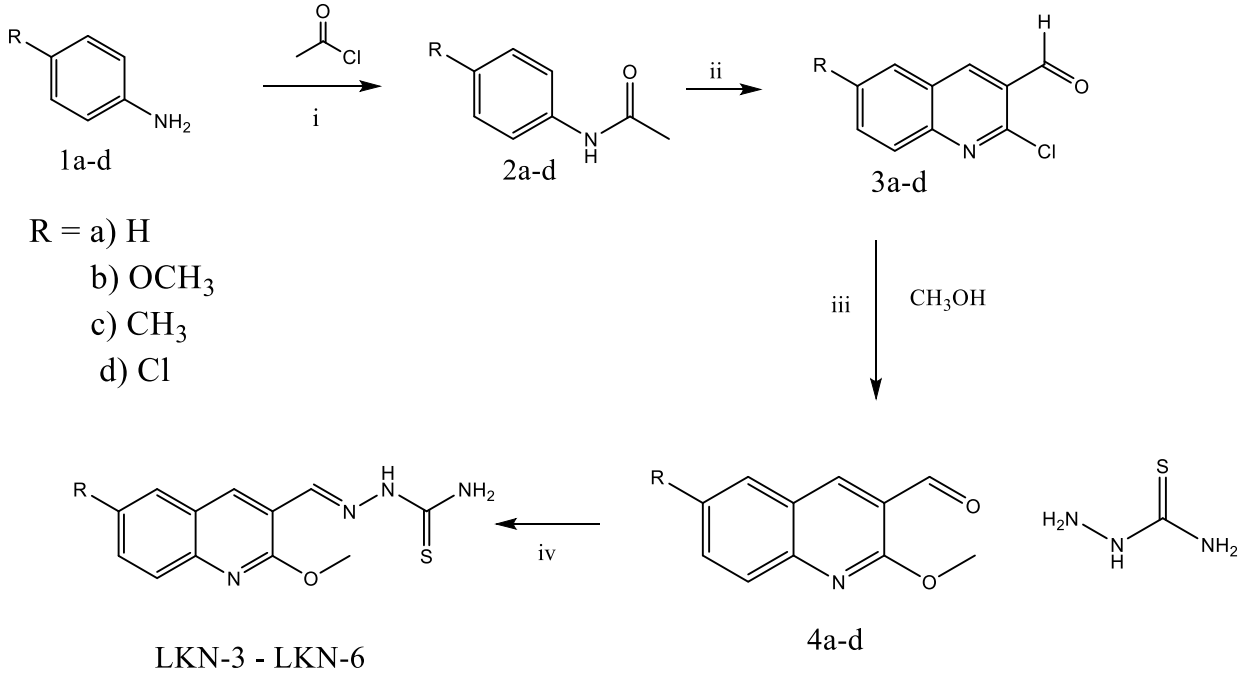

Scheme 2.2: Synthetic route for the synthesis of quinolone thiosemicarbazides. *Reagents and conditions*: (i) R-aniline (**1a-d**), TEA, DCM, acetyl chloride, r.t., 5 hrs; (ii) R-phenyl-acetamide (**2a-d**) $POCl_3$, DMF, 80 °C, 5 hrs; (iii) R-chloroquinoline-carbaldehyde (**3a-d**), KOH, MeOH, 70 °C, 2 hrs; (iv) R-methoxy-carbaldehyde (**4a-d**) thiosemicarbazide, MeOH, r.t., 1 h

The Vilsmeier Haack reaction mechanism, named after Anton Vilsmeier and Albert Haack, was used in the production of the final products depicted in **Scheme 2.2** above. The Vilsmeier Haack reaction mechanism is the chemical reaction of a substituted amide with phosphorus oxychloride and an electron-rich arene to produce an aryl aldehyde or ketone[52]. The Vilsmeier Haack Reagent is formed from DMF and phosphorus oxychloride. Depicted in the scheme below is an electrophilic aromatic substitution which leads to α-chloro amines, which are then rapidly hydrolyzed during work up to give the aldehydes.

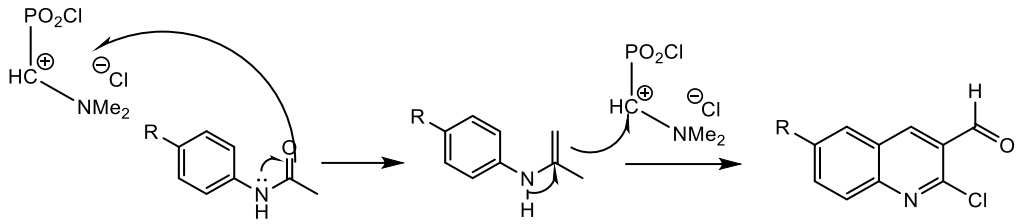

Scheme 2.3: Vilsmeier Haack Reaction Mechanism used to synthesize desired final products

2.1.2.1 Synthesis of acetanilides

Having rationalized the synthetic route to achieve target compounds **LKN-3** to **LKN-6**, seen in **Scheme 2.3** above, the first step in achieving desired compounds was to synthesize acetanilide derivatives. Commercially available anilines **1a-d** and acetyl chloride were used in the preparation of the desired acetanilide derivatives[53–55].

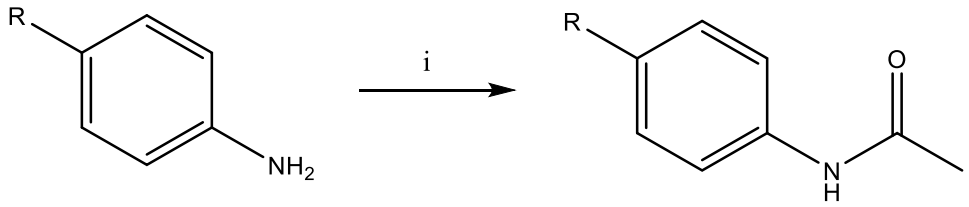

1a: R=H	2a: R= H	69.4%
1b: R= OCH_3	2b: R= OCH_3	87.3%
1c: R= Cl	2c: R= Cl	71%
1d: R=CH_3	2d: R= CH_3	74%

Scheme 2.4: *Reagents and conditions:* (i) Acetyl chloride, TEA, DCM, r.t., 5 hrs

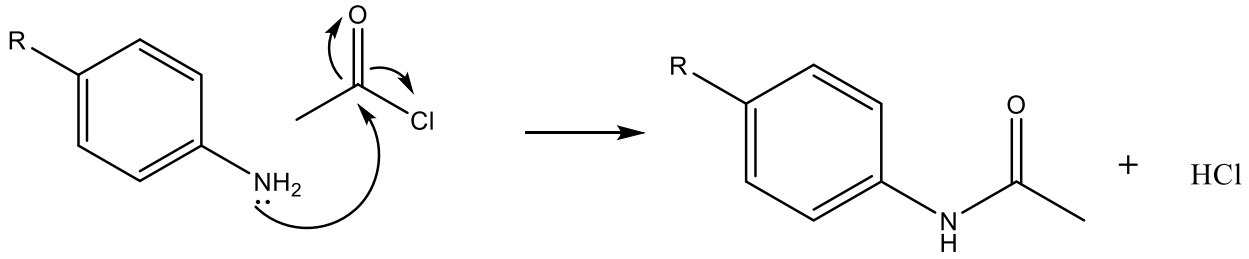

Scheme 2.5: Proposed mechanism of acetylation

The product was formed by nucleophilic substitution, the electron rich nucleophile which is NH_2 with a lone pair of electrons displaces the Cl atom bonded to the central carbon of the acetyl

chloride. How this works is due to the fact the Cl is more electrophilic than the carbon resulting in the carbon being more attracted to the electron-pair on the NH_2. The resultant compounds obtained ranged in yield from 69- 88%.

2.1.2.2 Synthesis of 2-Chloroquinoline-3-carbaldehydes

The second step in achieving the synthesis of the desired quinoline- thiosemicarbazone derivatives was to synthesize chloroquinoline- carbaldehyde derivatives. The synthesized acetanilides were used in a Vilsmeier- Haack methodology to synthesize the chloroquinoline- carbaldehyde derivatives as this method has been previously shown to yield quinolone scaffolds with chloro and formyl substituents.

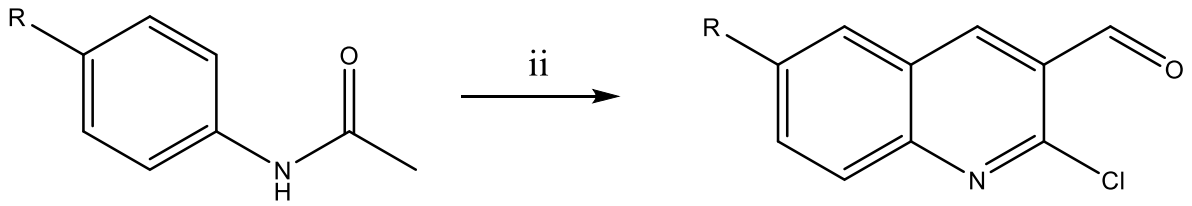

3a: R= H	18%
3b: R= OCH_3	11%
3c: R= Cl	83%
3d: R= CH_3	6.1%

Scheme 2.6: *Reagents and conditions*: (ii) $POCl_3$, DMF, 80 °C, 5 hrs

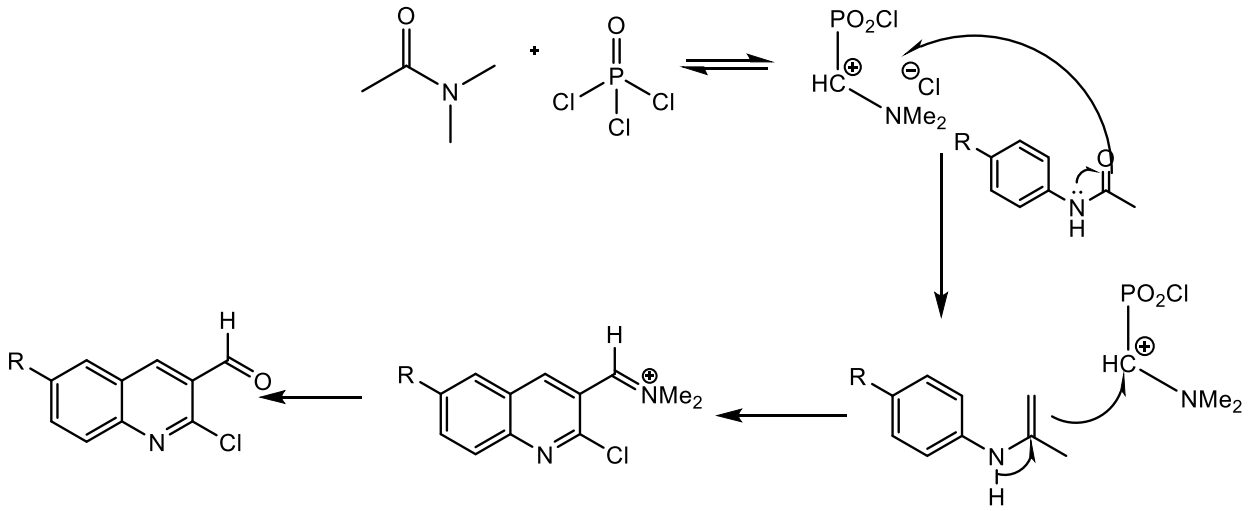

Scheme 2.7: a proposed mechanism for the synthesis of chloroquinoline-carbaldehydes

Dimethylformamide (DMF) acts as the nucleophile attacking the phosphoryl chloride ($POCl_3$), the resultant reagent reacts with the acetanilide resulting in a Vilsmeier-Haack reagent. On reaction with water this results in the desired product precipitating out. The resultant compounds obtained ranged in yield from 6- 83%.

2.1.2.3 Synthesis of Methoxyquinoline-3-carbaldehydes

After the successful synthesis of the chloroquinoline- carbaldehydes, the next step was the substitution of the chlorine group with a methoxy atom to synthesize methoxyquinoline-carbaldehydes.

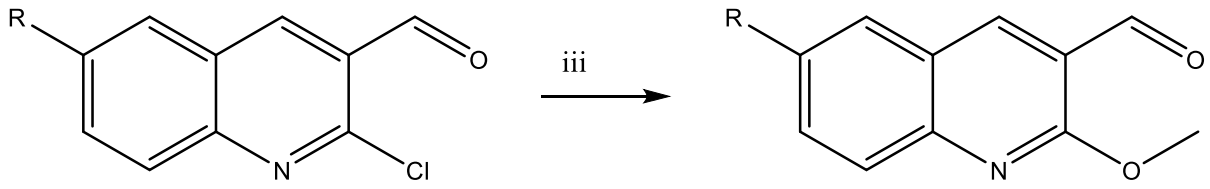

4a: R= H	51.2%
4b: R= OCH_3	64%
4c: R= Cl	26.1%
4d: R= CH_3	15%

Scheme 2.8: *Reagents and conditions*: (iii) KOH, CH_3OH, 70 °C, 2 hrs

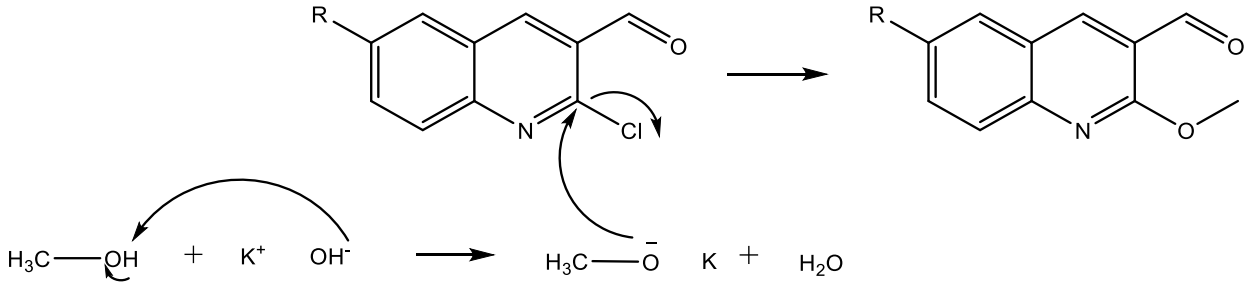

Scheme 2.9: a proposed mechanism for the synthesis of methoxyquinoline- carbaldehyde

Potassium hydroxide (KOH) was added to methanol to remove an acidic proton thus changing the methanol which is not a good nucleophile into a methoxide which is a good nucleophile capable of attacking the quinolone scaffold and resulting in a nucleophilic substitution substituting the good leaving group chloride with a methoxy group. The resultant compounds obtained ranged in yield from 15- 64%.

2.1.2.4 Synthesis of Quinoline-thiosemicarbazones

The final step was the substitution of the oxygen of the –CHO- group with the thiosemicarbazide resulting in the synthesis of the desired quinolone- thiosemicarbazone final products. This was achieved by reacting the 2-methoxyquinoline-3-carbaldehyde derivatives with thiosemicarbazide in a dehydrative nucleophilic substitution reaction using methanol as solvent and acetic acid as catalyst.

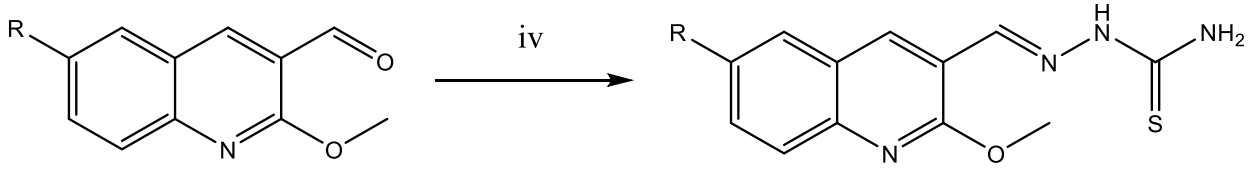

LKN-3: R= H	41%
LKN-4: R= OCH_3	20.3%
LKN-5: R= Cl	46%
LKN-6: R= CH_3	91%

Scheme 2.10: *Reagents and conditions*: (iv) thiosemicarbazide, MeOH, r.t., 1 hr.

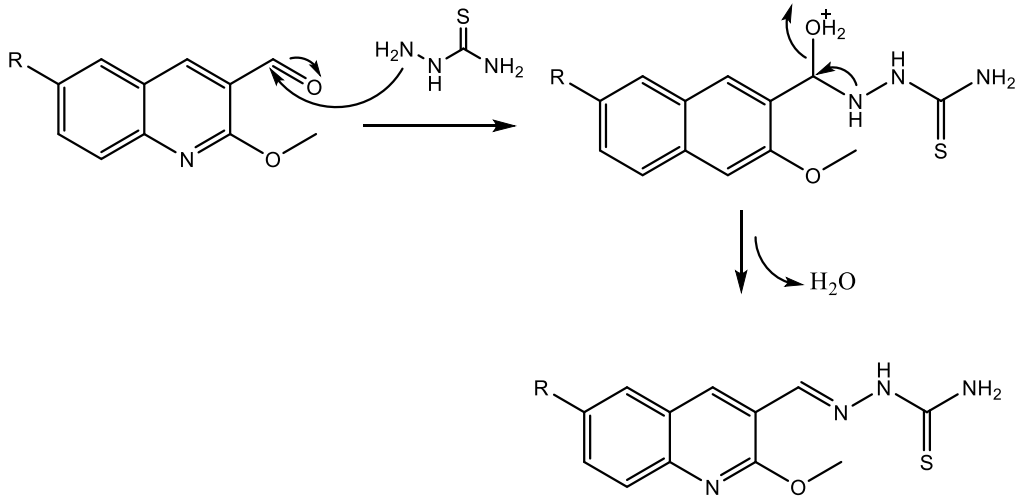

Scheme 2.11: a proposed mechanism for the synthesis of quinolone- thiosemicarbazones

The NH_2 moiety on the thiosemicarbazide acts as the nucleophile, and attacks the electrophilic carbonyl group, displacing the oxygen to give the desired quinolone-thiosemicarbazone final product. The resultant compounds obtained ranged in yield from 20- 91%.

2.1.3 Characterization of compounds

The compounds synthesized for this project were characterized using ^{1}H, ^{13}C NMR and infrared (IR) spectroscopic techniques.

2.1.3.1 Spectroscopic characterization of acetanilide's

The successful synthesis of acetanilides by the acetylation of anilines was confirmed by proton (^{1}H) and carbon-13 nuclear magnetic resonance spectroscopy technique. Literature reviews showed a correlation with synthesized acetanilides[56]. The spectrum for compound **1a** can be seen in **figure 2.1** below. For $^{1}HNMR$, the methyl moiety of $–COCH_3$- integrated to three protons resonates at 2.04 ppm, the –CONH- signal integrated to one proton appears downfield as a broad signal at ~ 9.95 ppm. For $^{13}CNMR$ spectrum, the characteristic signals for the methyl group can be seen at 24.06 ppm and the signal at 171.37 ppm can be attributed to the carbonyl carbon. This spectroscopic data confirmed the successful acetylation of the anilines.

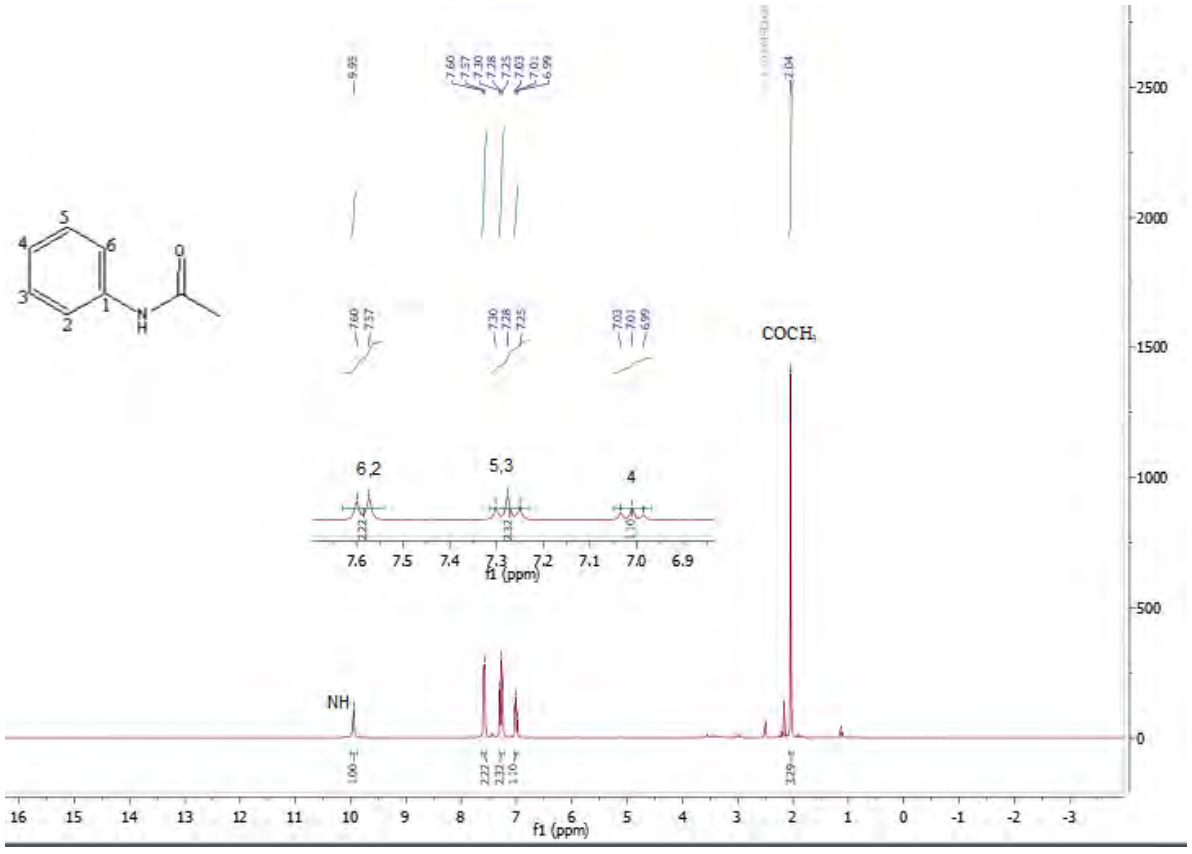

Figure 2.1: $^{1}HNMR$ spectrum of compound 1a

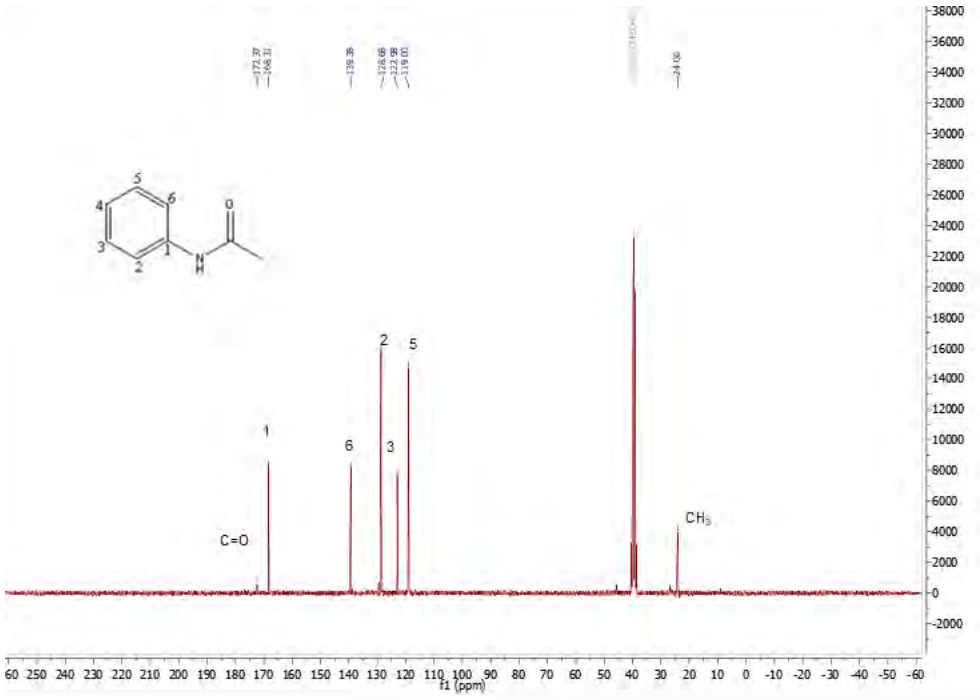

Figure 2.2: ^{13}CNMR spectrum of compound 1a

2.1.3.2 Spectroscopic characterization of chloroquinoline- carbaldehydes

The successful synthesis of chloroquinoline- carbaldehydes by a Vilsmeier- Haack reaction of acetanilides was confirmed by proton and Carbon-13 NMR spectroscopy technique. A literature review for chloroquinoline-carbaldehydes showed a correlation with the compounds synthesized[57]. The spectrum for compound **2a** is shown in **figure 2.3** below. The ^{1}H NMR spectrum for compound **2a** is shown in the **figure 2.3** below. For ^{1}HNMR the proton for the –CHO- group resonated at 10.37 ppm, aromatic protons resonated in the range of 8.98, - 7.75 ppm. As can be observed in the ^{1}HNMR spectrum below there is an increased number of protons compared to that of acetanilides, this increase in protons is a clear indication of the formation of a new aromatic ring. For the ^{13}CNMR spectrum, the signal at 189.84 ppm is assignable to the formyl carbon, this is a diagnostic signal conforming successful transformation.

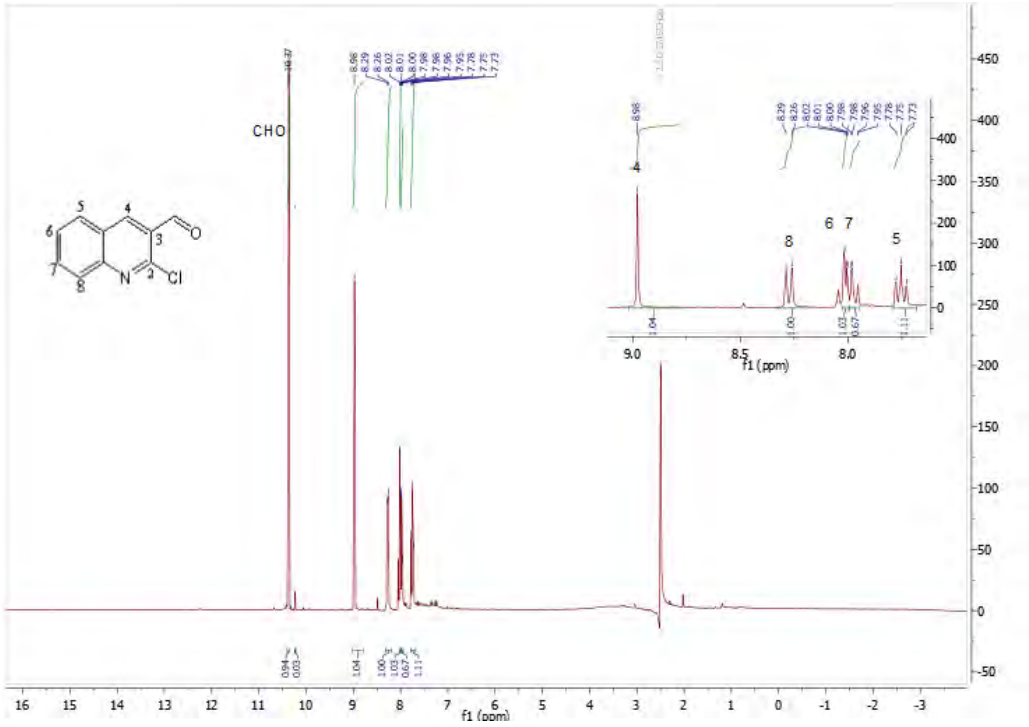

Figure 2.3: ^{1}HNMR spectrum of compound 2a

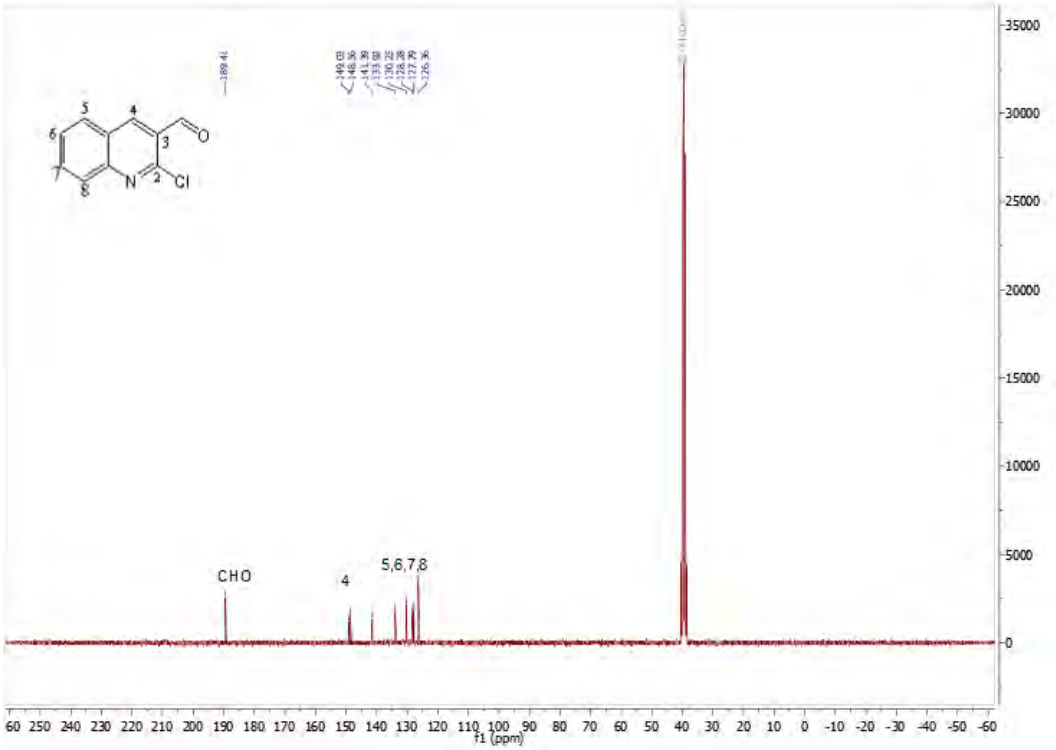

Figure 2.4: ^{13}CNMR spectrum of compound 2a

2.1.3.3 Spectroscopic characterization of methoxyquinoline-carbaldehydes

Proton and Carbon-13 NMR spectroscopic techniques were used to confirm the successful synthesis of 2- methoxyquinoline-3.carbaldehydes by the nucleophilic substitution of 2-chloroquinoline-3-carbaldehyde. For ^{1}HNMR, the singlet signal at 3.87 ppm, which integrated to three protons is assignable to methyl protons of –OCH_3- moiety while downfield the proton for the –CHO- group integrated at 10.46 ppm. For ^{13}CNMR the characteristic signals for –OCH_3- and –OCH- showed up on the spectrum at 55.92 and 189.55, respectively. The results from these spectra further confirm the successful synthesis of methoxyquinoline-carbaldehydes.

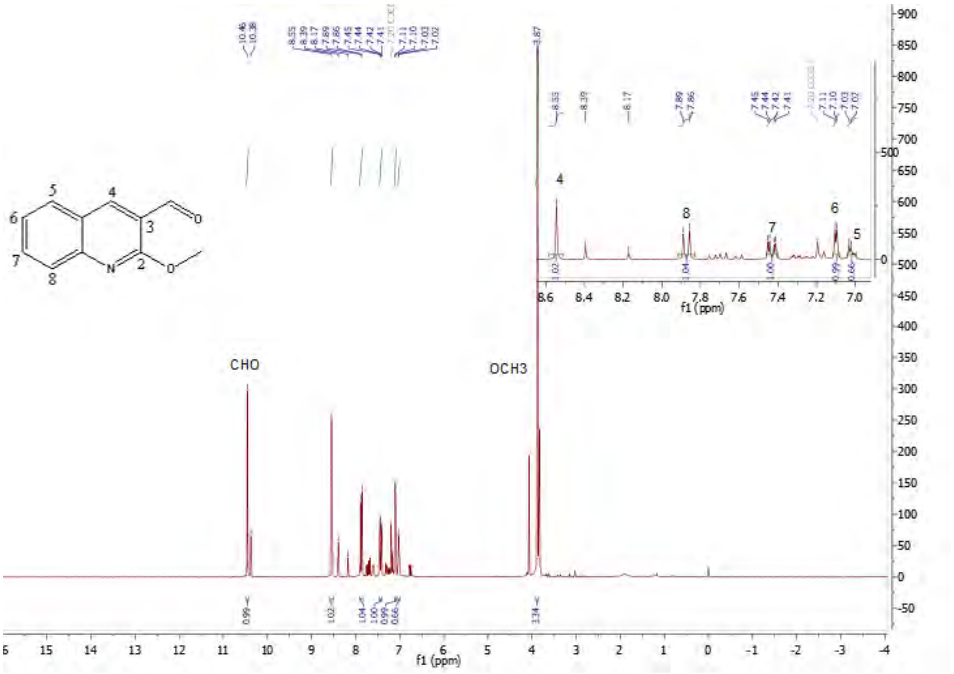

Figure 2.5: ^{1}HNMR spectrum of compound 3a

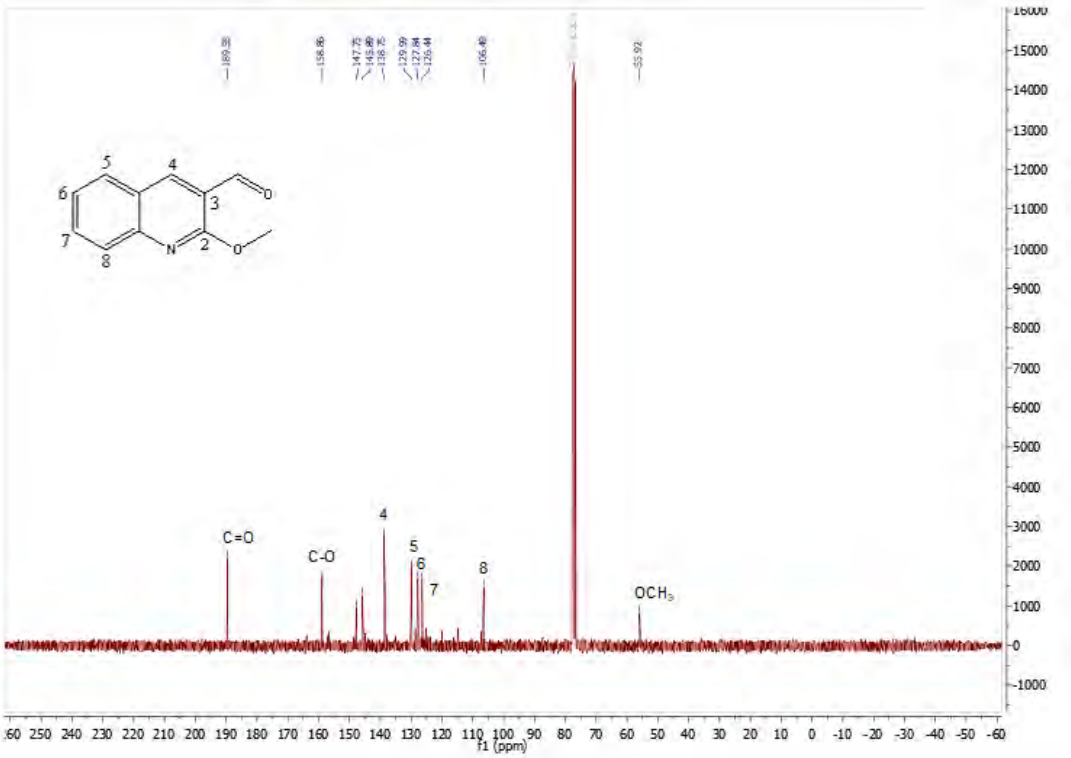

Figure 2.6: ^{13}CNMR spectrum of compound 3a

2.1.3.4 Spectroscopic characterization of quinolone-thiosemicarbazone derivatives

The successful synthesis of the desired quinolone- thiosemicarbazone final products was confirmed by proton and Carbon-13 nuclear magnetic resonance, infrared and liquid chromatography-mass spectroscopy techniques. The literature reviews showed a correlation with the synthesized quinolone- thiosemicarbazones[58,59]. In **figure 2.7** below the ^{1}HNMR spectrum for compound **LKN-3** can be seen, for this compound, the methyl protons of –OCH_3- group integrated for 3 protons resonated at 4.04 ppm, while downfield the –NH- and –CHN- signals integrated for one each resonated at 11.69 and 9.05 ppm respectively, the –NH_2- integrated for two and resonated at 8.36 ppm. For ^{13}CNMR spectrum, the characteristic signals for the –OCH_3- methyl group showed up on the spectrum at 53.73 ppm and the signal for the azomethine (C=N) group appeared at 159.33 ppm. The Infrared Spectroscopic data for **LKN-3** can be seen in the figure below, where the peak for NH, NH_2, C=N, and O-CH_3 can be seen at 3450, 3300, 1600 and 1100 respectively. The expected molecular weight for **LKN-3** is 260.32 g/mol, the results from the mass spectrometer for this compound give a molecular weight of 261.0816 g/mol giving a difference of 0.7616 from

the expected molecular weight. The results from these spectroscopic analyses further confirmed the successful synthesis of the quinolone- thiosemicarbazone derivatives.

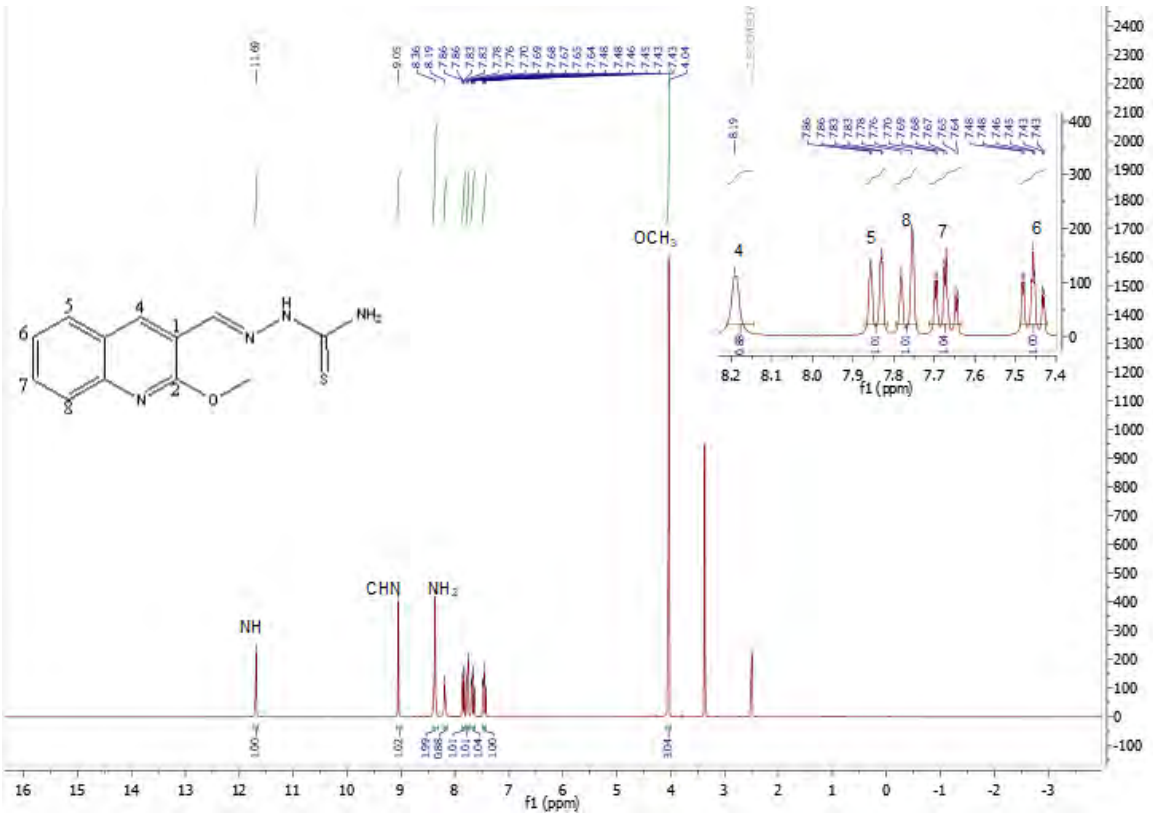

Figure 2.7: ^{1}HNMR spectrum of compound LKN-3

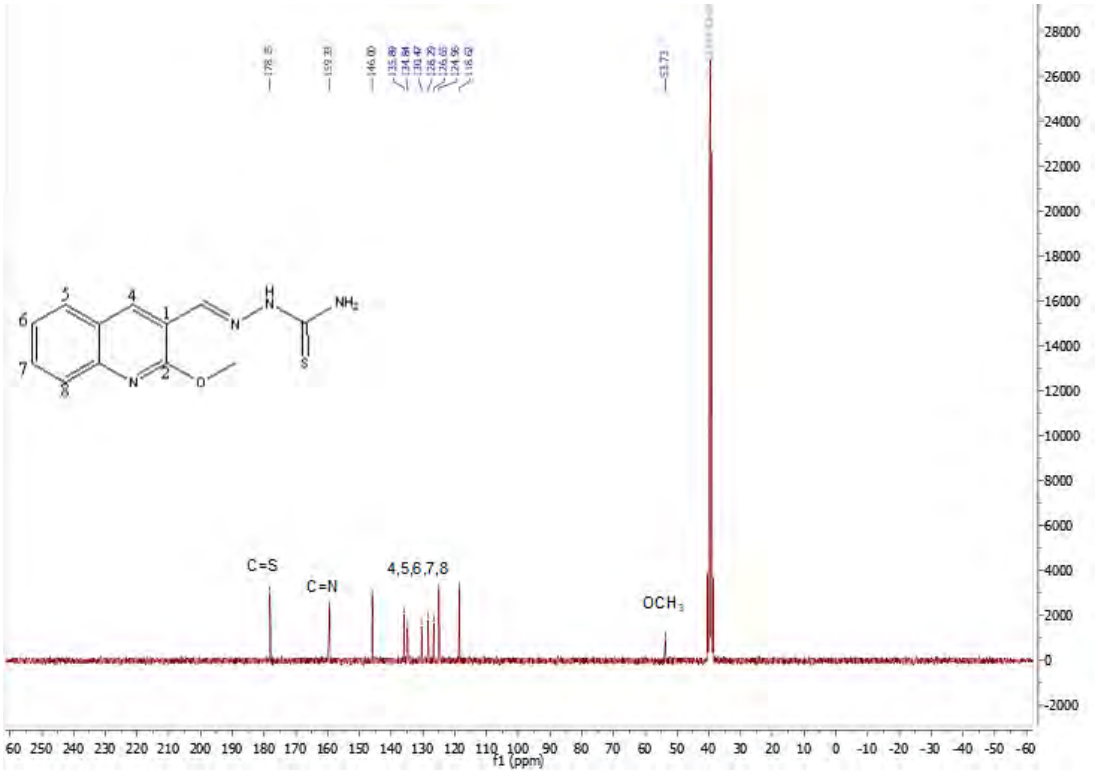

Figure 2.8: ^{13}CNMR spectrum of compound LKN-3

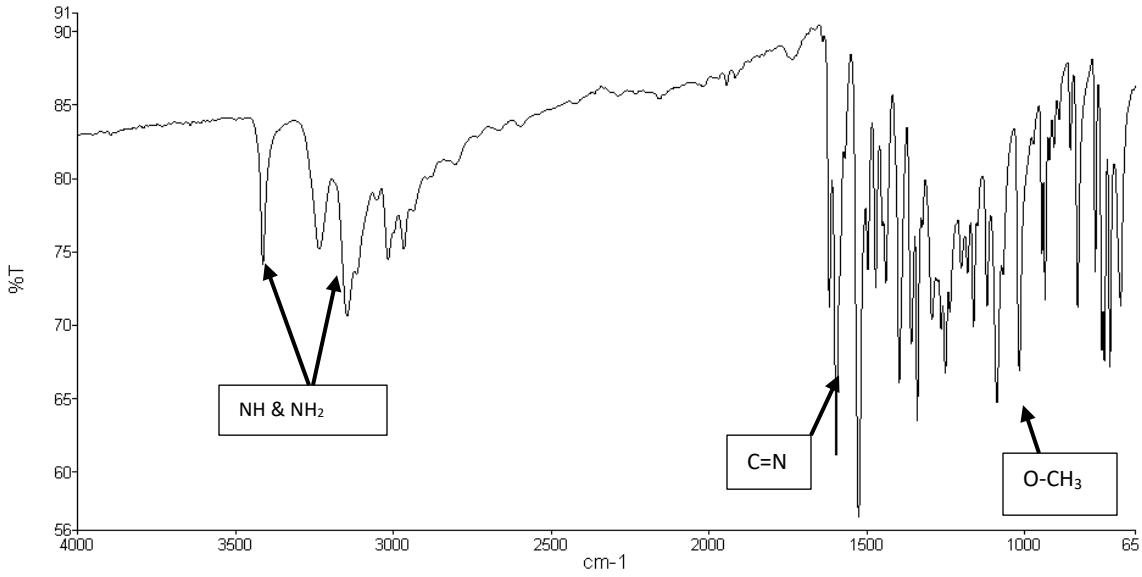

Figure 2.9: IR data for LKN-3

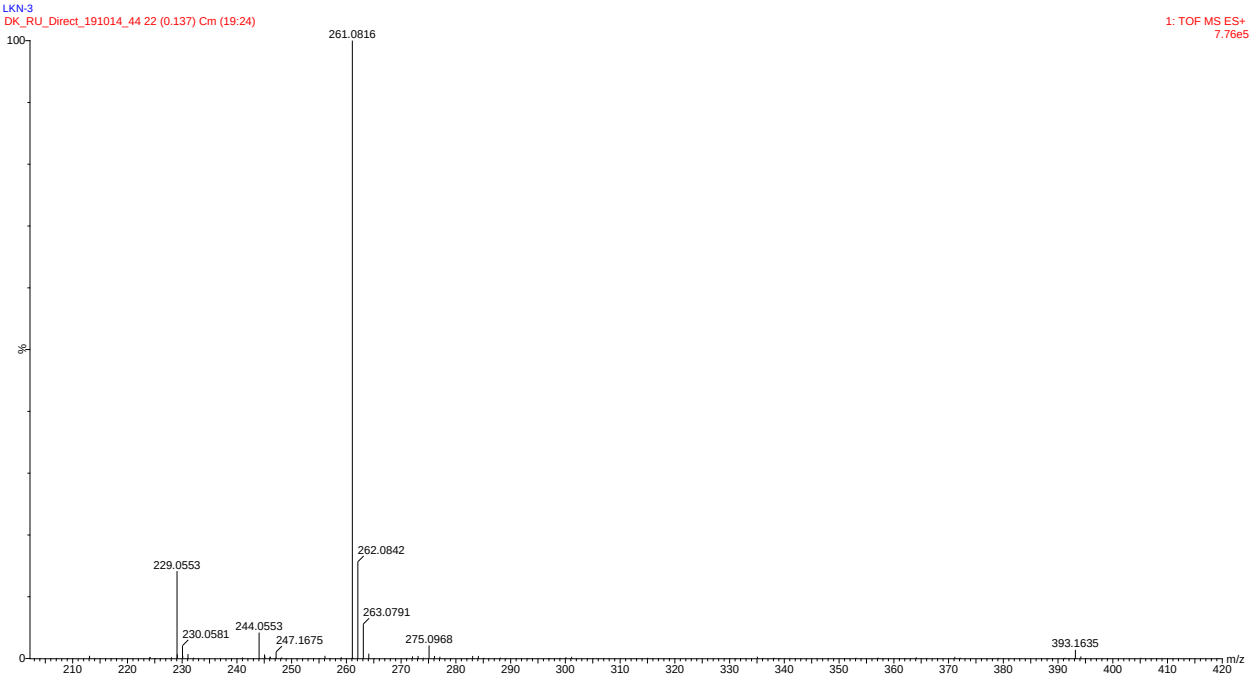

Figure 2.10: LCMS for LKN-3

2.1.4 Retrosynthetic Analysis of thiosemicarbazone based phenolic scaffolds

The synthesis for the thiosemicarbazone based phenolic scaffold group of compounds was thought to be achievable from the synthesis of phenyl- benzaldehydes reacted with commercially available thiosemicarbazide. The phenyl- benzaldehydes could be synthesized from bromo-hydroxy-benzaldehydes which could be synthesized from commercially available substituted bromophenols. The retrosynthetic analysis of these phenol thiosemicarbazone derivatives can be seen in **scheme 2.12** below.

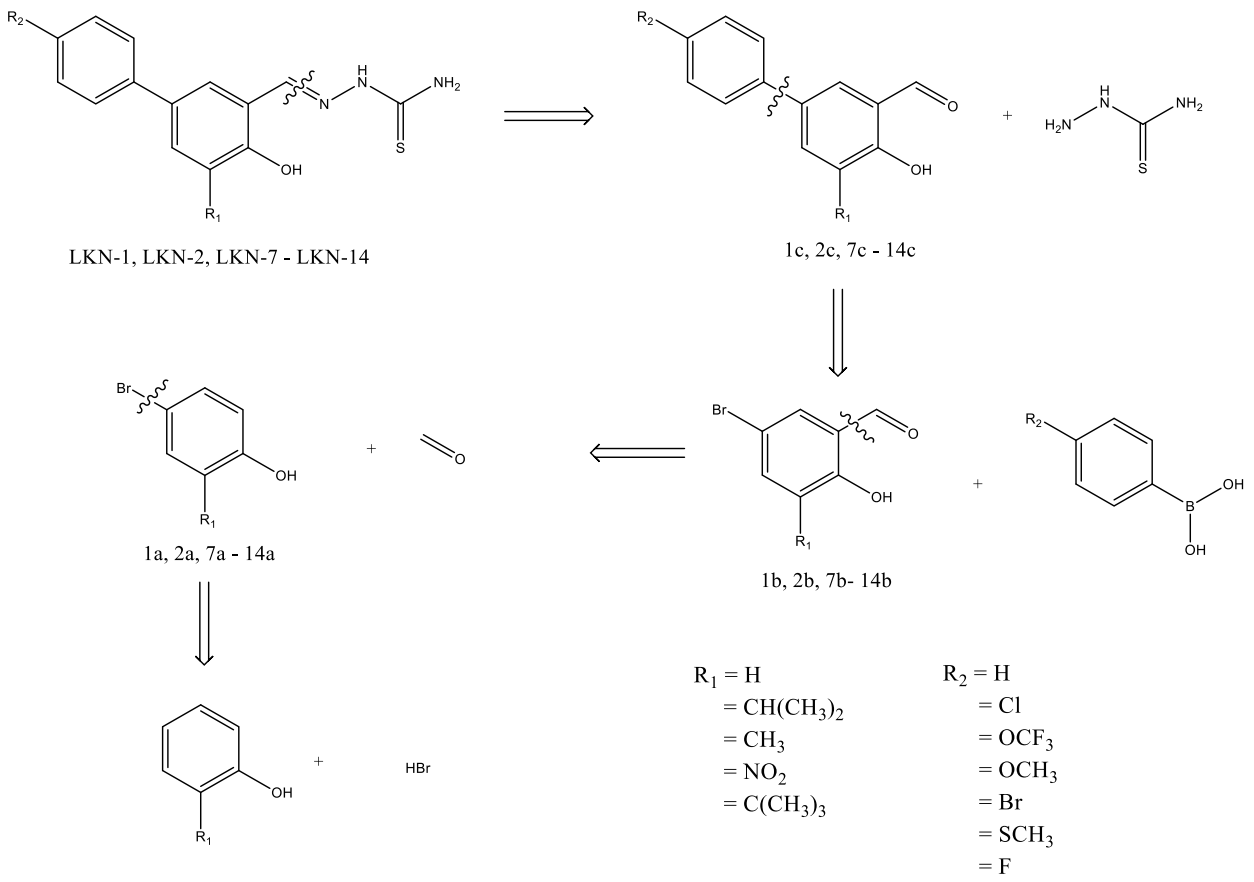

Scheme 2.12: Retrosynthetic analysis of thiosemicarbazone based phenolic scaffolds

2.1.5 Synthesis of thiosemicarbazone based phenolic scaffolds

The synthetic route proposed for the synthesis of various thiosemicarbazone based phenolic scaffolds can be seen in **scheme 2.13** below. This synthetic route was used to synthesize **LKN-1**, **LKN-2**, and **LKN-7** – **LKN-14**.

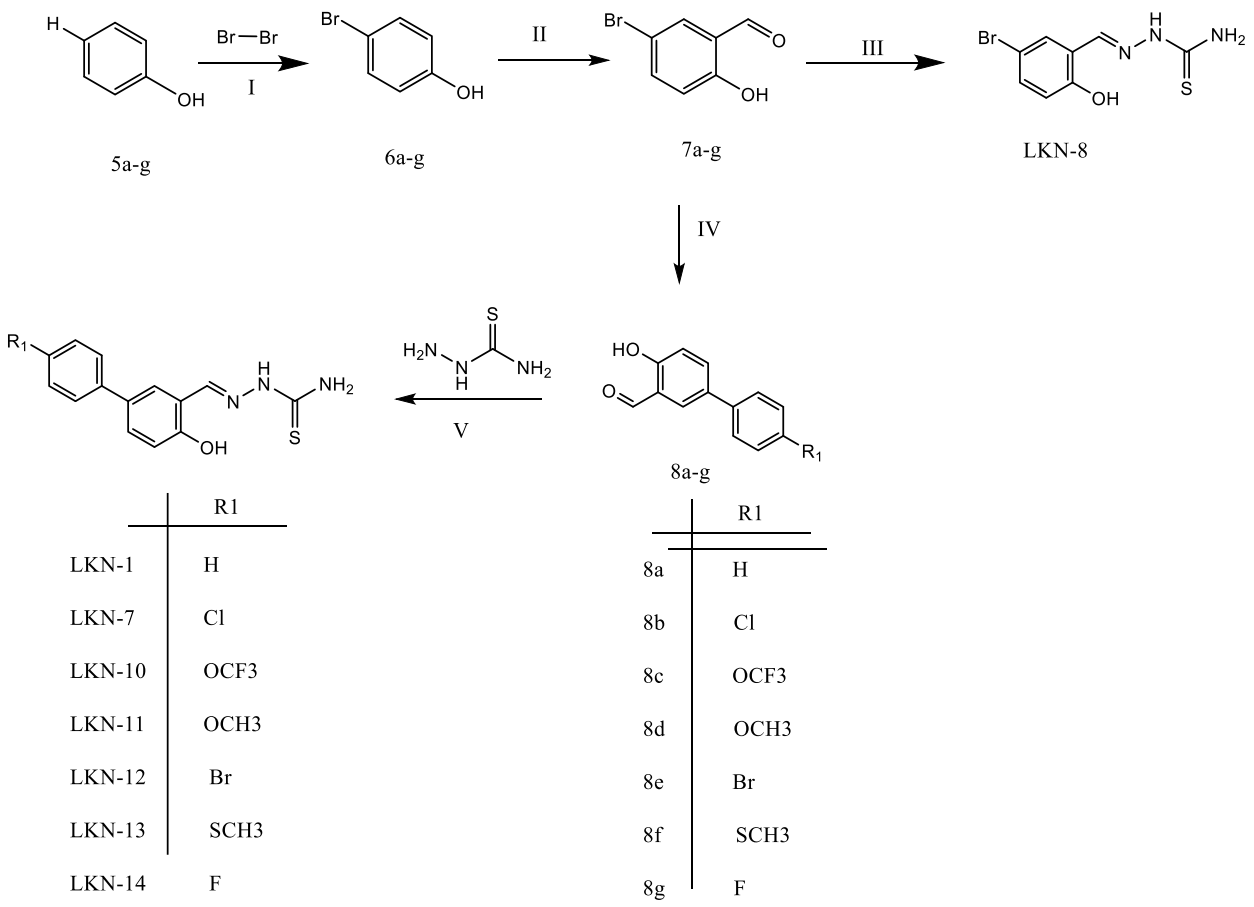

Scheme 2.13: Synthetic route for the synthesis of phenol-thiosemicarbazides. *Reagents and conditions*: (I) phenol, Br_2, $CHCl_3$, r.t., 24 hrs; (II) bromophenol (**6a-g**), C_2H_3N, $MgCl_2$, PFA, 82 °C, 3 hrs; (IV) bromohydroxy-benzaldehyde (**7a-g**), DME, K_2CO_3, R_1- phenylboronic acid, tetrakis(triphenylphosphine)palladium(0), 80 °C, 24 hrs; (IV) R_1phenyl-benzaldehyde (**8a-g**), thiosemicarbazide, MeOH, 60 °C, 24 hrs.

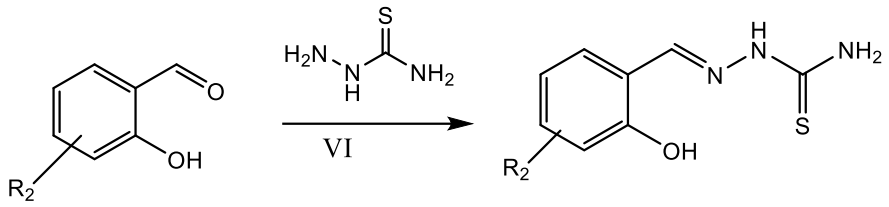

9a-b

	R_2
9a	NO_2
9b	NH_2

	R_2
LKN-2	NO_2
LKN-9	NH_2

Scheme 2.14: Synthetic route for the synthesis of phenol-thiosemicarbazides. *Reagents and conditions*: (VI) R_2-hydroxybenzaldehyde (**9a-b**), thiosemicarbazide, MeOH, 60 °C, 24 hrs.

Three final products in particular did not undergo the full reaction mechanism shown above in **scheme 2.14**, these compounds did not undergo the step of addition of a boronic acid, these compounds are namely **LKN-2**, **LKN-8** and **LKN-9.** The synthesis of **LKN-8** is shown in step III of **scheme 2.14** above. The synthetic route for **LKN-2** and **LKN-9** is depicted in **scheme 2.14** above.

2.5.5.1 Synthesis of substituted bromophenol

Having rationalized the synthetic route for synthesizing the phenolic-thiosemicarbazone scaffolds in **scheme 2.15** above, the first step in synthesizing these desired final products was to synthesize bromophenols from readily available phenols.

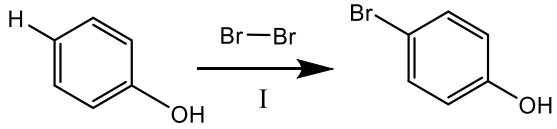

Scheme 2.15: *Reagents and conditions*: (I)phenol, Br_2, $CHCl_3$, r.t, 24 hrs

The reaction of bromine with the benzene ring is an example of an electrophilic aromatic substitution reaction, bromine acts as the electrophile forming a sigma bond to the benzene ring, yielding an intermediate. A proton is then removed from the intermediate to form a substituted benzene ring.

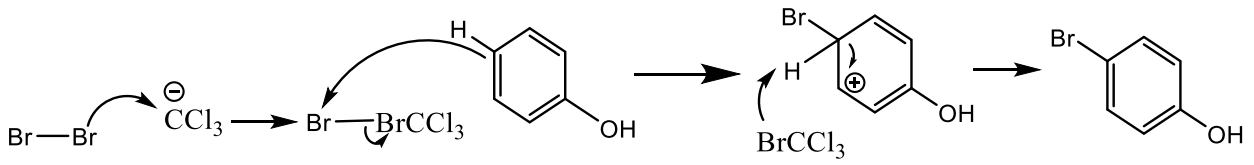

Scheme 2.16: a proposed mechanism for the synthesis of substituted bromophenols

Depicted above in **scheme 2.16** is the reaction mechanism for the synthesis of the desired bromophenols. In this reaction CCl_3 catalyzes the reaction acting as a lewis acid being more prone to attracting electrons towards itself and thus forming a bond with Br_2. This resultant bond causes one of the Br directly bonded to the Carbon atom to have a positive charge. Due to this positive nature of Br it becomes more prone to pulling an electron towards itself. Because of this the bond between the two Br atoms is weaker as the positive Br tries to steal an electron from the other, thus this Br when reacted with the phenol benzene ring reacts more easily with it and forms a bond with the ring. The carbon atom now starts to act as a base and gives an electron to a hydrogen which in turn gives an electron to the carbocation. This results in the reformation of the double bond and the formation of Hydrogen Bromide as a side product to the bromophenol which has been successfully synthesized.

2.1.5.2 Synthesis of Bromo-hydroxy-benzaldehyde

The second step in the synthesis of phenol- thiosemicarbazones was the synthesis of Bromo-hydroxy benzaldehydes, by the reaction of previously synthesized bromophenols with magnesium chloride, and paraformaldehyde in acetonitrile.

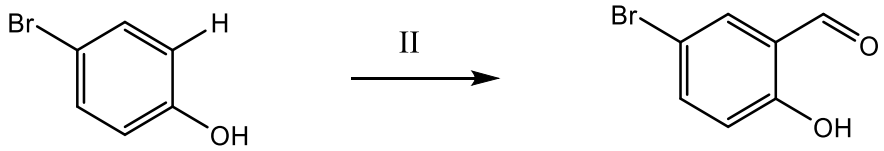

Scheme 2.17: *Reagents and conditions*: (II) bromophenol, C_2H_3N, $MgCl_2$, PFA, 82 °C, 3 hrs

The addition of the carbonyl group on to the bromophenol as seen in **scheme 2.17** above, is an example of a formylation reaction which are a form of electrophilic aromatic substitution. The direct reaction between phenol and paraformaldehyde is possible via the Casiraghi formylation. The Casiraghi research group reported that the reaction of paraformaldehyde and magnesium

phenoxides, these magnesiumphenoxides having been formed from the respective phenol and magnesium halide in benzene resulted in mono-formylation exclusively at the ortho-position respective to the hydroxyl group in the phenol[60].

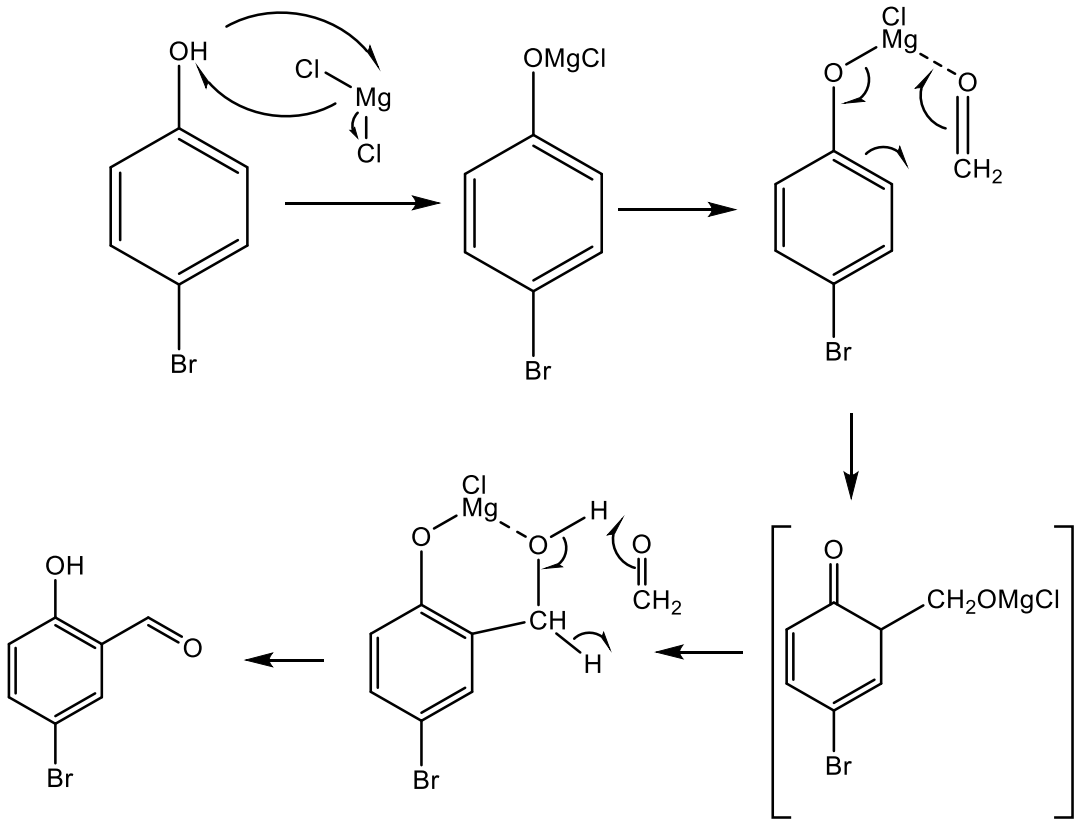

Scheme 2.18: a proposed mechanism for the synthesis of Bromo-hydroxy-benzaldehydes

The reaction with the phenol is initiated by the base system providing the salt. The phenoxymagnesium chloride intermediate formed reacts with paraformaldehyde resulting in a cyclohexadienone intermediate. This intermediate subsequently takes part in a redox reaction with paraformaldehyde in which salicylaldehyde is formed together with methanol as a side product.

2.1.5.3 Synthesis of phenyl-benzaldehyde

The third step was the synthesis of phenyl- benzaldehyde derivatives, the proposed synthetic route for synthesizing these phenyl-benzaldehydes involved reacting bromo-hydroxy-benzaldehydes

synthesized from previous reactions or commercially available 5-bromo-salicylaldehyde with various phenylboronic acids to synthesize phenyl-benzaldehyde derivatives.

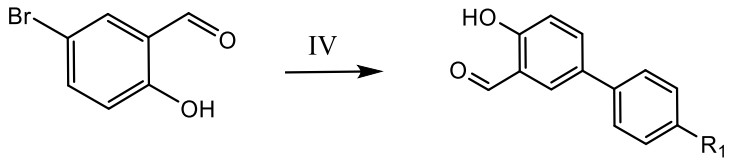

	R1
8a	H
8b	Cl
8c	OCF3
8d	OCH3
8e	Br
8f	SCH3
8g	F

Scheme 2.19: *Reagents and conditions*: (III) DME, K_2CO_3, R_1- phenylboronic acid, tetrakis(triphenylphosphine)palladium(0), 80 °C, 24 hrs

A palladium metal complex catalyzes the reaction of phenylboronic acids in an aqueous solvent as seen in **scheme 2.19**. Palladium catalyzed conjugate addition reactions are less developed than the copper or rhodium-catalyzed reaction, however the palladium-catalyzed reactions offer significant advantages[61]. For example, these palladium-catalyzed conjugate addition reactions utilize air-stable, functional group tolerant boron nucleophiles, many of which are commercially available. Furthermore, the reactions are typically not sensitive to water or oxygen[61]. These features together comprise an operationally simple and robust transformation.

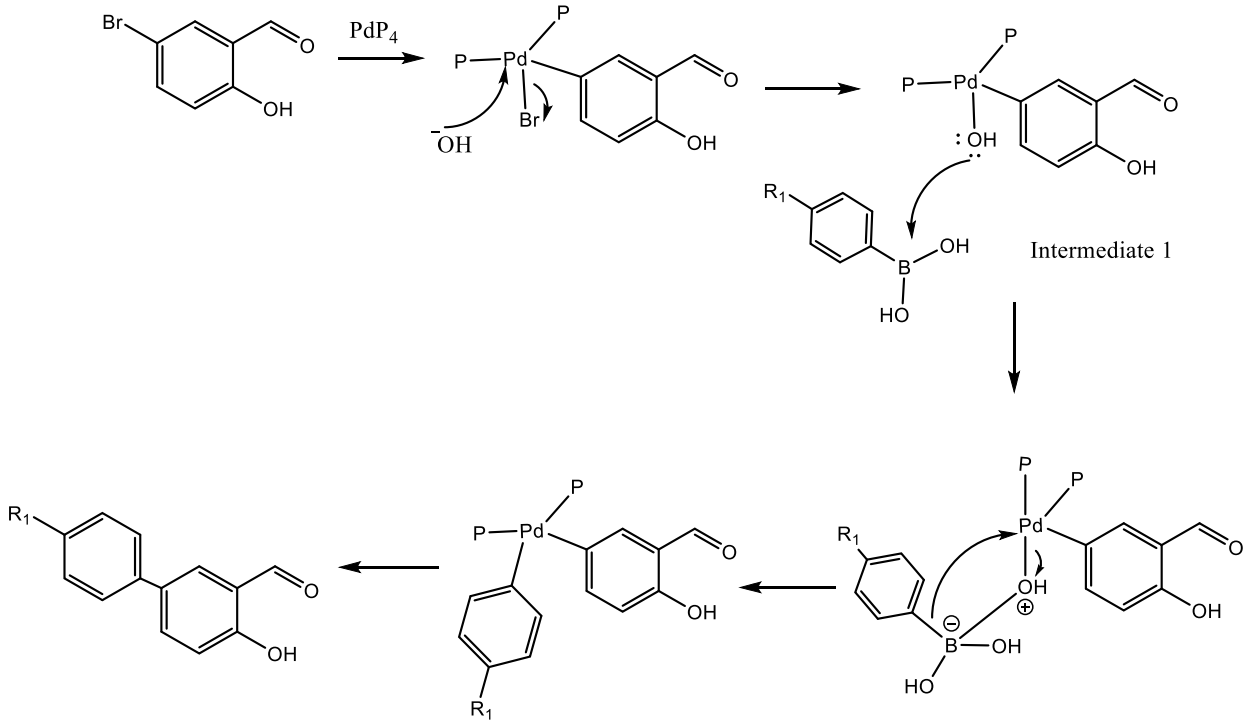

Scheme 2.20: a proposed mechanism for the synthesis of phenyl-benzaldehyde derivatives

The synthesis of these compounds was achieved by a number of steps, the first step being the oxidative addition of the palladium to the halide, followed by a hydroxide group attacking and kicking off the halide group. The next step involves the reaction of the complex with boronic acid which reacts with the first intermediate in transmetalation to afford the second intermediate. A reductive elimination follows this step to give the desired product and regenerate the original Pd(0) species.

2.1.5.4 Synthesis of thiosemicarbazone based phenolic scaffolds

The final step in the synthetic route was the synthesis of phenol-thiosemicarbazones, where the carbonyl group was substituted with thiosemicarbazide resulting in the desired final compounds.

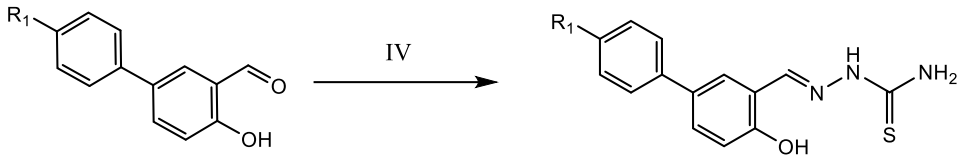

	R_1	
LKN-1	H	44.4%
LKN-7	Cl	94.2%
LKN-10	OCF_3	77%
LKN-11	OCH_3	18%
LKN-12	Br	38.2%
LKN-13	SCH_3	92.3%
LKN-14	F	92%

Scheme 2.21: *Reagents and conditions*: (IV) thiosemicarbazide, MeOH, 60 °C, 24 hrs

Thiosemicarbazides are greatly utilized in organic chemistry, demonstrating their importance in the synthesis of various heterocycles[62]. The formation of C-N and C=N bonds as opposed to the N-N bond formation is reflected in their extensive use for the preparation of these heterecycles in excellent yields. Thiosemicarbazides are polyfunctional compounds possessing nucleophilic properties, with the internal nitrogen of the hydrazine fragment being a softer nucleophilic center than the more powerful terminal nitrogen[63]. Reagents which are susceptible to nucleophilic attack by the terminal nitrogen undergo cyclisation to afford heterocyclic compounds in excellent yields even under mild reaction conditions[63]

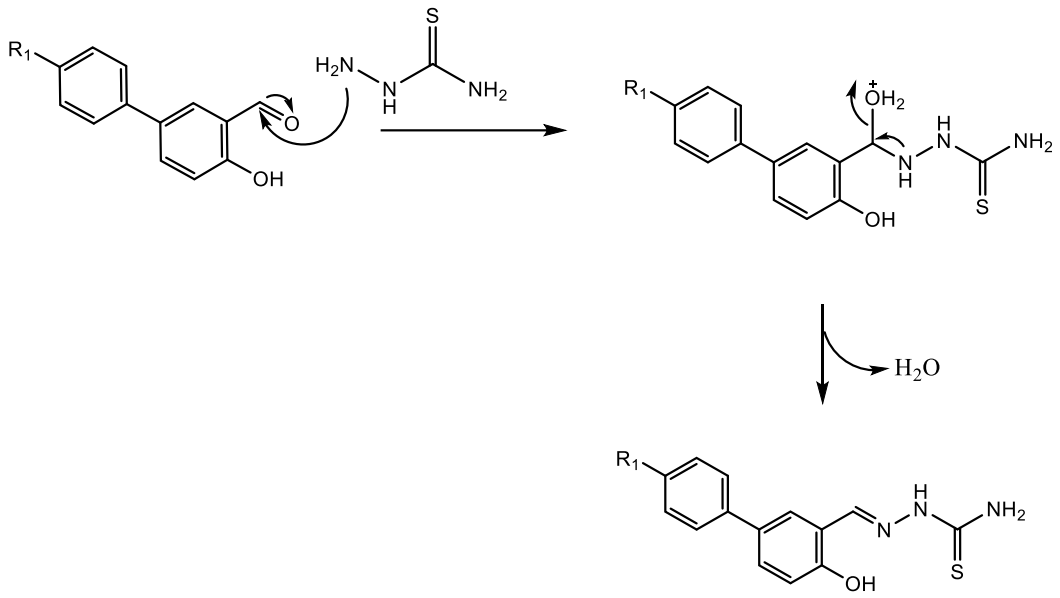

Scheme 2.22: the proposed synthetic route for the synthesis of thiosemicarbazone based phenolic scaffolds.

The synthesis of the phenol-thiosemicarbazones is an example of nucleophilic substitution, the NH_2 group on the thiosemicarbazide acts as the nucleophile attacking the carbon of the carbonyl group and knocking off the oxygen substituting it with the thiosemicarbazide to give the desired phenol-thiosemicarbazone derivatives.

2.1.6 Characterization of thiosemicarbazone based phenolic scaffolds

The compounds prepared during this project were characterized using ^{1}H, ^{13}C NMR and infrared (IR) spectroscopic techniques.

2.1.6.1 Spectroscopic characterization of bromophenols

The successful synthesis of bromophenols by electrophilic aromatic substitution was confirmed by proton (^{1}H) and carbon-13 (^{13}C) nuclear magnetic resonance spectroscopy techniques. There was a correlation between the synthesized bromophenols and those of the previous studies[64,65]. The ^{1}H spectrum for compound **5a** can be seen in the figure below, in the spectrum below the methyl groups can be seen resonating at 3.45 ppm while downfield the signal for –OH- resonated at 9.98 ppm. For the ^{13}CNMR spectrum the characteristic signals for –COH- and the methyl groups

numbered 7, 8 and 9 showed up at 152.01, 32.41, 24.08 and 23.80 respectively. The results from the spectroscopic analysis confirmed the successful synthesis of bromophenols.

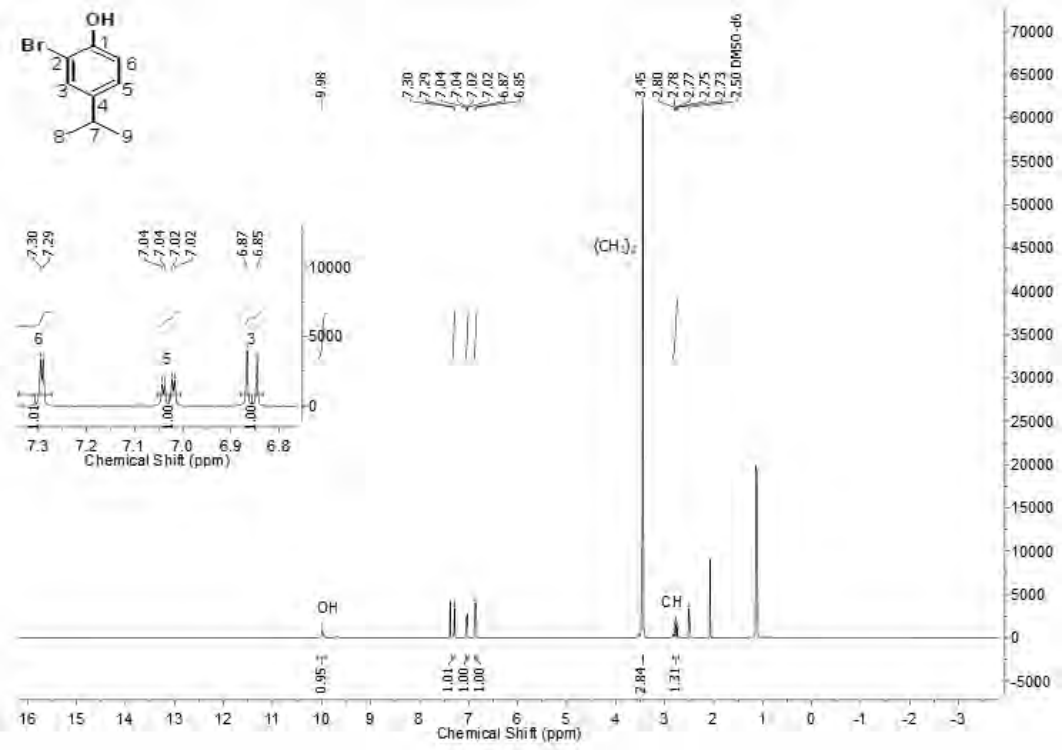

Figure 2.11: ^{1}HNMR spectrum of compound 5a

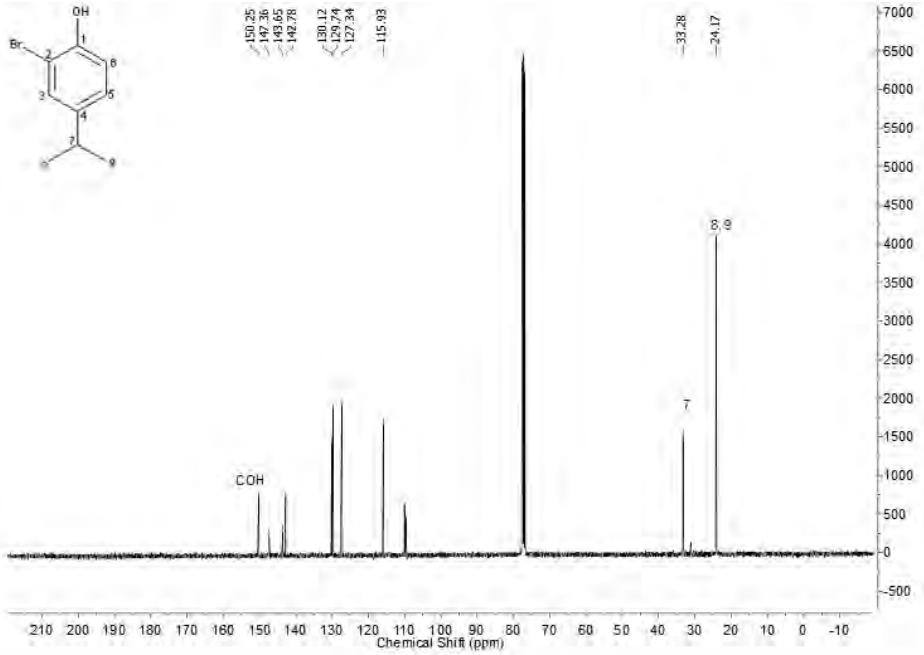

Figure 2.12: ^{13}CNMR spectrum of compound 5a

2.5.6.2 Spectroscopic characterization of Bromo-hydroxy-benzaldehydes

The successful synthesis of bromo-hydroxy-benzaldehydes was confirmed by proton and carbon-13 nuclear magnetic resonance spectroscopy techniques. There was a correlation between synthesized bromo-hydroxy-benzaldehydes and those found in literature[66]. The ^{1}HNMR spectrum for compound **6b** is shown in the figure below where the methyl group integrates for 3 and resonated at 2.33 ppm, downfield the signals for –CHO- and –OH- resonated at 11.38 ppm and 9.80 ppm respectively. For ^{13}CNMR the characteristic signals for the methyl group resonated at 20.15 ppm, the signal for the carbonyl carbon appeared at 196.11 ppm and the signal for –COH- resonated at 156.03 ppm. The analysis of these NMR spectra further proved the successful synthesis of compound **6b**.

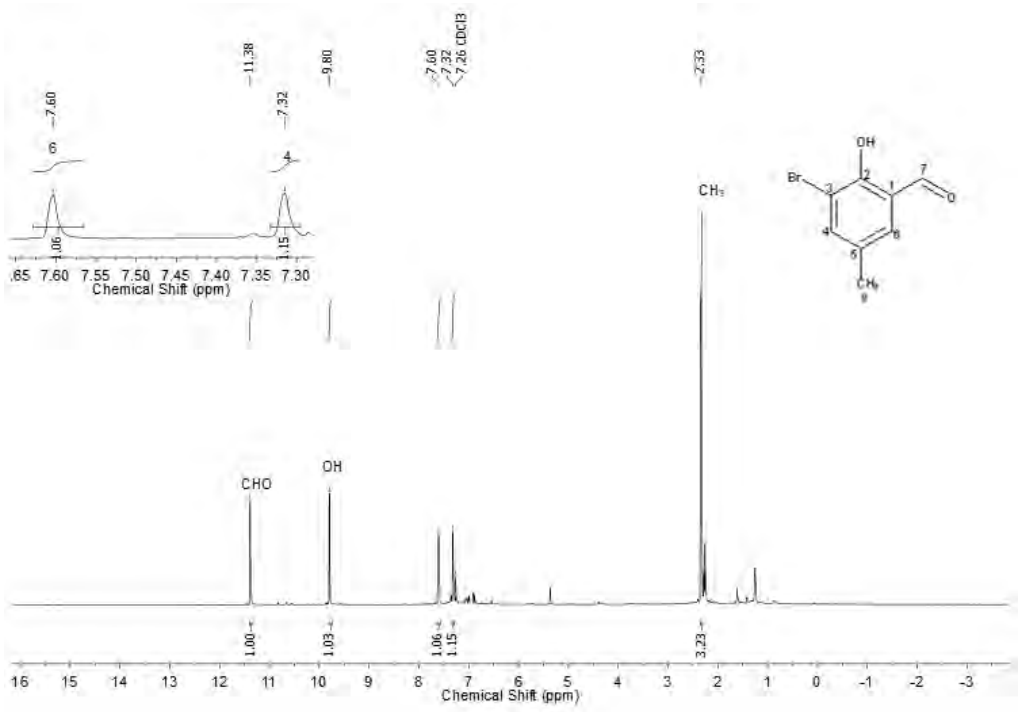

Figure 2.13: ^{1}HNMR for compound 6b

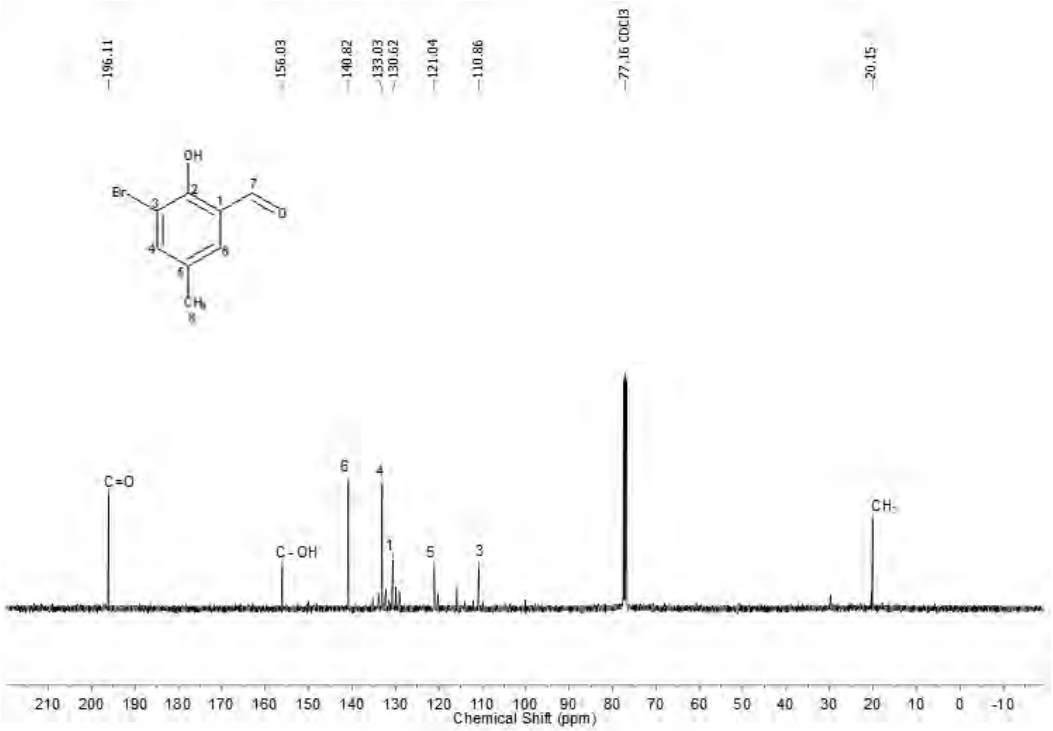

Figure 2.14: ^{13}CNMR for compound 6b

2.1.6.3 Spectroscopic characterization of phenyl-benzaldehydes

The successful synthesis of phenyl-benzaldehyde derivatives was confirmed by proton and carbon-13 nuclear magnetic resonance spectroscopy techniques. After reviewing various literature there was a correlation with the synthesized phenyl-benzaldehydes[67]. The ^{1}HNMR spectrum for the proton for the –CHO- group resonated at 10.31 ppm and the signals for protons 9,13 and 10,12 resonated at 7.63-7.61 ppm and 7.46-7.42 ppm respectively, there is also a significant increase in the number of protons indicating the formation of a new aromatic ring. For the ^{13}CNMR the characteristic signals for the –CHO- and –C-OH- group showed up on the spectrum at 191.84 ppm and 160.34 ppm respectively, there is a significant increase in the number of signals.

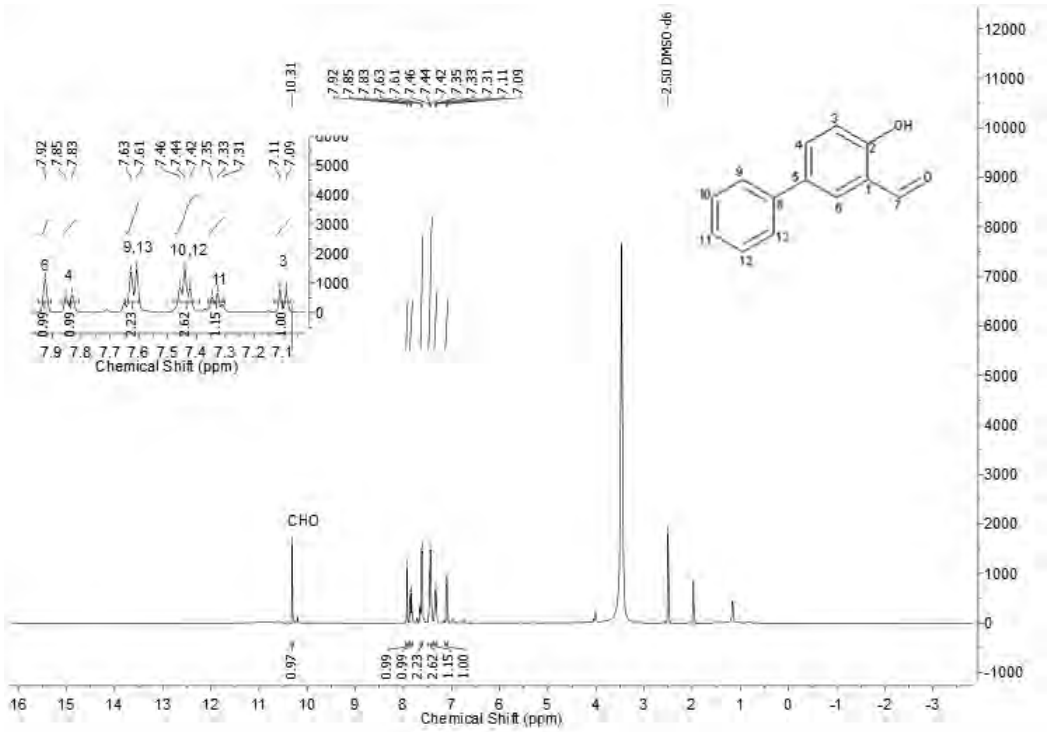

Figure 2.15: ^{1}HNMR for compound 7a

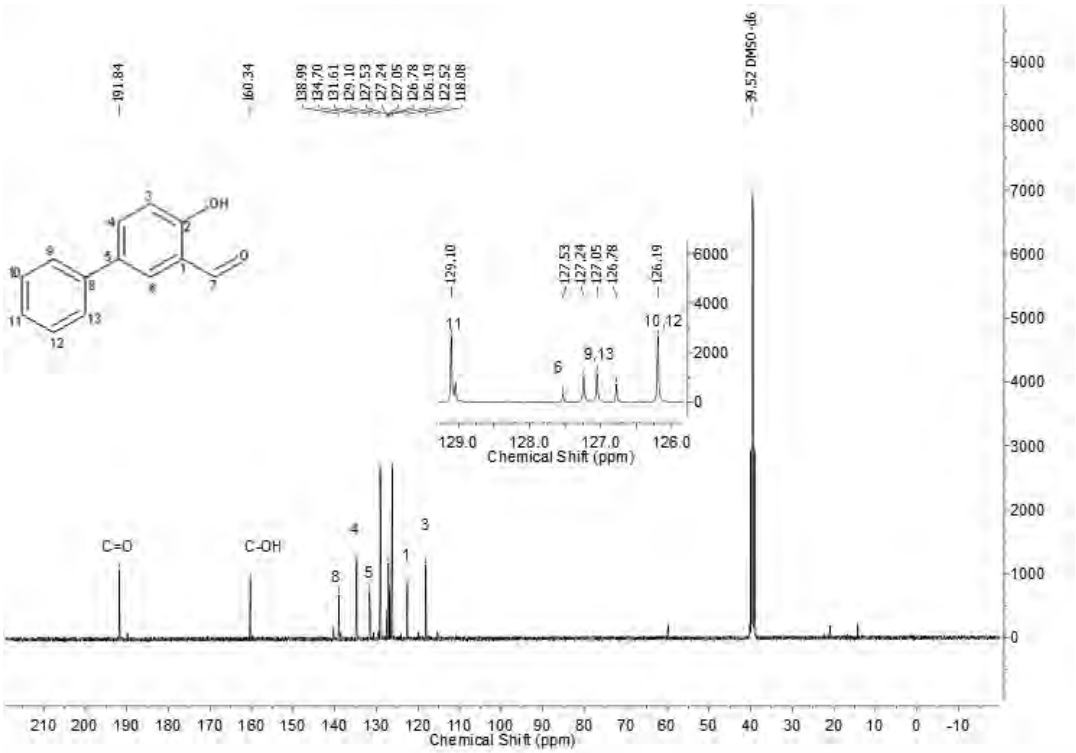

Figure 2.16: ^{13}CNMR for compound 7a

2.1.6.4 Spectroscopic characterization of phenol-thiosemicarbazones

The successful synthesis of the desired final phenol-thiosemicarbazone derivatives was confirmed by several spectroscopic techniques such as the proton, carbon-13, mass spectroscopy, and infrared spectroscopic techniques. The literature reviewed showed a correlation with this synthesized phenol-thiosemicarbazone derivatives[59]. The ^{1}HNMR spectrum for compound **LKN-1** can be seen in figure 8 below, the proton for the –NH- group resonated at 11.40 ppm with the protons for the –OH- group and the –NH_2- group resonated at 10.11 ppm and 8.43 ppm respectively. For the ^{13}CNMR spectrum the characteristic signals for the -C=S-, –COH- and –C=N- groups showed up on the spectrum at 177.73 ppm, 156.18 ppm and 139.72 ppm, respectively. Infrared spectroscopy data can be seen in figure 9 below shows the peak for the phenol group at about 3450, the peaks for NH and NH_2 appearing between 3200 and 3300 and C=N appearing at about 1600. The expected molecular weight for **LKN-1** is 271.34 g/mol, as seen below in figure 10, the mass spectrometry results for this final product was 272.0855 g/mol which is a difference of 0.7475 between the expected molecular weight and the molecular weight shown by the mass spectrometer.

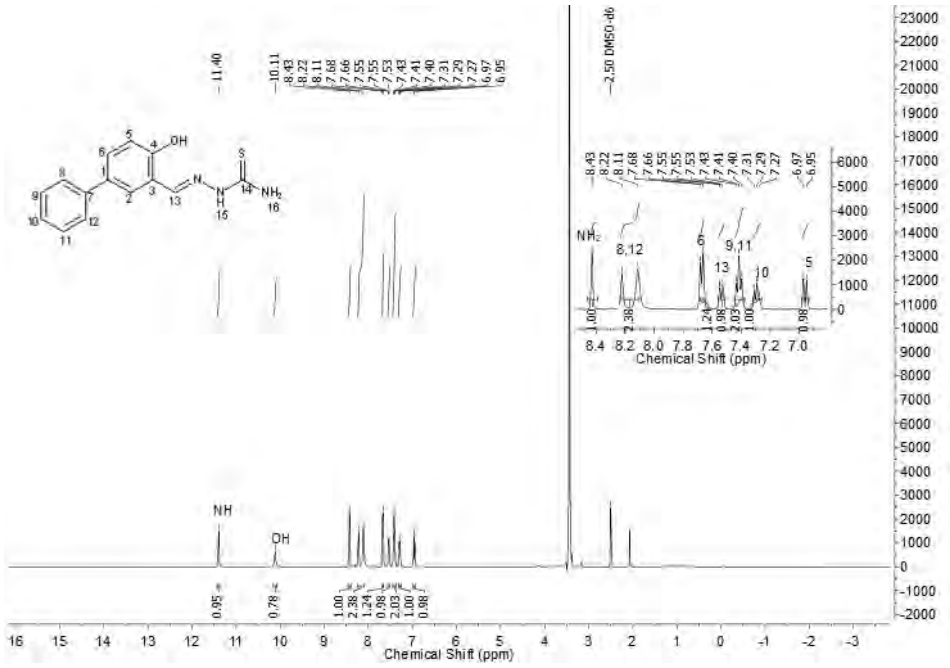

Figure 2.17: ^{1}HNMR for compound LKN-1

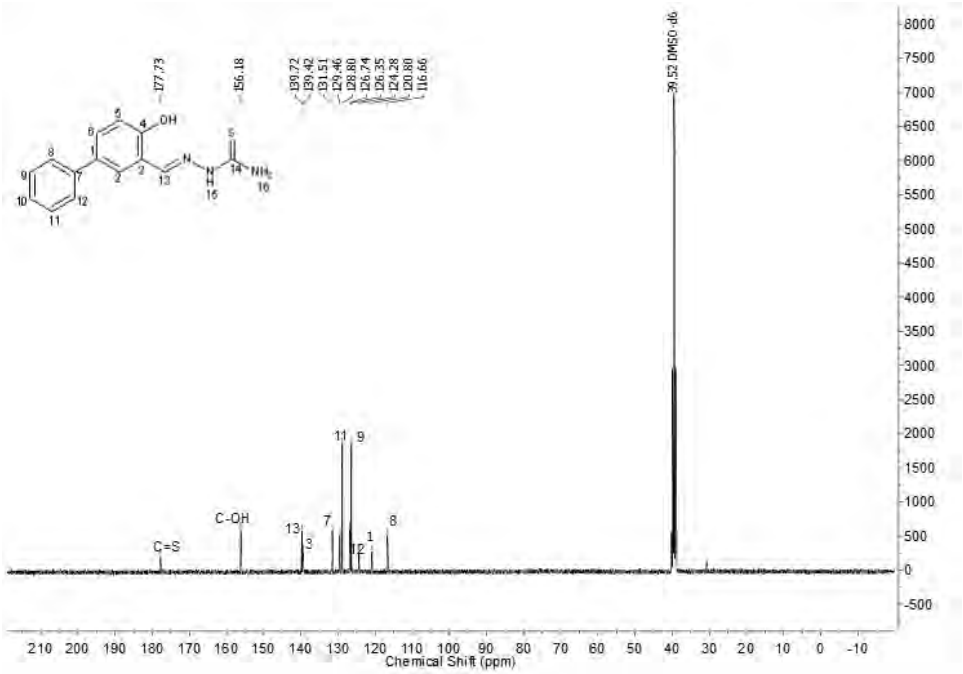

Figure 2.18: ^{13}CNMR for compound LKN-1

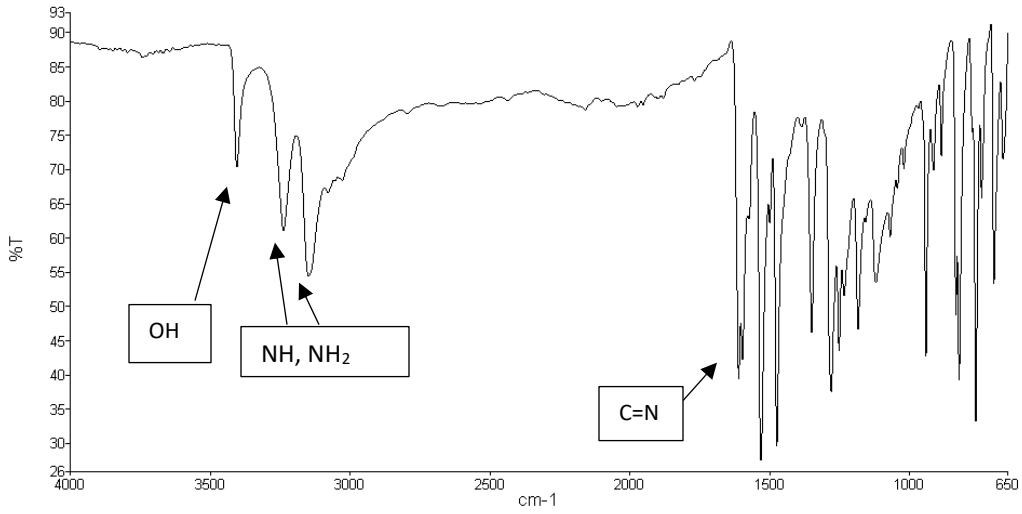

Figure 2.19: IR for final product LKN-1

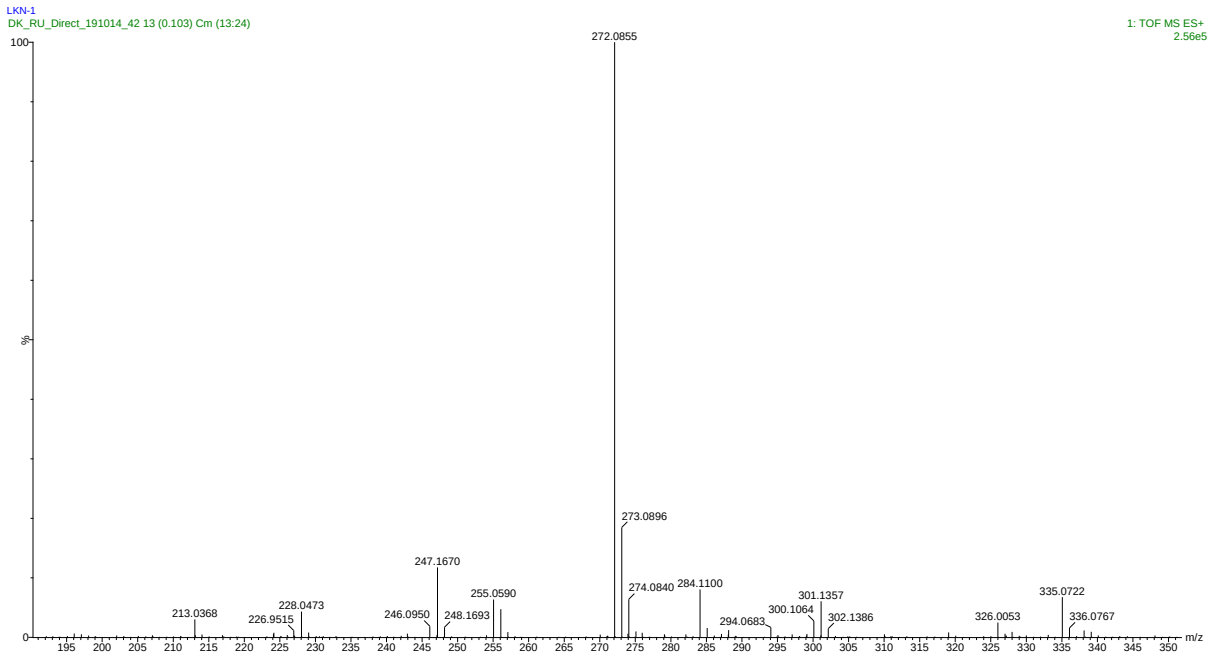

Figure 2.20: LCMS data for LKN-1

2.2 Conclusion

In conclusion, out of the fourteen final compounds synthesized the results, seen above, for two of those compounds didn't coincide with expected results. Leading to the conclusion that for thesetwo compounds the expected product was not synthesized. These two compounds are **LKN-5** and **LKN-6**

Elemental analysis is a process whereby a sample is analyzed for its elemental and sometimes isotopic composition. A CHNS analyzer was used to analyze these samples and the results were given as percentage values. These percentage values are then compared with the expected percentage values for elements C, H, N and S with a margin of error of 0.5 difference allowed between the expected and the actual results, should the difference be greater than the margin of error then a conclusion can be drawn that the compound either has some impurities or the analyzed compound is not the expected synthesized product.

The infrared spectrum of a sample is recorded by passing a beam of infrared light through the sample. When the frequency of the IR is the same as the vibrational frequency of a bond or collection of bonds, absorption occurs. This technique is commonly used for analyzing samples with covalent bonds. Simple spectra are obtained from samples with few IR active bonds and high levels of purity.

Mass spectrometry is a detection method that relies on the mass-to-charge ratio of a compound. Following chromatographic separation, molecules are ionized using an energy source. These ionized molecules then pass through a set of magnets, which further separates molecules based on their mass-to-charge ratio. Detection is performed based on charged particles striking a detector and creating current. The detector only detects charges and cannot differentiate based on mass. The magnetic separation provides the selectivity of the methodology. Thus two molecules that are ionized at the same time, but have different masses can be detected independently using MS detection. Similarly, two molecules that are ionized at the same time and have different masses, but have different charges can be detected independently using MS detection.

There was insufficient product remaining to successfully run and elemental analysis for **LKN-5**. However IR and MS were run for this compound, the IR data shows sharp peaks at 2950, 2900 and 1200 corresponding to expected peaks for this compound. However, the data from the mass spectrometer gives a much greater value for the molecular weight than expected leading to the conclusion that either this product has several impurities or rather the expected product was not synthesized.

The elemental analysis results for **LKN-6** differed greatly from the expected values, the difference was greater than the margin of error. We expected NH and NH_2 peaks for **LKN-6** around 3500-3000 and a sharp peak was expected at 1200-1180 however these peaks were not observed. The calculated mass with the highest percentage was 295.0423 g/mol, the expected molecular weight for this product was 294.76 g/mol, the difference between these two values is 0.2823 which is a relatively low value. The results from elemental analysis and IR are enough to conclude that the expected product was not synthesized or had impurities, however, the results from MS indicate that despite previous results from IR and elemental analysis the desired product was synthesized possibly with several impurities.

With the exception of these two compounds (**LKN-5** and **LKN-6**), the elemental, NMR, IR and MS analyses confirm that the expected compounds were synthesized successfully.

CHAPTER 3

IN VITRO ANTIPLASMODIAL EVALUATION OF THIOSEMICARBAZONE DERIVATIVES

3.1 Introduction

The main objective of this research was to synthesize and subject the resulting compounds to biological evaluation for their potential *in vitro* antiparasitic activity. The synthesized compounds were tested for their ability to inhibit plasmodial growth using the chloroquine-sensitive (CQS) 3D7 strain of the human malaria parasite *Plasmodium falciparum*, with chloroquine (CQ) included as the control drug. The compounds were also cross-screened for their potential activity against nagana *Trypanosoma brucei brucei*, which is a causative agent of animal African trypanosomiasis. Anti-trypanosomal activity of the compounds was evaluated against *T.b. brucei* 427 strain using pentamidine (PMD) as reference compound. The cytotoxicity potential of synthesized compounds was evaluated using human cervix adenocarcinoma (HeLa) cells with emetine (EMT) included as a standard drug. All experimental details relating to biological tests have been done in collaboration with the Centre for Chemico- and Biomedical Research at Rhodes University.

3.2 Biological results and discussion

3.2.1 In vitro cytotoxicity assay of thiosemicarbazone derivatives

To assess the overt cytotoxicity of the compounds, each test compound was incubated with Hela cells at a fixed concentration of 20 μM. Compounds were tested in duplicate and standard deviations (SD) were derived. Except compound **LKN-10**, none of the compounds showed human cytotoxicity risk and percentage HeLa viability of >80 was often observed at 20 μM concentration of test compounds. The bar graph (**Figure 3.1**) shows the percentage of HeLa cell viability obtained for the individual compounds. Compound **LKN-10** reduced viability of HeLa cells to below 25%, and it was thus put forward to determine its IC_{50} value. The IC_{50} value of compound **LKN-10** by plotting percentage viability against Log (compound concertation) and the IC_{50} (50% inhibitory concentration) obtained from the resulting dose-response curve by non-linear regression (**Figure 3.2**). For comparative purposes, emetine as a drug standard gave IC_{50} value of 0.02 μM and compound **LKN-10** showed moderate cytotoxic risk with IC_{50} value of 9.59 μM.

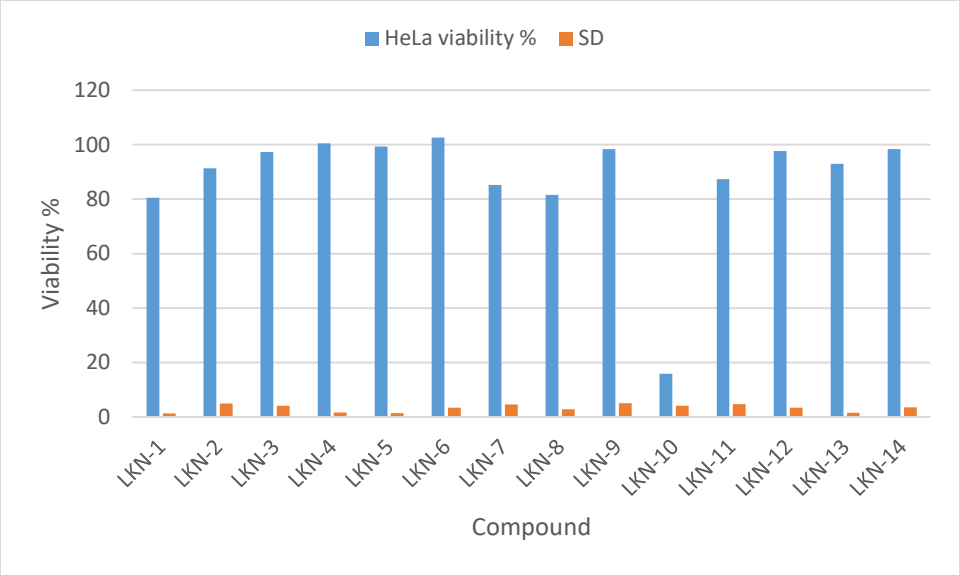

Figure 3.1: Cell toxicity (HeLa cell viability) screening data of the individual compounds (20 µM).

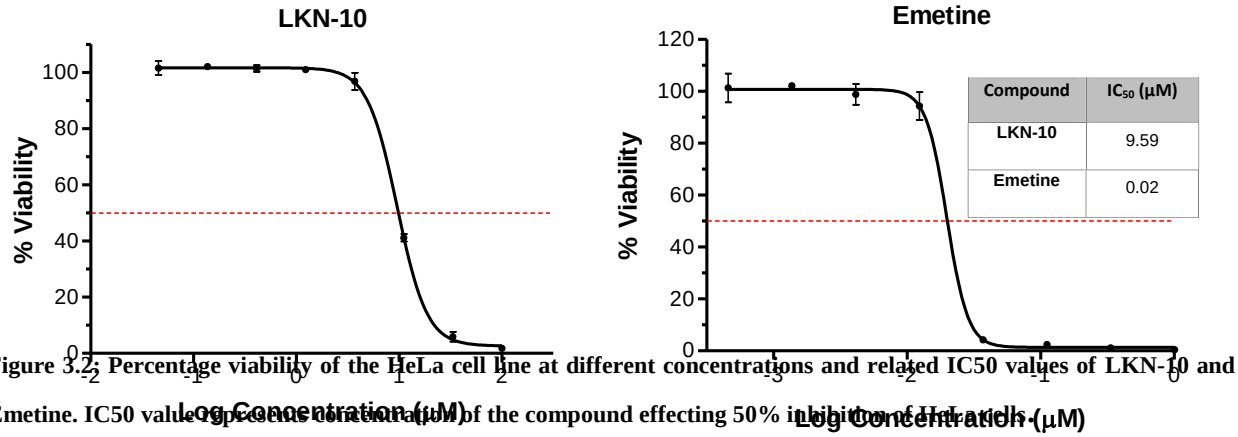

Figure 3.2: Percentage viability of the HeLa cell line at different concentrations and related IC50 values of LKN-10 and Emetine. IC50 value represents concentration of the compound effecting 50% inhibition of HeLa cells.

3.2.2 In vitro activity malaria assay of thiosemicarbazone compounds

To assess the effect of synthesized compounds against malaria parasite, the thiosemicarbazone derivatives were subjected to initial single point screening using a concentration of 20 µM of test compounds against the 3D7 strain of *P. falciparum*. Compounds were tested in duplicate and standard deviations (SD) derived. For comparative purposes, CQ was used as a standard. The graph (**Figure 3.3**) is showing the percentage parasite viability and ±SD obtained for the individual compounds. These compounds generally did not affect *P. falciparum* viability at 20 µM, this could probably be due to poor solubility of the compounds in screening media. Compound **LKN-11** ,however, showed activity against 3D7 strain of the *P. falciparum* parasite, and since it reduced the parasite viability to below 50% threshold **LKN-11** was subjected to further screening to determine the IC_{50} value. **LKN-11** demonstrated moderate antimalarial activity, with IC_{50} value of 6.69 µM.

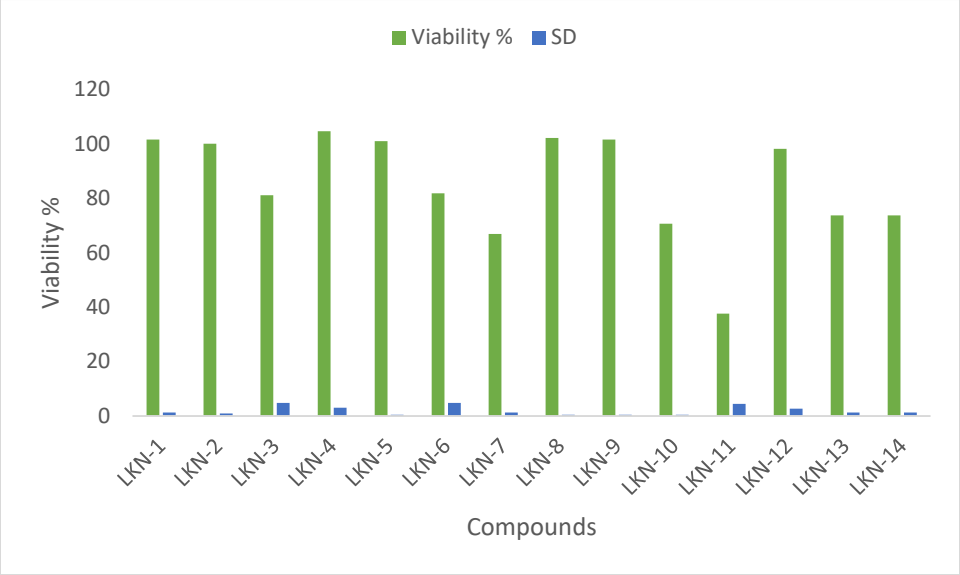

Figure 3.3: In vitro antimalarial screening assay of the synthesised thiosemicarbazone derivatives (20 µM).

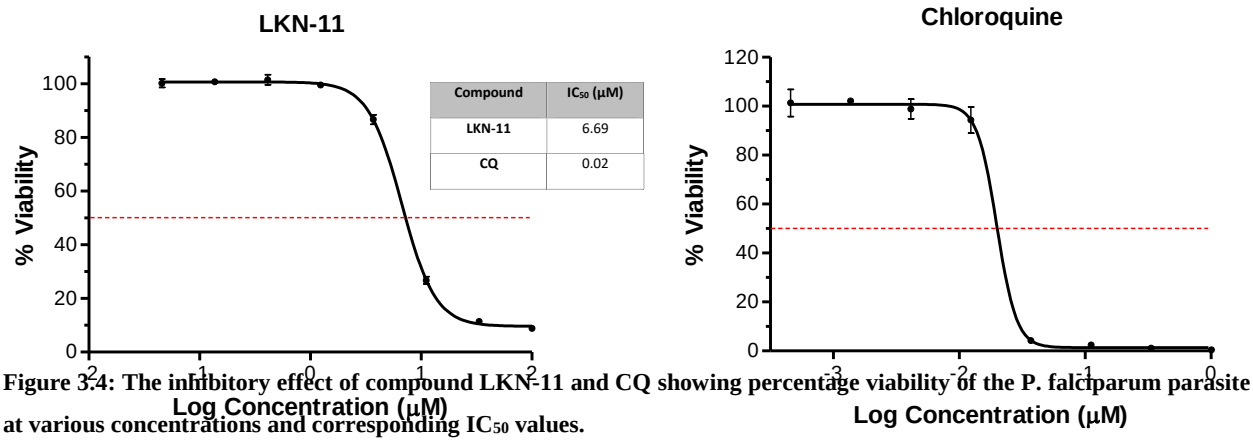

Figure 3.4: The inhibitory effect of compound LKN-11 and CQ showing percentage viability of the P. falciparum parasite at various concentrations and corresponding IC_{50} values.

3.3 Conclusion

In summary, the synthesised compounds were biologically evaluated for cytotoxicity and antiplasmodial activity using HeLa and 3D7 CQS strain of the human malaria parasite *P. falciparum*. Compound **LKN-10** showed a significant cytotoxic effect on the viability of HeLa cells, and inhibited the cell growth of HeLa cells with the IC_{50} value of 9.59 µM. Compound **LKN-11** produced a significant decrease in pLDH with a percentage parasite viability of 37. 6% at 20 , and displayed moderate activity against 3D7 sensitive strain of *P. falciparum* with IC_{50} of 6.69 µM. The only difference in structure of **LKN-11** in comparison to the other diaryl phenol thiosemicarbazones is the methoxy group, and the reason for the effectiveness of **LKN-11** may be linked to the methoxy group. A study by Tse *et al.* showed a significant increase in potency of a compound after the addition of a methoxy group.[68] Another study by *Yadav et al*. also demonstrated that the presence of methoxy groups at position 2 and 4 in chalcone derivatives appeared to be favorable for antimalarial activity.[69] Despite low cytotoxicity risk, the rest of other compounds were not effective against 3D7 strain of *P. falciparum*. Future work should include in depth investigation into diaryl phenol thiosemicarbazones with para-substituted oxygen containing groups, as they seem to play required role in the degradation of malaria.

CHAPTER 4
EXPERIMENTAL PROCEDURES AND METHODS

4.1 Experimental and general methods

All chemicals and solvents used in the synthesis of compounds were obtained from Sigma-Aldrich (Pty) Ltd. and Merck (Pty) Ltd. and were used without further purification. Compounds were purified by column chromatography using silica gel 60 Å, 70 – 230 mesh (0.068 – 0.2 mm) from Merck. The ^{1}H and ^{13}C NMR spectra were recorded on Bruker Biospin 300, Avance II 400 or Avance II 600 MHz spectrometers at room temperature unless stated otherwise. The deuterated solvents were used in the analysis of various compounds and these included DMSO-d_6 with chemical shifts of 2.5 ppm in ^{1}H and 39.5 ppm in ^{13}C NMR, and $CDCl_3$-*d* with chemical shifts of 7.26 ppm in ^{1}H and 77.2 ppm in ^{13}C NMR. The spectra were processed using MestReNova version 11.0 software and the chemical shifts were recorded in parts per million (ppm) and the *J*-coupling constants are in Hertz (Hz). The high-resolution mass spectrometry (HRMS) analysis was performed on a Waters Synapt G2 Mass spectrometer using electron spray ionization in the positive ionization mode (ESI+), Central Analytical Facilties (CAF), Stellenbosch University. The infrared (IR) spectra were recorded on PerkinElmer 100 FT-IR Spectrometer. Elemental microanalysis was performed on Elementar Analysensysteme varioMICRO V1.6.2 GmbH analysis system. Melting points were determined using Stuart melting point apparatus SMP30 and were reported as obtained.

For screening compound LKN-11 against malaria parasites, the compound was added to parasite cultures in 96-well plates and incubated for 48h in a 37 ºC CO_2 incubator. The compound was tested in a range extending from 100 µM to 0.0457 µM (3 fold-dilution series). For each compound concentration, the % parasite viability was calculated. Compound **LKN-11** was tested in triplicate wells, and a standard deviation (SD) was derived. For each compound, percentage viability is then plotted against Log (compound concentration) and the IC_{50} (50% inhibitory concentration) obtained from the resulting dose-response curve by non-linear regression. For comparative purposes, Chloroquine was used as a drug standard (duplicate) and yields IC_{50} values in the range 0.01-0.05 µM. It can be seen in the results observed in the table and graph below that the higher the concentration of LKN-11 the lower the % viability.

4.2 General Procedure for quinolone thiosemicarbazones

A mixture of anilines **1a-d** (0.044 mol) and triethylamine (0.066 mol) in DCM (20 mL) was stirred on an ice bath. Thereafter, acetyl chloride (0.044 mol) in DCM (30 mL) was added dropwise and the reaction was allowed to stir for five hours at room temperature. Water-DCM extraction was performed using a separating funnel and the bottom layer was collected, this extraction was performed 2-3 times to ensure as much of the desired product was extracted. The collected product was dried using a drying tube while the mixture was heating over a hotplate, the remaining solvent was removed using the rotary evaporator. Purification of the product was performed by recrystallization using water and ethanol as solvents.

_N_-Phenylacetamide (3a)

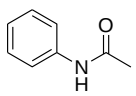

Brown solid (4110 mg, 69%). M.p.: 114.8– 115.3 °C (Lit.[70] 111 – 115 °C). ^{1}H NMR (300 MHz, DMSO-*d*$_6$): δ_H = 9.95 (s, 1H, NH), 7.59 (d, *J* = 9.0 Hz, 2H, Ar-H), 7.28 (t, *J* = 9.0 Hz, 2H, Ar-H), 7.01 (t, *J* = 6.0 Hz, 1H, Ar-H), 2.04 (s, 1H, CH_3); ^{13}C NMR (75 MHz, DMSO-*d*$_6$): δ_C = 172.4, 168.3, 139.4, 128.7, 122.9, 119.0, 24.1.

N-(4-Methoxyphenyl)acetamide (4a)

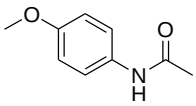

Silver solid (11.32 g, 87%). M.p.: 127.5 – 128.2 °C (Lit.[71] 128 – 130 °C). ^{1}H NMR (300 MHz, DMSO-*d*$_6$): δ_H = 10.37 (s, 3H, O-CH_3), 10.22 (s, 3H, CH_3), 8.98 (s, 1H, NH), 8.27 (d, *J* = 9.0 Hz, 1H, Ar-H), 7.99 (dd, *J* = 6.0 Hz, 2H, Ar-H), 7.75 (t, *J* = 9.0 Hz, 1H, Ar-H); ^{13}CNMR (75 MHz, DMSO-*d*$_6$): δ_C = 166.7, 131.0, 122.05, 114.04, 55. 5, 24.3.

N-(p-Tolyl)acetamide (5a)

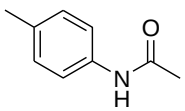

Orange solid (5.15 g, 71%). M.p.: 148.8 – 150 °C (Lit.[72,73] 148 – 151 °C). ^{1}HNMR (300 MHz, DMSO-*d*$_6$): δ_H = 10.04 (s, 1H, NH), 7.72 (d, *J* = 9.0 Hz, 2H, Ar-H), 7.35 (d, *J* = 9.0 Hz, 2H, Ar-H), 2.36 (s, 3H, Ar-CH_3), 2.30 (s, 3H, CH_3); ^{13}CNMR (75 MHz, DMSO-*d*$_6$): δ_C = 168.5, 137.3, 132.3, 129.4, 119.5, 24.3, 20.8.

N-(4-Chlorophenyl)acetamide (6a)

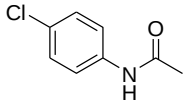

White solid (9.83 g, 74%). M.p.: 176.9 – 178.2 °C (Lit.[74] 178 – 179 °C). ^{1}HNMR (300 MHz, DMSO-d_6): δ_H = 7.64 (s, 1H, NH), 7.45 (d, 2H, J = 9.0 Hz, Ar-H), 7.24 (d, J = 6.0 Hz, 2H, Ar-H), 2.15 (s, 3H, CH_3); ^{13}CNMR (75 MHz, DMSO-d_6): δ_C = 168.6, 136.5, 129.2, 128.9, 121.1, 50.8.

4.3 General procedure for synthesis of chloroquinoline carbaldehyde derivatives

A flask containing DMF (20 mL) was cooled in ice to 0 °C. Thereafter, phosphorus oxychloride ($POCl_3$) (0.12 mol) was added dropwise under nitrogen and the resultant reaction mixture was warm up to room temperature and heated at 70 °C for about 10 minutes. After cooling down in ice to 35 °C, acetanilides **3a-6a** (0.03 mol) were each slowly added to the reaction mixture, which was allowed to warm to room temperature and stirred for five hours at 80 ºC under nitrogen. The solution was poured into a beaker filled halfway with ice and allowed to stir until a precipitate formed. The precipitate was filtered, wash with ice cold water and dried to give desired aldehydes.

2-Chloroquinoline-3-carbaldehyde (3b)

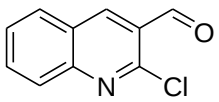

Yellow solid (1.04 g, 18%). M.p.: 149.4 – 150.2 °C (Lit.[75,76] 148– 150 °C). ^{1}H NMR (300 MHz, DMSO-d_6): δ_H = 10.37 (s, 1H, CHO), 8.98 (s, 1H, Ar-H), 8.28 (d, J = 9.0 Hz, 1H, Ar-H), 8.01 (t, J = 3.0 Hz, 1H, Ar-H), 7.97 (dd, J = 3.0 and 6.0 Hz, 1H, Ar-H), 7.75 (t, J = 9.0 Hz, 1H, Ar-H). ^{13}C NMR (75 MHz, DMSO-d_6): δ_C = 189.8, 149.5, 148.9, 141.8, 134.3, 130.7, 128.7, 128.2, 127.8, 126.4.

2-Chloro-6-methoxyquinoline-3-carbaldehyde (4b)

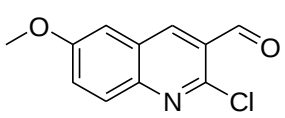

Orange solid (0.76 g, 11%). M.p.: 147.1 – 148 °C (Lit.[77] 146 – 151 °C). ^{1}H NMR (300 MHz, DMSO-d_6): δ_H = 10.46 (s, 1H, CHO), 8.19 (s, 1H, Ar-H), 7.75 (d, J = 9.0 Hz, 2H, Ar-H), 7.62 (d, J = 9.0 Hz, 1H, Ar-H), 7.19 (s, 1H, Ar-H), 3.84 (s, 3H, O-CH_3); ^{13}C NMR (75 MHz, DMSO-d_6): δ_C = 163.8, 159.1, 156.9, 143.75, 137.9, 135.8, 130.0, 129.6, 116.2, 114.6, 55.5.

2-Chloro-6-methylquinoline-3-carbaldehyde (5b)

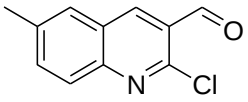

Orange solid (0.34 g, 6%). M.p.: 123 – 124.7 °C (Lit.[78] 120 – 125 °C). ^{1}H NMR (300 MHz, DMSO-*d*$_6$): δ_H = 10.15 (s, 1H, CHO), 8.55 (s, 1H, Ar-H), 7.55 (d, *J* = 9.0 Hz, 1H, Ar-H), 7.47 (d, *J* = 9.0 Hz, 1H, Ar-H), 7.08 (d, *J* = 9.0 Hz, 1H, Ar-H), 2.23 (s, 1H, CH_3); ^{13}C NMR (75 MHz, DMSO-*d*$_6$): δ_C = 137.3, 132.2, 130.9, 130.5, 129.8, 129.4, 120.5, 120.1, 119.5, 31.2, 20.9.

2,6-Dichloroquinoline-3-carbaldehyde (6b)

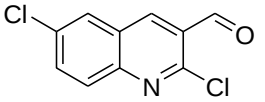

Brown solid (5.13 g, 83%). M.p.: 189.8 – 191.2 °C (Lit.[79] 191 – 192 °C). ^{1}H NMR (300 MHz, DMSO-*d*$_6$): δ_H = 10.55 (s, 1H, CHO), 8.67 (s, 1H, Ar-H), 7.91 (d, *J* = 3.0 Hz, 1H, Ar-H), 7.76 (d, *J* = 3.0 Hz, 1H, Ar-H), 7.73 (d, *J* = 3.0 Hz, 1H, Ar-H); ^{13}C NMR (75 MHz, DMSO-*d*$_6$): δ_C = 188.9, 150.3, 147.9, 139.3, 134.5, 134.1, 130.1, 128.2, 127.2, 126.9.

4.4 General procedure for synthesis of 2-methoxyquinoline-3-carbaldehyde derivatives

Potassium hydroxide (4.0 mmol) was added to methanol (10 mL) to a solution of **3b-6b** (3.0 mmol) in methanol (40 mL). The resultant reaction mixture was allowed reflux in methanol for two hours. Thereafter, water (10 mL) was added and the mixture left stirring at room temperature until the precipitates formed, which was filtered, washed with ice cold water and dried overnight.

2-Methoxyquinoline-3-carbaldehyde (3c)

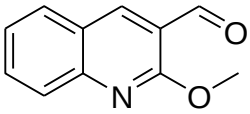

Pale yellow solid (250 mg, 51%). M.p.: 91.8 – 92.3 °C (Lit.[80] 92 – 93 °C). ^{1}H NMR (300 MHz, $CDCl_3$): δ_H = 10.46 (s, 1H, OCH), 8.55 (s, 1H, Ar-H), 7.87 (d, *J* = 9.0 Hz, 1H, Ar-H), 7.43 (q, *J* = 6.0 Hz, *J* = 3.0 Hz, 1H, Ar-H), 7.11 (d, *J* = 3.0 Hz, 1H, Ar-H), 7.03 (d, *J* = 3.0 Hz, 1H, Ar-H); ^{13}C NMR (75 MHz, $CDCl_3$): δ_C = 189.9, 158.9, 147.8, 145.9, 138.8, 129.9, 127.8, 126.4, 106.5, 55.9.

2,6-Dimethoxyquinoline-3-carbaldehyde (4c)

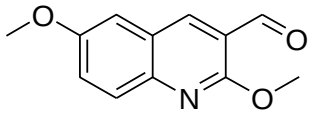

Yellow solid (530 mg, 64%). M.p.: 122 – 123.8 °C (Lit.[81] 121 – 125 °C). ^{1}H NMR (300 MHz, $CDCl_3$): δ_H = 10.46 (s, 1H, CHO), 8.55 (s, 1H, Ar-H), 7.88 (d, *J* = 9.0 Hz, 1H, Ar-H), 7.43 (dd, *J* = 3.0 and 6.0 Hz, 1H, Ar-H), 7.11 (d, *J* = 3.0 Hz, 1H, Ar-H), 7.03 (d, *J* = 3.0 Hz, 1H, Ar-H), 4.07 (s, 3H, OCH_3), 3.87 (s, 3H, OCH_3); ^{13}C NMR (75 MHz, $CDCl_3$): δ_C = 189.6, 158.9, 147.8, 145.9, 138.8, 129.9, 127.8, 126.4, 106.5, 55.9.

2-Methoxy-6-methylquinoline-3-carbaldehyde (5c)

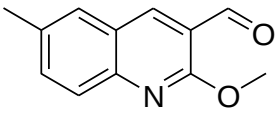

Brown solid, Yield (180 mg, 15%). M.p.: 144.2 – 145.9 °C (Lit.[82] 113 – 115 °C). ^{1}H NMR (300 MHz, $CDCl_3$): δ_H = 9.99 (s, 1H, CHO), 8.34 (s, 1H, Ar-H), 7.47 (d, *J* = 9.0 Hz, 1H, Ar-H), 7.08 (d, *J* = 9.0 Hz, 1H, Ar-H), 3.39 (s, 3H, OCH_3), 2.52 (s, 3H, CH_3); ^{13}C NMR (75 MHz, $CDCl_3$): δ_C = 197.2, 160.4, 148.1, 147.4, 143.7, 140.1, 134.6, 134.1, 131.1, 130.7, 55.1, 21.5.

6-Chloro-2-methoxyquinoline-3-carbaldehyde (6c)

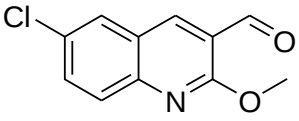

Brown solid. Yield (700 mg, 26.1%). M.p.: 182.1 – 183.2 °C. ^{1}H NMR (300 MHz, $CDCl_3$): δ_H = 10.43 (s, 1H, CHO), 8.47 (s, 1H, Ar-H), 7.84 (d, *J* = 3.0 Hz, 1H, Ar-H), 3.44 (s, 3H, OCH_3); ^{13}C NMR (75 MHz, $CDCl_3$): δ_C = 189.4, 165.2, 151.2, 134.1, 132.5, 130.0, 128.5, 128.1, 126.4, 124.3, 51.4.

4.5 General procedure for synthesis of substituted bromophenols

The substituted phenol (~500 mg) was dissolved in chloroform (10 mL) and allowed to stir for 5 minutes in an ice bath. A 1 molar equivalent of bromine was dissolved in chloroform (2 mL) and added dropwise to the phenol mixture in chloroform. Thereafter, the reaction mixture was allowed warm to room temperature and left stirring overnight. The mixture was dried using a drying tube and water was added to remove excess unreacted bromine, the solid was allowed to dry in a drying fume hood overnight.

4-Bromo-2-isopropylphenol (1.1)

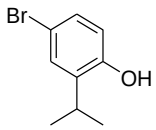

Yellow solid (540 mg, 72%). M.p.: 47.5 – 48.3 °C (Lit.[83] 48 – 49 °C). ^{1}H NMR (400 MHz, DMSO-d_6): δ_H = 9.98 (s, 1H, Ar-OH), 7.29 (d, *J* = 4.0 Hz, 1H, Ar-H), 7.03 (dd, *J* = 4.0 and 12.0 Hz, 1H, Ar-H), 6.86 (d, *J* = 8.0 Hz, 1H, Ar-H), 3.45 (s, 6H, CH_3), 2.77 (q, *J* = 12.0 Hz, 1H, CH); ^{13}C NMR (100 MHz, DMSO-d_6): δ_C = 152.0, 140.8, 130.4, 126.6, 116.3, 109.1, 32.4, 24.1, 23.8.

2-*B*romo-4-methoxyphenol (1.2)

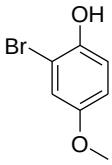

Dark brown solid (568 mg, 57%). M.p.: 42 – 43.7 °C (Lit.[84] 43 – 47 °C). ^{1}H NMR (400 MHz, DMSO-*d*$_6$): δ_H = 7.06 (s, 1H, Ar-H), 6.98 (d, *J*= 4.0 Hz, 1H, Ar-H), 6.77 (dd, *J*= 4.0 Hz and 8.0 Hz, 1H, Ar-H), 5.68 (s, 1H, Ar-OH), 3.85 (s, 3H, OCH_3); ^{13}C NMR (100 MHz, DMSO-*d*$_6$): δ_C = 151.3, 150.6, 115.3, 115.2, 114.8, 111.8, 57.4.

2-Bromo-4-nitrophenol (1.3)

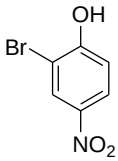

Dark orange solid (2.56 g, 85%). M.p.: 112 – 113.2 °C (Lit.[85] 111 – 115 °C). ^{1}H NMR (400 MHz, DMSO-*d*$_6$): δ_H = 8.37 (s, 1H, Ar-OH), 8.34 (d, *J* = 4.0 Hz, 1H, Ar-H), 8.12 (dd, *J* = 4.0 and 12.0 Hz, 1H, Ar-H), 7.09 (s, 1H, Ar-OH); ^{13}C NMR (100 MHz, DMSO-*d*$_6$): δ_C = 160.7, 139.9, 128.9, 125.2, 115.9, 111.1.

2-Bromo-4-(tert-butyl)phenol (1.4)

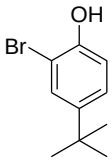

Yellow liquid (422 mg, 42%). M.p.: 55 – 55.9 °C (Lit.[86,87] 51 °C). ^{1}H NMR (400 MHz, DMSO-*d*$_6$): δ_H = 11.97 (s, 1H, Ar-OH), 8.36 (d, *J* = 12.0 Hz, 1H, Ar-H), 8.12 (dd, *J* = 4.0 and 8.0 Hz, 1H, Ar-H), 7.10 (d, *J* = 8.0 Hz, 1H, Ar-H), 1.98 (s, 9H, CCH_3); ^{13}C NMR (100 MHz, DMSO-*d*$_6$): δ_C = 161.1, 140.3, 129.2, 125.6, 116.3, 109.8, 35.8, 31.1.

4.6 Synthesis of Bromo-hydroxybenzaldehydes

The brominated phenol (183 mmol) dissolved in acetonitrile (28 mL) was treated with magnesium chloride (2 mol eq), paraformaldehyde (7 mol eq) and triethylamine (3 mol eq). The reaction mixture was heated under reflux for 3 hours. Thereafter, hydrochloric acid (1 N) was added to the resulting reaction mixture and the product extracted with ethyl acetate (4 × 20 mL). The organic layer was washed with aqueous sodium chloride and dried using magnesium sulphate, which was filtered and solvent reduced a rotary evaporator to give an oily residue. The residue was purified using column chromatography with a mobile phase of 90% Petroleum Ether: 10% Ethyl Acetate.

3-Bromo-2-hydroxy-5-isopropylbenzaldehyde (2.1)

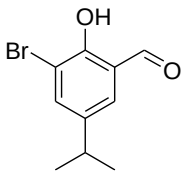

Pale yellow solid (198 mg, 37%). M.p.: 135.4 – 136.7 °C. ^{1}H NMR (400 MHz, $CDCl_3$): δ_H = 11.12 (s, 1H, Ar-OH), 10.02 (s, 1H, CHO), 7.74 (d, *J* = 4.0 Hz, 1H, Ar-H), 7.11 (d, *J* = 4.0 Hz, 1H, Ar-H), 3.43 (s, 6H, CCH_3); ^{13}C NMR (100 MHz, $CDCl_3$): δ_C = 193.1, 158.1, 144.2, 134.5, 125.4, 120.9, 109.8, 35.4, 27.1.

5-Bromo-2-hydroxy-3-methylbenzaldehyde (2.2)

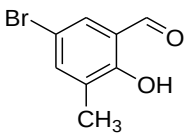

Orange solid (240 mg, 61%). M.p.: 111 – 112.4 °C. ^{1}HNMR (400 MHz, $CDCl_3$): δ_H = 11.38 (s, 1H, CHO), 9.80 (s, 1H, Ar-OH), 7.67 (d, *J* = 4.0 Hz, 1H, Ar-H), 7.32 (d, *J*= 4.0 Hz, 1H, Ar-H), 2.33 (s, 3H, Ar- CH_3); ^{13}CNMR (100 MHz, $CDCl_3$): δ_C = 196.1, 156.0, 140.8, 133.0, 130.6, 121.0, 110.9, 20.2.

3-Bromo-2-hydroxy-5-nitrobenzaldehyde (2.3)

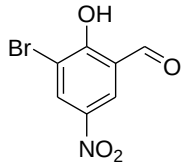

Orange solid (582.7 mg, 23%). M.p.: 152 - 153 °C (Lit.[88] 149 – 150 °C). ^{1}H NMR (400 MHz, $CDCl_3$): δ_H = 8.42 (dd, *J* = 4.0 Hz and 8.0 Hz, 1H, Ar-H), 7.12 (d, *J* = 4.0 Hz, 1H, Ar-H); ^{13}C NMR (100 MHz, $CDCl_3$): δ_C = 195.2, 168.3, 145.8, 129.5, 125.0, 118.4, 111.8.

4.7 General procedure for synthesis of phenylbenzaldehydes

A solution of the bromo-hydroxy-benzaldehyde (15.6 mmol) in dimethoxyethane (30 mL) and water (10 mL) was purged with nitrogen for about 15 minutes. Subsequently, K_2CO_3 (23.2 mmol), phenylboronic acid (15.5 mmol) and tetrakis(triphenylphosphine)palladium (0) (0.675 mmol) were added and the reaction mixture was heated to reflux under nitrogen overnight. The reaction mixture was filtered over celite to give a solution, which was dried using magnesium sulphate and the solvent was concentrated using a rotary evaporator to give a solid residue. The residue was purified using silica gel column chromatography with a mobile phase of 90% Petroleum Ether: 10% Ethyl Acetate to give a purified solid compound.

4-Hydroxy-[1,1'-biphenyl]-3-carbaldehyde (3.1)

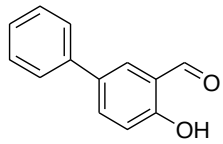

Mustard solid (423.8 mg, 42%). M.p.: 118.5 – 119.2 °C (Lit.[89] 99 – 101 °C). ^{1}H NMR (400 MHz, DMSO-d_6): δ_H = 10.31 (s, 1H, Ar-OH), 7.92 (s, 1H, Ar-H), 7.84 (d, *J* = 8.0 Hz, 1H, Ar-H), 7.62 (d, *J* = 8.0 Hz, 2H, Ar-H), 7.44 (t, *J* = 8.0 Hz, 3H, Ar-H), 7.33 (t, *J* = 4.0 Hz, Ar-H), 7.10 (d, *J* = 4.0 Hz, 1H, Ar-H); ^{13}C NMR (100 MHz, DMSO-d_6): δ_C = 191.8, 160.3, 134.7, 129.1, 127.5, 127.2, 127.1, 126.8, 126.2, 122.5, 118.1.

4'-Chloro-4-hydroxy-[1,1'-biphenyl]-3-carbaldehyde (3.7)

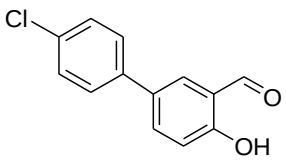

Brown solid (77.7 mg, 8%). M.p.: 98.4 – 98.9 °C (Lit.[90,91] 85 – 87 °C). ^{1}H NMR (400 MHz, DMSO-d_6): δ_H = 11.34 (s, 1H, Ar-OH), 10.24 (s, 1H, CHO), 8.10 (s, 1H, Ar-H), 7.72 (d, J = 8.0 Hz, 2H, Ar-H), 7.58 (dd, J = 4.0 and 8.0 Hz, 1H, Ar-H), 7.32 (d, J = 8.0 Hz, 1H, Ar-H),7.14 (d, J = 8 .0 Hz, 1H, Ar-H); ^{13}C NMR (100 MHz, DMSO-d_6): δ_C = 182.2, 161.4, 140.6, 137.2, 132.1, 131.5, 129.1, 127.5, 121.2, 118.5, 115.9.

4-Hydroxy-4'-(trifluoromethoxy)-[1,1'-biphenyl]-3-carbaldehyde (3.10)

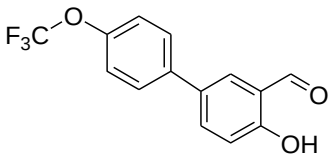

White solid. Yield (350 mg, 23%). M.p.: 132 – 132.8 °C. ^{1}H NMR (400 MHz, DMSO-d_6): δ_H = 11.42 (s, 1H, Ar-OH), 10.91 (s, 1H, CHO), 8.11 (s, 1H, Ar-H), 7.89 (dd, J = 4.0 and 8.0 Hz, 1H, Ar-H), 7.72 (d, J = 8.0 Hz, 2H, Ar-H), 7.57 (d, J = 8.0 Hz, 2H, Ar-H), 7.19 (d, J = 8.0 Hz, 1H, Ar-H); ^{13}C NMR (75 MHz, DMSO-d_6): δ_C = 195.1, 165.1, 152.9, 141.0, 136.9, 135.1, 133.2, 130.5, 127.7, 125.2, 124.9, 122.1, 120.2.

4-Hydroxy-4'-methoxy-[1,1'-biphenyl]-3-carbaldehyde (3.11)

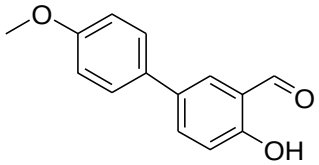

Yellow solid (380 mg, 25.3%). M.p.: 110.8 – 111.5°C. ^{1}H NMR (400 MHz, DMSO-d_6): δ_H = 10.51 (s, 1H, Ar-OH), 9.87 (s, 1H, CHO), 8.03 (s, 1H, Ar-H), 7.93 (dd, J = 4.0 and 8.0 Hz, 1H, Ar-H), 7.77 (d, J = 4.0 Hz, 2H, Ar-H), 7.29 (d, J = 8.0 Hz, 1H, Ar-H), 7.12 (d, J = 8.0 Hz, 2H, Ar-H), 3.82 (s, 3H, OCH_3); ^{13}C NMR (100 MHz, DMSO-d_6): δ_C = 197.2, 172.3, 170.7, 142.1, 139.9, 138.2, 136.9, 133.2, 124.7, 120.2, 117.9, 55.9.

4'-Bromo-4-hydroxy-[1,1'-biphenyl]-3-carbaldehyde (3.12)

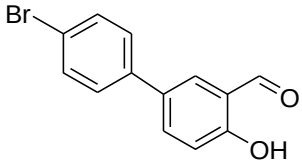

Yellow solid (550 mg, 28%). M.p.: 103 – 103.7 °C. ^{1}H NMR (400 MHz, DMSO-d_6): δ_H = 10.98 (s, 1H, Ar-H), 9.52 (s, 1H, CHO), 8.14 (s, 1H, Ar-H), 7.85 (d, J = 8.0 Hz, 2H, Ar-H), 7.57 (dd, J = 4.0 and 8.0 Hz, 2H, Ar-H), 7.41 (d, J = 4.0 Hz, 1H, Ar-H), 7.12 (d, J = 8.0 Hz, 1H, Ar-H); ^{13}CNMR (100 MHz, DMSO-d_6): δ_C = 189.2, 163.9, 147.2, 146.8, 140.7, 129.1, 122.0, 119.2, 117.4.

4-Hydroxy-4'-(methylthio)-[1,1'-biphenyl]-3-carbaldehyde (3.13)

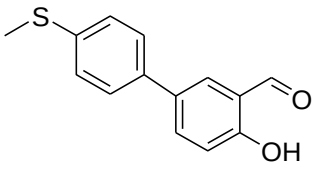

Dark orange solid (130 mg, 8%). M.p.: 117.3 – 118.9 °C. ^{1}H NMR (400 MHz, DMSO-d_6): δ_H = 12.26 (s, 1H, Ar-OH), 8.11 (d, J = 4.0 Hz, 1H, Ar-H), 7.78 (dd, J = 4.0 and 8.0 Hz, 1H, Ar-H), 7.61 (d, J = 8.0 Hz, 2H, Ar-H), 7.40 (t, J = 8.0 Hz, 2H, Ar-H), 7.29 (t, J = 8.0 Hz, 1H, Ar-H), 6.98 (d, J = 8.0 Hz, 1H, Ar-H), 2.72 (s, 3H, SCH_3); ^{13}C NMR (100 MHz, DMSO-d_6): δ_C = 161.8, 139.9, 135.1, 132.1, 129.6, 128.9, 127.2, 126.7, 119.9, 118.5, 26.3.

4'-Fluoro-4-hydroxy-[1,1'-biphenyl]-3-carbaldehyde (3.14)

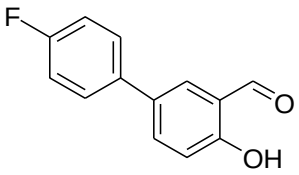

Yellow solid. Yield (461 mg, 23%). M.p.: 122.1 – 123.5 °C (Lit.[92] 91 – 93 °C). ^{1}H NMR (400 MHz, DMSO-d_6): δ_H = 10.01 (s, 1H, Ar-OH), 9.82 (s, 1H, CHO), 8.31 (s, 1H, Ar-H), 7.84 (t, J = 8.0 Hz, 2H, Ar-H), 7.63 (d, J = 4.0 Hz, 1H, Ar-H), 7.37 (t, J = 4.0 Hz, 2H, Ar-H), 7.21 (d, J = 8.0 Hz, 1H, Ar-H); ^{13}C NMR (100 MHz, DMSO-d_6): δ_C = 197.9, 164.2, 163.1, 140.4, 136.9, 135.9, 134.2, 132.0, 124.2, 121.9, 121.9, 118.5, 118.1.

4.8 General procedure for synthesis of thiosemicarbazone derivatives

Thiosemicarbazide (0.70 mmol) was dissolved in warm methanol (5 mL) followed by a catalytic amount of acetic acid. Subsequently, aldehyde **4a-d** (0.7 mmol) were each added into the reaction mixture and then allowed to reflux for 1 hour. Upon cooling the solution to ambient temperature, the precipitate was filtered using gravity filtration and the solid product was allowed to dry in a drying fume hood.

(E)-2-((2-Methoxy-6-methylquinolin-3-yl)methylene)hydrazine-1-carbothioamide (LKN-3)

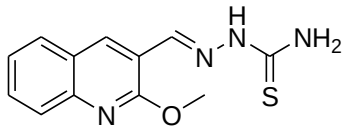

Off white solid (130 mg, 41%). M.p.: 275.1 – 276.8 °C. ν_{max}(IR)/cm^{-1} 3250 and 3100 (NH and NH_2), 1600 (C=N), 1100 (C-O); ^{1}H NMR (300 MHz, DMSO-d_6): δ_H = 11.69 (s, 1H, NH), 9.05 (s, 1H, HCN), 8.38 (s, 1H, NH_2'), 8.19 (s, 1H, NH_2'), 7.81 (d, J = 6.0 Hz, 2H, Ar-H), 7.67 (d, J = 6.0 Hz, 1H, Ar-H), 7.46 (t, J = 3.0 Hz, 1H, Ar-H), 4.04 (s, 3H, O-CH_3), 3.37 (s, 1H, Ar-H); ^{13}C NMR (75 MHz, DMSO-d_6): δ_C = 178.2, 159.3, 148.7, 146.0, 135.9, 134.8, 130.5, 128.3, 126.7, 124.8, 118.6, 53.7. m/z (ESI$^+$) calcd for $C_{12}H_{13}N_4OS$ $[M+H]^+$: 261.0805, found 261.0816; EA: Calcd (%) C (55.37), H (4.65), N (21.52), S (12.32). Found C (54.77), H (4.49), N (21.00), S (12.19).

(E)-2-((2,6-Dimethoxyquinolin-3-yl)methylene)hydrazine-1-carbothioamide (LKN-4)

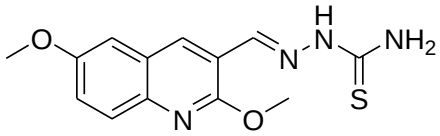

Yellow solid (150 mg, 20%). M.p.: 242.3 – 243.5 °C. ν_{max}(IR)/cm^{-1} 3200 and 3150 (NH and NH_2), 1550 (C=N), 1200 and 1050 (C-O); ^{1}H NMR (300 MHz, DMSO-d_6): δ_H = 11.77 (s, 1H, NH), 9.92 (s, 1H, HCN), 8.47 (s, 1H, NH_2'), 7.85 (d, *J* = 3.0 Hz, 1H, Ar-H), 7.55 (s, 1H, NH_2'), 7.28 (d, *J*= 6.0 Hz, 1H, Ar-H), 7.02 (dd, *J*= 3.0 and 6 Hz, 1H, Ar-H), 6.77 (d, *J*= 3.0 Hz, 1H, Ar-H), 3.89 (s, 3H, O-CH_3), 3.52 (s, 3H, O-CH_3). ^{13}C NMR (75 MHz, DMSO-d_6): δ_C = 178.8, 168.9, 158.4, 143.5, 139.6, 137.5, 129.1, 128.6, 123.5, 119.5, 107.1, 31.1, 24.4. *m/z* (ESI$^+$) calcd for $C_{13}H_{14}N_4O_2S$ $[M+H]^+$: 291.0910, found 291.0923; EA: Calcd (%) C (53.78), H (4.86), N (19.30), S (11.04). Found C (56.94), H (2.09), N (12.89), S (7.01)

(E)-2-((2-Methoxy-6-methylquinolin-3-yl)methylene)hydrazine-1-carbothioamide (LKN-5)

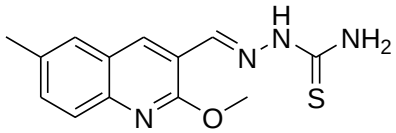

Orange solid (110 mg, 91%). M.p.: 315.1 – 315.8 °C. ν_{max}(IR)/cm^{-1} 2900 (CH_3), 1600 (C=N), 1100 (C-O); ^{1}HNMR (300 MHz, DMSO-d_6): δ_H = 9.85 (s, 1H, HCN), 9.16 (s, 1H, NH_2'), 7.91 (s, 1H, NH_2'), 7.50 (d, *J* = 3.0 Hz, 1H, Ar-H), 7.42 (d, *J* = 6.0 Hz, 1H, Ar-H), 7.35 (dd, *J*= 3.0 and 9 Hz, 2H, Ar-H), 3.50 (s, 3H, O-CH_3), 2.07 (s, 3H, Ar- CH_3); ^{13}CNMR (75 MHz, DMSO-d_6): δ_C = 178.8, 173.2, 167.5, 158.8, 156.6, 154.4, 152.4, 138.4, 137.2, 129.5, 119.5, 55.8, 31.1. *m/z* (ESI$^+$) calcd for $C_{13}H_{14}N_4OS$ $[M+H]^+$: 275.0961, found 239.1552; EA: Calcd (%) C (59.92), H (5.14), N (20.42), S (11.69). Found C (58.48), H (4.88), N (19.56), S (10.97).

(E)-2-((6-Chloro-2-methoxyquinolin-3-yl)methylene)hydrazine-1-carbothioamide (LKN-6)

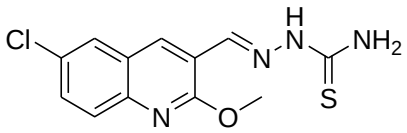

Dark brown solid (420 mg, 46%). Melting point: 293.5 – 294.2 °C. ν_{max}(IR)/cm^{-1} 1550 (C=N), 1050 (C-O); ^{1}HNMR (300 MHz, DMSO-d_6): δ_H = 11.73 (s, 1H, NH), 8.94 (s, 1H, NH_2'), 8.75 (d, *J*= 6.0 Hz, 1H, Ar-H), 8.32 (s, 1H, NH_2'), 8.15 (d, *J*= 9.0 Hz, 1H, Ar-H), 7.89 (d, *J*= 3.0 Hz, 1H, Ar-H), 7.66 (t, *J*= 3.0 Hz, Ar-H), 7.39 (dd, *J*= 3.0 and 6 Hz, 1H, Ar-H), 3.75 (s, 3H, O-CH_3); ^{13}CNMR (75 MHz, DMSO-d_6): δ_C = 178.1, 167.9, 147.8, 145.9, 130.9, 130.1, 129.7, 129.5, 126.2, 123.1, 123.0, 52.6. *m/z* (ESI$^+$) calcd for $C_{12}H_{11}ClN_4OS$ $[M+H]^+$: 294.7570, found 295.0424; EA: Calcd (%) C (48.90), H (3.76), N (19.01), S (10.88). Found C (58.70), H (2.83), N (8.52), S (2.63).

(E)-2-((4-Hydroxy-[1,1'-biphenyl]-3-yl)methylene)hydrazine-1-carbothioamide (LKN-1)

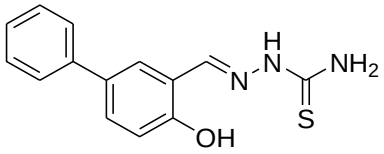

Pale yellow solid (88.7 mg, 44%). M.p.: 303.7 – 304.9 °C. ν_{max}(IR)/cm^{-1} 3400 (OH), 3200 and 3150 (NH and NH_2), 1600 (C=N); ^{1}H NMR (400 MHz, DMSO-*d*$_6$): δ_H = 11.40 (s, 1H, NH), 10.11 (s, 1H, OH), 8.43 (s, 1H, HCN), 8.22 (s, 2H, NH_2'), 8.11 (s, 1H, NH_2'), 7.65 (d, *J* = 4.0 Hz, 1H, Ar-H), 7.54 (d, *J* = 8.0 Hz, 1H, Ar-H), 7.47 (dd, *J*= 4.0 and 12.0 Hz, 2H, Ar-H), 7.41 (t, *J* = 4.0 Hz, 2H, Ar-H), 7.29 (t, *J* = 8.0 Hz, 1H, Ar-H), 6.96 (d, *J* = 4.0 Hz, 1H, Ar-H); ^{13}C NMR (100 MHz, DMSO-*d*$_6$): δ_C = 177.7, 156.2, 139.7, 139.4, 131.5, 129.5, 128.8, 126.7, 126.4, 124.3, 120.8, 116.7. *m/z* (ESI$^+$) calcd for $C_{14}H_{13}N_3OS$ $[M+H]^+$: 272.0852, found 272.0855; EA: Calcd (%) C (61.97), H (4.83), N (15.49), S (11.82). Found C (60.84), H (6.49), N (14.99), S (11.51).

(*E*)-2-(2-Hy droxy-3-nitrobenzylidene)hydrazine-1-carbothioamide (LKN-2)

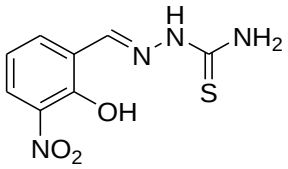

Yellow solid (364.7 mg, 84%). M.p.: 249.7 – 250.0 °C. ν_{max}(IR)/cm^{-1} 3450 (OH), 3300 and 3100 (NH and NH_2), 1615 (C=N); ^{1}H NMR (400 MHz, DMSO-*d*$_6$): δ_H = 11.55 (s, 1H, NH), 10.48 (s, 1H, OH) 8.42 (d, *J* = 4.0 Hz, 1H, HCN), 8.33 (s, 1H, NH_2'), 8.24 (s, 1H, NH_2'), 8.11 (d, *J* =4.0 Hz, 1H, Ar-H), 8.01 (t, *J* = 4.0 Hz, 1H, Ar-H), 7.06 (t, *J* = 8.0 Hz, 1H, Ar-H); ^{13}C NMR (100 MHz, DMSO-*d*$_6$): δ_C = 178.5, 151.4, 137.8, 136.9, 133.6, 126.8, 125.2, 120.2. *m/z* (ESI$^+$) calcd for $C_8H_8N_4O_3S$ $[M+H]^+$: 241.0390, found 241.0407; EA: Calcd (%) C (40.00), H (3.36), N (23.32), S (13.35). Found C (39.67), H (3.64), N (22.76), S (13.65).

(E)-2-((4'-Chloro-4-hydroxy-[1,1'-biphenyl]-3-yl)methylene)hydrazine-1-carbothioamide (LKN-7)

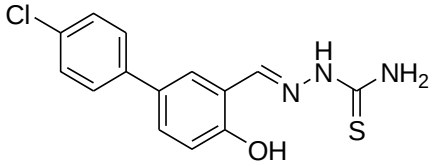

Yellow solid. Yield: (73.2 mg, 94.2%). M.p.: 191.9 – 192.5°C. ν_{max}(IR)/cm^{-1} 3400 (OH), 3250 and 3100 (NH and NH_2), 1600 (C=N); ^{1}H NMR (400 MHz, DMSO-*d*$_6$): δ_H = 11.47 (s, 1H, NH), 10.01 (s, 1H, OH), 8.48 (d, *J*= 4.0 Hz, 1H, HCN), 8.22 (s, 1H, NH_2'), 8.14 (s, 1H, NH_2'), 7.85 (dd, *J*= 4.0 and 12.0 Hz, 2H, Ar-H), 7.54 (dd, *J*= 4.0 and 8.0 Hz, 3H, Ar-H), 7.31 (d, *J*= 4.0 Hz, 1H, Ar-H), 7.12 (d, *J*= 8.0 Hz, 1H, Ar-H); ^{13}C NMR (100 MHz, DMSO-*d*$_6$): δ_C = 182.8, 161.2, 153.4, 142.7, 140.1, 134.9, 134.2, 130.6, 129.8, 126.4, 115.8,

115.3. *m/z* (ESI^+) calcd for $C_{14}H_{11}ClN_3OS$ $[M+H]^+$: 306.0462, found 279.0955; EA: Calcd (%) C (54.99), H (3.96), N (13.74), S (10.48). Found C (42.97), H (7.44), N (23.76), S (17.94).

(E)-2-(5-Bromo-2-hydroxybenzylidene)hydrazine-1-carbothioamide (LKN-8)

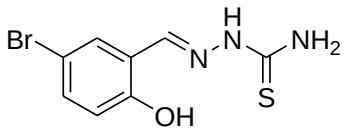

Light yellow solid (112.4 mg, 96%). M.p.: 250.1 – 251.3 °C. ν_{max}(IR)/cm^{-1} 3250 (OH), 1600 (C=N); ^{1}H NMR (400 MHz, DMSO-d_6): δ_H = 11.47 (s, 1H, NH), 9.56 (s, 1H, OH), 8.82 (s, 1H, HCN), 8.65 (s, 1H, NH_2'), 8.29 (s, 1H, NH_2'), 8.21 (d, *J* = 8.0 Hz, 1H, Ar-H), 7.58 (s, 1H, Ar-H), 7.41 (d, *J* = 4.0 Hz, 1H, Ar-H); ^{13}C NMR (100 MHz, DMSO-d_6): δ_C = 177.7, 150.3, 141.4, 134.4, 130.6, 128.3, 122.0, 111.2. *m/z* (ESI^+) calcd for $C_8H_8BrN_3OS$ $[M+H]^+$: 273.9644, found 289.976; EA: Calcd (%) C (35.05), H (2.94), N (15.33), S (11.67). Found C (37.40), H (3.48), N (14.87), S (11.72).

(E)-2-(4-Amino-2-hydroxybenzylidene)hydrazine-1-carbothioamide (LKN-9)

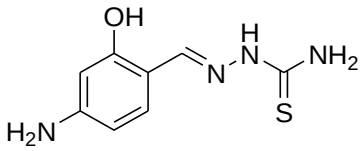

Brown solid (51.1 mg, 4%). M.p.: 191.3 - 192.9 °C. ν_{max}/ cm^{-1} 3200(OH), 1750 (C=N); ^{1}HNMR (400 MHz, DMSO-d6): δ_H = 8.63 (s, 1H, OH), 8.42 (s, 1H, HCN), 8.18 (s, 1H, NH_2'), 8.03 (s, 1H, NH_2'), 7.56 (d, *J*= 4.0 Hz, 1H, Ar-H), 7.19 (d, *J*= 4.0 Hz, 1H, Ar-H), 7.01 (dd, *J*= 4.0 and 8.0 Hz, 1H, Ar-H) 4.52 (s, 1H, Ar-NH_2'), 3.36 (s, 1H, Ar-NH_2'); ^{13}C NMR (100 MHz, DMSO-d_6): δ_C = 182.8, 161.4, 158.2, 157.0, 132.1, 110.2, 106.5, 104.8. *m/z* (ESI^+) alcd for $C_8H_{10}N_4OS$ $[M+H]^+$: 211.0648, found 211.0654 ; EA: Calcd (%) C (45.70), H (4.79), N (26.65), S (15.25). Found C (18.93), H (5.38), N (40.87), S (31.24).

(E)-2-((4-Hydroxy-4'-(trifluoromethoxy)-[1,1'-biphenyl]-3-yl)methylene)hydrazine-1-carbothioamide (LKN-10*)*

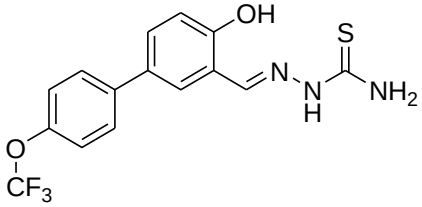

Peach solid (270 mg, 77%). M.p.: 342.2 – 343.0 °C. ν_{max}(IR)/cm^{-1} 3300 and 3250 (NH and NH_3), 3150 (OH), 1650 (C=N), 1100 (C-O); ^{1}H NMR(400 MHz, DMSO-d_6): δ_H = 11.41 (s, 1H, NH), 10.19 (s, 1H, OH), 8.41 (s, 1H, HCN), 8.26 (s, 1H, NH_2'), 8.14 (s, 1H, NH_2'), 7.78 (dd, *J* = 4.0 and 12.0 Hz, 2H, Ar-H), 7.55 (d, *J* = 8.0 Hz, 2H, Ar-H), 7.39 (dd, *J* = 4.0 and 12.0 Hz, 1H, Ar-H), 7.21 (d, *J*= 4.0 Hz, 1H, Ar-H), 7.08 (d, *J* = 8.0 Hz, 1H, Ar-H); ^{13}C NMR (75 MHz, DMSO-d_6): δ_C = 177.8,

156.5, 147.3, 139.2, 138.9, 131.2, 130.1, 129.5, 128.2, 124.5, 121.4, 120.9, 119.4, 116.7. *m/z* (ESI^+) calcd for $C_{15}H_{12}F_3N_3O_2S$ $[M+H]^+$: 356.0675, found 356.0674; EA: Calcd (%) C (50.70), H (3.40), N (11.83), S (9.02). Found C (44.4), H (3.82), N (17.80), S (14.23).

(E)-2-((4-Hydroxy-4'-methoxy-[1,1'-biphenyl]-3-yl)methylene)hydrazine-1-carbothioamide (LKN-11)

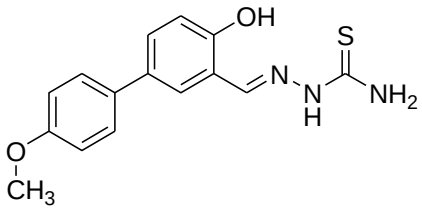

Pale yellow solid (68.4 mg, 18%). M.p.: 313.6 – 314.5 °C. ν_{max}(IR)/cm^{-1} 3400 and 3350 (NH and NH_2), 1550 (C=N), 1200 (C-O); ^1H NMR (300 MHz, DMSO-d_6): δ_H = 11.41 (s, 1H, NH), 10.01 (s, 1H, OH), 8.43 (s, 1H, HCN), 8.31 (s, 1H, NH_2'), 8.22 (s, 1H, NH_2'), 7.84 (d, *J* = 8.0 Hz, 2H, Ar-H), 7.62 (dd, *J* = 4.0 and 8.0 Hz, 1H, Ar-H), 7.49 (dd, *J* = 4.0 and 12.0 Hz, 1H, Ar-H), 6.98 (d, *J* = 8.0 Hz, 1H, Ar-H), 6.94 (dd, *J* = 4.0 and 8.0 Hz, 2H, Ar-H), 3.78 (s, 3H, O-CH_3); ^{13}C NMR (100 MHz, DMSO-d_6): δ_C = 177.7, 158.3, 155.6, 139.4, 134.2, 132.2, 131.2, 128.9, 127.4, 126.3, 123.6, 120.7, 116.5, 114.1, 55.2. *m/z* (ESI^+) calcd for $C_{15}H_{15}N_3O_2S$ $[M+H]^+$: 302.0958, found 302.0981 ; EA: Calcd (%) C (59.78), H (5.62), N (13.94), S (10.64). Found C (59.88), H (4.86), N (13.56), S (10.61).

(E)-2-((4'-Bromo-4-hydroxy-[1,1'-biphenyl]-3-yl)methylene)hydrazine-1-carbothioamide (LKN-12)

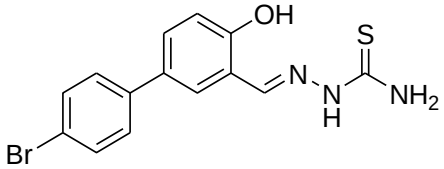

Off white solid (210 mg, 38%). M.p.: 174.1 – 175.6 °C. ν_{max}(IR)/cm^{-1} 3200 and 3150 (NH and NH_2), 1600 (C=N); ^1H NMR (400 MHz, DMSO-d_6): δ_H = 9.89 (s, 1H, OH), 8.64 (s, 1H, HCN), 8.41 (s, 1H, NH_2'), 8.36 (s, 1H, NH_2'), 8.15 (d, *J* = 4.0 Hz, 1H, Ar-H), 7.90 (d, *J* = 8.0 Hz, 2H, Ar-H), 7.65 (d, *J* = 8.0 Hz, 2H, Ar-H), 7.56 (dd, *J* = 4.0 and 8.0 Hz, 1H, Ar-H), 6.95 (d, *J* = 8.0 Hz, 1H, Ar-H); ^{13}C NMR (75 MHz, DMSO-d_6): δ_C = 181.6, 178.8, 178.0, 171.7, 156.8, 152.2, 141.3, 139.2, 131.9, 128.8, 119.7, 116.5. *m/z* (ESI^+) calcd for $C_{14}H_{12}BrN_3OS$ $[M+H]^+$: 349.9957, found 350.9858; EA: Calcd (%) C (48.01), H (3.45), N (12.00), S (9.15). Found C (24.05), H (5.64), N (37.05), S (28.77).

(E)-2-((4-Hydroxy-4'-(methylthio)-[1,1'-biphenyl]-3-yl)methylene)hydrazine-1-carbothioamide (LKN-13)

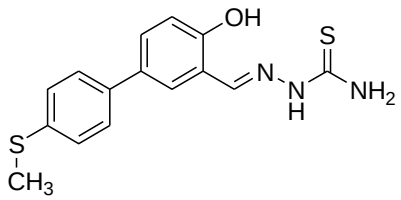

Yellow solid (120 mg, 92%). M.p.: 322.5 – 323.4 °C. ν_{max}(IR)/cm^{-1} 3450 (OH), 3200 and 3150 (NH and NH_2), 1600 (C=N); ^{1}H NMR (400 MHz, DMSO-*d*$_6$): δ_H = 11.43 (s, 1H, NH), 10.11 (s, 1H, OH), 8.43 (s, 1H, HCN), 8.16 (s, 1H, NH_2'), 8.09 (s, 1H, NH_2'), 7.85 (d, *J*= 4.0 Hz, 1H, Ar-H), 7.66 (d, *J* = 8.0 Hz, 2H, Ar-H), 7.54 (dd, *J* = 4.0 and 8.0 Hz, 1H, Ar-H), 7.31 (d, *J* = 8.0 Hz, 2H, Ar-H), 6.96 (d, *J* = 8.0 Hz, 1H, Ar-H), 3.38 (s, 3H, S- CH_3); ^{13}C NMR (100 MHz, DMSO-*d*$_6$): δ_C = 192.0, 178.1, 160.6, 156.5, 139.6, 136.8, 131.2, 129.5, 127.2, 126.8, 124.3, 122.9, 118.5, 117.0, 28.5. *m/z* (ESI$^+$) calcd for $C_{15}H_{15}N_3OS_2$ $[M+H]^+$: 318.0729, found 318.0735; EA: Calcd (%) C (56.76), H (4.76), N (13.24), S (20.20). Found C (58.02), H (4.80), N (11.59), S (19.34).

(E)-2-((4'-Fluoro-4-hydroxy-[1,1'-biphenyl]-3-yl)methylene)hydrazine-1-carbothioamide (LKN-14)

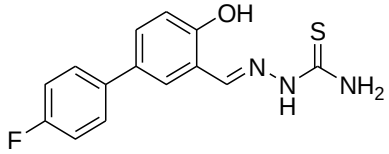

Off white solid (422 mg, 92%). M.p.: 282.5 – 283.9 °C. ν_{max}(IR)/cm^{-1} 3450 (OH), 3200 and 3150 (NH and NH_2), 1600 (C=N); ^{1}H NMR (400 MHz, DMSO-*d*$_6$): δ_H = 11.41 (s, 1H, NH), 10.03 (s, 1H, OH), 8.43 (s, 1H, HCN), 8.23 (s, 1H, NH_2'); 8.18 (s, 1H, NH_2'), 7.72 (dd, *J* = 4.0 and 12.0 Hz, 2H, Ar-H), 7.52 (dd, *J* = 4.0 and 8.0 Hz, 1H, Ar-H), 7.39 (d, *J* = 4.0, 1H, Ar-H), 7.23 (t, *J* = 8.0 Hz, 2H, Ar-H), 6.96 (d, *J* = 8.0 Hz, 1H, Ar-H); ^{13}CNMR (100 MHz, DMSO-*d*$_6$): δ_C = 178.1, 163.1, 160.6, 156.5, 150.4, 139.5, 136.6, 130.8, 129.7, 128.6, 124.6, 121.2, 117.0, 115.1. *m/z* (ESI$^+$) calcd for $C_{14}H_{12}FN_3OS$ $[M+H]^+$: 290.0758, found 290.0763 ; EA: Calcd (%) C (58.12), H (4.18), N (14.52), S (11.08). Found C (56.93), H (3.74), N (15.09), S (11.91)

CHAPTER 5

Conclusion

The aims and objectives for this research were the identification and characterization of novel thiosemicarbazone based derivatives as possible antiparasitic agents. Various thiosemicarbazones were synthesized to generate a structurally diversed compound library. This was to enable proper and in-depth correlation on how the different substituents would affect the viability of parasitic cells.

Quinolines are among the most commonly used antimalarials, with chloroquine having been the most used drug with a quinolone moiety for decades before the emergence of drug resistant strains. The quinolines and thiosemicarbazides were hybridized in an attempt to synthesize hybrid compounds which would target more than one target in the malaria parasite in an attempt to make these compounds more potent and more effective against malaria. However, it was observed that of the synthesized quinolone-thiosemicarbazone hybrid compounds all had little to no effect on HeLa and *P. falciparum* cells, meaning these compounds were ineffective at inhibiting the growth of malaria cells in vitro. This could either indicate that these hybrid compounds were completely ineffective at inhibiting cell growth of malaria cells, it could also be an indication of a need for further investigation to assess the effectiveness of quinolone-thiosemicarbazones.

Work done on α-aminocresols by Burckhalter and co-workers displayed the importance of having the hydroxyl group in the ortho position to the α-amino group. The synthesis of phenol-thiosemicarbazone scaffolds followed this ortho substitution of phenol groups in relation to the thiosemicarbazone moiety in an attempt to increase the activity of these compounds. It is also though that certain phenols are effective against the metabolically active late trophozoite schizont stages of the malaria parasite. Thus, there is a possibility that these hybrid compounds could in turn target two different stages of the malaria lifecycle, thus increasing their effectiveness. One compound from this set of hybrid compound was effective in inhibiting cell growth of *P. falciparum* and that synthesized compound was

LKN-11, which was a phenol-thiosemicarbazone species with a para-substituted methoxy-phenyl group which may have played a role in the compounds efficacy at inhibiting cell growth. Future work should entail further investigation into possible effects the methoxy-phenyl groups could play.

REFERENCES

1. The chemical structure of p -cymene. | Download Scientific Diagram. https://www.researchgate.net/figure/The-chemical-structure-of-deferoxamine-DFO_fig1_263741518. Accessed January 11, 2021.
2. Walcourt A, Loyevsky M, Lovejoy DB, Gordeuk VR, Richardson DR. Novel aroylhydrazone and thiosemicarbazone iron chelators with anti-malarial activity against chloroquine-resistant and -sensitive parasites. *Int J Biochem Cell Biol*. 2004;36(3):401-407. doi:10.1016/S1357-2725(03)00248-6
3. Greenbaum DC, Mackey Z, Hansell E, et al. Synthesis and structure-activity relationships of parasiticidal thiosemicarbazone cysteine protease inhibitors against Plasmodium falciparum, Trypanosoma brucei, and Trypanosoma cruzi. *J Med Chem*. 2004;47(12):3212-3219. doi:10.1021/jm030549j
4. Butler AR, Khan S, Ferguson E. A brief history of malaria chemotherapy. *J R Coll Physicians Edinb*. 2010;40(2):172-177. doi:10.4997/JRCPE.2010.216
5. Plasmodium species (Malaria) - Infectious Disease Advisor. https://www.infectiousdiseaseadvisor.com/home/decision-support-in-medicine/infectious-diseases/plasmodium-species-malaria/. Accessed March 23, 2020.
6. Malaria. https://www.who.int/news-room/fact-sheets/detail/malaria. Accessed March 23, 2020.
7. Ashley EA, White NJ. The duration of Plasmodium falciparum infections. *Malar J*. 2014;13(1). doi:10.1186/1475-2875-13-500
8. van Damme W. *Malaria Control during Mass Population Movements and Natural Disasters*. Vol 17.; 2004. doi:10.1093/jrs/17.1.145
9. Autino B, Noris A, Russo R, Castelli F. Epidemiology of malaria in endemic areas. *Mediterr J Hematol Infect Dis*. 2012;4(1). doi:10.4084/MJHID.2012.060
10. WHO | World malaria report 2019. https://www.who.int/malaria/publications/world-malaria-report-2019/en/. Accessed March 6, 2020.
11. WHO | World malaria report 2019. *WHO*. 2020.
12. More pregnant women and children protected from malaria, but accelerated efforts and funding needed to reinvigorate global response, WHO report shows. https://www.who.int/news-room/detail/04-12-2019-more-pregnant-women-and-children-protected-from-malaria-but-accelerated-efforts-and-funding-needed-to-reinvigorate-global-response-who-report-shows. Accessed March 5, 2020.
13. Rowe AK, Rowe SY, Snow RW, et al. The burden of malaria mortality among African children in the year 2000. *Int J Epidemiol*. 2006;35(3):691-704. doi:10.1093/ije/dyl027
14. WHO/UNICEF. *Africa Malaria Report*.; 2003. http://mosquito.who.int/amd2003/amr2003/pdf/amr2003.pdf.

15. Gething PW, Casey DC, Weiss DJ, et al. Mapping plasmodium falciparum mortality in Africa between 1990 and 2015. *N Engl J Med*. 2016;375(25):2435-2445. doi:10.1056/NEJMoa1606701

16. Prevention C-C for DC and. CDC - Malaria - About Malaria - Biology. 2020.

17. Life-cycle-malaria-parasite.jpg (300×400). https://cdn.britannica.com/47/123347-004-5CEDBD29/Life-cycle-malaria-parasite.jpg. Accessed March 5, 2020.

18. Tse EG, Korsik M, Todd MH. The past, present and future of anti-malarial medicines. *Malar J*. 2019;18(1):1-21. doi:10.1186/s12936-019-2724-z

19. Nussenzweig RS, Vanderberg J, Most H, Orton C. Protective immunity produced by the injection of X-irradiated sporozoites of plasmodium berghei. *Nature*. 1967;216(5111):160-162. doi:10.1038/216160a0

20. Draper SJ, Sack BK, King CR, et al. Malaria Vaccines: Recent Advances and New Horizons. *Cell Host Microbe*. 2018;24(1):43-56. doi:10.1016/j.chom.2018.06.008

21. van Schalkwyk DA. History of Antimalarial Agents. In: *ELS*. Chichester, UK: John Wiley & Sons, Ltd; 2015:1-5. doi:10.1002/9780470015902.a0003624.pub3

22. MMV. History of antimalarials | Medicines for Malaria Venture. Medicine for malaria Venture. https://www.mmv.org/malaria-medicines/history-antimalarials. Published 2020. Accessed March 2, 2021.

23. Heller LE, Roepe PD. Artemisinin-based antimalarial drug therapy: Molecular pharmacology and evolving resistance. *Trop Med Infect Dis*. 2019;4(2):89. doi:10.3390/tropicalmed4020089

24. Delves M, Plouffe D, Scheurer C, et al. The activities of current antimalarial drugs on the life cycle stages of plasmodium: A comparative study with human and rodent parasites. *PLoS Med*. 2012;9(2). doi:10.1371/journal.pmed.1001169

25. Delves M, Lafuente-Monasterio MJ, Upton L, et al. Fueling Open Innovation for Malaria Transmission-Blocking Drugs: Hundreds of Molecules Targeting Early Parasite Mosquito Stages. *Front Microbiol*. 2019;10:2134. doi:10.3389/fmicb.2019.02134

26. Deslyper G, Doherty DG, Carolan JC, Holland C V. The role of the liver in the migration of parasites of global significance. *Parasites and Vectors*. 2019;12(1):1-11. doi:10.1186/s13071-019-3791-2

27. Stanway RR, Bushell E, Chiappino-Pepe A, et al. Genome-Scale Identification of Essential Metabolic Processes for Targeting the Plasmodium Liver Stage. *Cell*. 2019;179(5):1112-1128.e26. doi:10.1016/j.cell.2019.10.030

28. *Medicinal Chemistry of Neglected and Tropical Diseases*.; 2019. doi:10.1201/9781351011655

29. Group WGS. Gametocyte carriage in uncomplicated Plasmodium falciparum malaria following treatment with artemisinin combination therapy: a systematic review and meta-analysis of individual patient data. *BMC Med*. 2016;14(1):79. doi:10.1186/s12916-016-

0621-7

30. Thomas A, Antony J. Synthesis and In-vitro Anti-Cancer Screening of N 1 [(Substituted Phenyl)Benzylidene]Benzohydrazides.

31. Alam M, Verma G, Shaquiquzzaman M, Marella A, Akhtar M, Ali M. A review exploring biological activities of hydrazones. *J Pharm Bioallied Sci*. 2014;6(2):69. doi:10.4103/0975-7406.129170

32. Trotsko N, Golus J, Kazimierczak P, et al. Design, synthesis and antimycobacterial activity of thiazolidine-2,4-dione-based thiosemicarbazone derivatives. *Bioorg Chem*. 2020;97. doi:10.1016/j.bioorg.2020.103676

33. Beteck RM, Seldon R, Jordaan A, et al. New quinolone-based thiosemicarbazones showing activity against plasmodium falciparum and mycobacterium tuberculosis. *Molecules*. 2019;24(9). doi:10.3390/molecules24091740

34. de Araújo Neto LN, do Carmo Alves de Lima M, de Oliveira JF, et al. Synthesis, cytotoxicity and antifungal activity of 5-nitro-thiophene-thiosemicarbazones derivatives. *Chem Biol Interact*. 2017;272:172-181. doi:10.1016/j.cbi.2017.05.005

35. de Oliveira Paiva R, Ferreira Kneipp L, Marins Goular C, Almeida Albuquerque M, Echevarria A. *ANTIFUNGAL ACTIVITIES OF THIOSEMICARBAZONES AND SEMICARBAZONES AGAINST MYCOTOXIGENIC FUNGI Atividade Antifúngica de Tiosemicarbazonas e Semicarbazonas Frente a Fungos Micotoxigênicos*. Vol 38.; 2014.

36. Thanh ND, Duc HT, Duyen VT, Tuong PM, Quoc N. Synthesis and antibacterial and antifungal activities of N-(tetra-O-acetyl-β-d-glucopyranosyl)thiosemicarbazones of substituted 4-formylsydnones. *Chem Cent J*. 2015;9(1):60. doi:10.1186/s13065-015-0138-8

37. Pelosi G, Bisceglie F, Bignami F, et al. Antiretroviral activity of thiosemicarbazone metal complexes. *J Med Chem*. 2010;53(24):8765-8769. doi:10.1021/jm1007616

38. Pham VH, Dung Phan TP, Phan DC, Vu BD. Synthesis and bioactivity of thiosemicarbazones containing adamantane skeletons. *Molecules*. 2020;25(2):324. doi:10.3390/molecules25020324

39. Heffeter P, Pape VFS, Enyedy ÉA, Keppler BK, Szakacs G, Kowol CR. Anticancer thiosemicarbazones: Chemical properties, interaction with iron metabolism, and resistance development. *Antioxidants Redox Signal*. 2019;30(8):1062-1082. doi:10.1089/ars.2017.7487

40. Linciano P, Moraes CB, Alcantara LM, et al. Aryl thiosemicarbazones for the treatment of trypanosomatidic infections. *Eur J Med Chem*. 2018;146:423-434. doi:10.1016/j.ejmech.2018.01.043

41. Beteck RM, Seldon R, Jordaan A, et al. New quinolone-based thiosemicarbazones showing activity against plasmodium falciparum and mycobacterium tuberculosis. *Molecules*. 2019;24(9). doi:10.3390/molecules24091740

42. Sarkar S, Siddiqui AA, Saha SJ, et al. Antimalarial activity of small-molecule

benzothiazole hydrazones. *Antimicrob Agents Chemother*. 2016;60(7):4217-4228. doi:10.1128/AAC.01575-15

43. Cabantchik ZI, Moody-Haupt S, Gordeuk VR. Iron chelators as anti-infectives; malaria as a paradigm. *FEMS Immunol Med Microbiol*. 1999;26(3-4):289-298. doi:10.1111/j.1574-695x.1999.tb01401.x

44. Smith HJ, Meremikwu MM. Iron-chelating agents for treating malaria. *Cochrane Database Syst Rev*. 2003. doi:10.1002/14651858.cd001474

45. Tang J, Zhang J, Transition O, Complexes M. Thiosemicarbazone Derivative Luminescent Zinc Complexes as Bio- probes for Imaging Molecular Events in Live Cells Five-membered Rings with More than Two Heteroatoms and Fused Carbo- cyclic Derivatives. In: *Comprehensive Heterocyclic Chemistry III*. 1st editio. ; 2017.

46. Divatia SM, Rajani DP, Rajani SD, Patel HD. Novel thiosemicarbazone derivatives containing benzimidazole moiety: Green synthesis and anti-malarial activity. *Arab J Chem*. 2014. doi:10.1016/j.arabjc.2014.09.007

47. Serda M, Kalinowski DS, Rasko N, et al. Exploring the anti-cancer activity of novel thiosemicarbazones generated through the combination of retro-fragments: Dissection of critical structure-activity relationships. *PLoS One*. 2014;9(10). doi:10.1371/journal.pone.0110291

48. Lee BJ, Singh A, Chiang P, et al. Antimalarial Activities of Novel Synthetic Cysteine Protease Inhibitors. *Antimicrob Agents Chemother*. 2003;47(12):3810-3814. doi:10.1128/AAC.47.12.3810-3814.2003

49. Rosenthal P, Sijwali P, Singh A, Shenai B. Cysteine Proteases of Malaria Parasites: Targets for Chemotherapy. *Curr Pharm Des*. 2005;8(18):1659-1672. doi:10.2174/1381612023394197

50. Mallari JP, Guiguemde WA, Guy RK. Antimalarial activity of thiosemicarbazones and purine derived nitriles. *Bioorganic Med Chem Lett*. 2009;19(13):3546-3549. doi:10.1016/j.bmcl.2009.04.142

51. Divatia SM, Rajani DP, Rajani SD, Patel HD. Novel thiosemicarbazone derivatives containing benzimidazole moiety: Green synthesis and anti-malarial activity. *Arab J Chem*. 2014. doi:10.1016/j.arabjc.2014.09.007

52. Wikipedia Contributors. No Title. Wikipedia. doi:980036970

53. Palling DJ, Jencks WP. Nucleophilic Reactivity toward Acetyl Chloride in Water. *J Am Chem Soc*. 1984;106(17):4869-4876. doi:10.1021/ja00329a040

54. Ghosh R, Maiti S, Chakraborty A. Facile catalyzed acylation of alcohols, phenols, amines and thiols based on ZrOCl 2·8H 2O and acetyl chloride in solution and in solvent-free conditions. *Tetrahedron Lett*. 2005;46(1):147-151. doi:10.1016/j.tetlet.2004.10.164

55. Csihony S, Mehdi H, Horváth IT. In situ infrared spectroscopic studies of the Friedel-Crafts acetylation of benzene in ionic liquids using AlCl3 and FeCl3. *Green Chem*. 2001;3(6):307-309. doi:10.1039/b107515m

56. Meth-Cohn O, Narine B, Tarnowski B. A versatile new synthesis of quinolines and related fused pyridines. Part 5. The synthesis of 2-chloroquinoline-3-carbaldehydes. *J Chem Soc Perkin Trans 1*. 1981;(0):1520-1530. doi:10.1039/P19810001520

57. Doltra A, Dietrich T, Schneeweis C, et al. Magnetic Resonance Imaging of Cardiovascular Fibrosis and Inflammation: From Clinical Practice to Animal Studies and Back Cardiovascular MRI View project Magnetic Resonance Imaging of Cardiovascular Fibrosis and Inflammation: From Clinical Practice to Ani. *Biomed Res Int*. 2013;676489(10):1-2. doi:10.1155/2013

58. Proposed mechanism for the isomerisation of α-pinene oxide by a Lewis... | Download Scientific Diagram. https://www.researchgate.net/figure/A-proposed-mechanism-for-the-synthesis-of_fig4_271580535. Accessed March 11, 2020.

59. Hussein MA, Iqbal MA, Umar MI, Haque RA, Guan TS. Synthesis, structural elucidation and cytotoxicity of new thiosemicarbazone derivatives. *Arab J Chem*. 2019;12(8):3183-3192. doi:10.1016/j.arabjc.2015.08.013

60. Ramos-Tomillero I, Paradís-Bas M, De Pinho Ribeiro Moreira I, Bofill JM, Nicolás E, Albericio F. Formylation of electron-rich aromatic rings mediated by dichloromethyl methyl ether and TiCl4: Scope and limitations. *Molecules*. 2015;20(4):5409-5422. doi:10.3390/molecules20045409

61. Shockley SE, Holder JC, Stoltz BM. Palladium-Catalyzed Asymmetric Conjugate Addition of Arylboronic Acids to α,β-Unsaturated Cyclic Electrophiles. doi:10.1021/acs.oprd.5b00169

62. Metwally MA, Bondock S. Thiosemicarbazides : Synthesis and reactions Thiosemicarbazides : synthesis and reactions. 2011;(May 2020). doi:10.1080/17415993.2011.601869

63. Mustafa S, Nair V, Chittoor J, Krishnapillai S. Synthesis of 1, 2, 4-Triazoles and Thiazoles from Thiosemicarbazide and its Derivatives. *Mini Rev Org Chem*. 2005;1(4):375-385. doi:10.2174/1570193043403082

64. Bromination of benzene (video) | Khan Academy. https://www.khanacademy.org/science/organic-chemistry/aromatic-compounds/reactions-benzene/v/bromination-of-benzene. Accessed March 13, 2020.

65. Jim Clark. Reactions of Alkenes with Bromine - Chemistry LibreTexts. Jun 5. https://chem.libretexts.org/Bookshelves/Organic_Chemistry/Supplemental_Modules_(Organic_Chemistry)/Reactions/Addition_Reactions/Electrophilic_Addition_Reactions/Reactions_of_Alkenes_with_Bromine. Published 2019. Accessed March 13, 2020.

66. ORTHO-FORMYLATION OF PHENOLS; PREPARATION OF 3-BROMOSALICYLALDEHYDE. *Org Synth*. 2005;82:64. doi:10.15227/orgsyn.082.0064

67. Dikusar EA, Potkin VI. Synthesis and properties of substituted benzaldehyde phenylhydrazones. *Russ J Gen Chem*. 2009;79(5):953-956. doi:10.1134/S1070363209050144

68. Tse EG, Korsik M, Todd MH. The past, present and future of anti-malarial medicines.

Malar J. 2019;18(1). doi:10.1186/s12936-019-2724-z

69. Yadav N, Dixit SK, Bhattacharya A, et al. Antimalarial Activity of Newly Synthesized Chalcone Derivatives In Vitro. *Chem Biol Drug Des*. 2012;80(2):340-347. doi:10.1111/j.1747-0285.2012.01383.x

70. N-phenylacetamide - 103-84-4, C8H9NO, density, melting point, boiling point, structural formula, synthesis. https://www.chemsynthesis.com/base/chemical-structure-3538.html. Accessed June 12, 2020.

71. N-(4-Methoxyphenyl)acetamide 97% | Sigma-Aldrich. https://www.sigmaaldrich.com/catalog/product/aldrich/428264?lang=en&region=ZA. Accessed June 12, 2020.

72. Eliel EL, Burgstahler AW, Rivard DE, Haefele L. The Methyl Esters of 3-Hydroxyphthalic Acid. Selective Reduction of Monomethyl Phthalates with Lithium Aluminum Hydride. *J Am Chem Soc*. 1955;77(19):5092-5095. doi:10.1021/ja01624a042

73. N-(4-methylphenyl)acetamide - 103-89-9, C9H11NO, density, melting point, boiling point, structural formula, synthesis. https://www.chemsynthesis.com/base/chemical-structure-7637.html. Accessed June 12, 2020.

74. Gowda BT, Foro S, Fuess H. N-(4-Chloro-phen-yl)acetamide: A redetermination. *Acta Crystallogr Sect E Struct Reports Online*. 2007;63(8). doi:10.1107/S1600536807031893

75. 2-CHLOROQUINOLINE-3-CARBALDEHYDE | 73568-25-9. https://www.chemicalbook.com/ChemicalProductProperty_EN_CB1451393.htm. Accessed June 12, 2020.

76. Shiri M, Pourabed R, Zadsirjan V, Sodagar E. Highly selective organocatalytic three-component reaction of 2-chloroquinoline-3-carbaldehydes, 6-aminouracils, and cyclic methylene active compounds. *Tetrahedron Lett*. 2016;57(49):5435-5438. doi:10.1016/j.tetlet.2016.10.057

77. Alfa Aesar meso-Hydrobenzoin, 99% | Fisher Scientific. https://www.fishersci.com/shop/products/2-chloro-6-methoxyquinoline-3-carboxaldehyde-99/AAH2697306. Accessed June 12, 2020.

78. CAS#:73568-27-1 | 2-Chloro-6-methylquinoline-3-carbaldehyde | Chemsrc. https://www.chemsrc.com/en/cas/73568-27-1_57324.html. Accessed June 12, 2020.

79. 2,6-Dichloroquinoline-3-carbaldehyde 73568-41-9 MSDS, Safety Technical Specifications _ MSDS. http://www.molbase.com/en/msds_73568-41-9-moldata-397910.html. Accessed June 12, 2020.

80. 2-METHOXY-QUINOLINE-3-CARBALDEHYDE | 139549-06-7. https://www.chemicalbook.com/ChemicalProductProperty_EN_CB8743608.htm. Accessed June 12, 2020.

81. Ibrahim TS, Bokhtia RM, AL-Mahmoudy AMM, et al. Design, synthesis and biological evaluation of novel 5-((substituted quinolin-3-yl/1-naphthyl) methylene)-3-substituted imidazolidin-2,4-dione as HIV-1 fusion inhibitors. *Bioorg Chem*. 2020;99:103782.

doi:10.1016/j.bioorg.2020.103782

82. Rajeev P V., Rajendran SP. Facile synthesis of 1-hydroxy-5-methoxy-benzo[f][2,7]naphthyridines. *Synth Commun*. 2010;40(19):2837-2843. doi:10.1080/00397910903320258

83. 4-Bromo-2-isopropylphenol | C9H11BrO | ChemSpider. http://www.chemspider.com/Chemical-Structure.11462712.html?rid=d79e6559-1972-4dd9-928f-51daadb442ca&page_num=0#suppInfoTab. Accessed June 12, 2020.

84. 2-Bromo-4-methoxyphenol | C7H7BrO2 | ChemSpider. http://www.chemspider.com/Chemical-Structure.262559.html. Accessed June 12, 2020.

85. 2-Bromo-4-nitrophenol ≥98.0% | Sigma-Aldrich. https://www.sigmaaldrich.com/catalog/product/aldrich/689858?lang=en&region=ZA. Accessed June 18, 2020.

86. 57-50-1 CAS MSDS (Sucrose) Melting Point Boiling Point Density CAS Chemical Properties. https://www.chemicalbook.com/ChemicalProductProperty_US_CB7416419.aspx. Accessed June 18, 2020.

87. 2-Bromo-4-tert-butylphenol | C10H13BrO | ChemSpider. http://www.chemspider.com/Chemical-Structure.67695.html#suppInfoTab. Accessed June 18, 2020.

88. 3-Bromo-2-hydroxy-5-nitrobenzaldehyde supplier - CAS 16789-84-7 - EC-000.1542. https://exchemistry.com/chem-catalog/product-1542.html. Accessed June 19, 2020.

89. 4-Hydroxy-3-biphenylcarbaldehyde | C13H10O2 | ChemSpider. http://www.chemspider.com/Chemical-Structure.11447468.html#suppInfoTab. Accessed June 19, 2020.

90. Hegen O, Virovets A V., Timoshkin AY, Scheer M. The Lewis-Base-Stabilized Diphenyl-Substituted Arsanylborane: A Versatile Building Block for Arsanylborane Oligomers. *Chem - A Eur J*. 2018;24(62):16521-16525. doi:10.1002/chem.201804341

91. Raju BC, Tiwari AK, Kumar JA, et al. α-Glucosidase inhibitory antihyperglycemic activity of substituted chromenone derivatives. *Bioorganic Med Chem*. 2010;18(1):358-365. doi:10.1016/j.bmc.2009.10.047

92. Raju BC, Tiwari AK, Kumar JA, et al. α-Glucosidase inhibitory antihyperglycemic activity of substituted chromenone derivatives. *Bioorganic Med Chem*. 2010;18(1):358-365. doi:10.1016/j.bmc.2009.10.047